Journal of Ophthalmology

Retinitis Pigmentosa: Disease Mechanisms, Diagnosis, and Therapies

Guest Editors: Xinhua Shu, Ji-jing Pang, Houbin Zhang, and David Mansfield

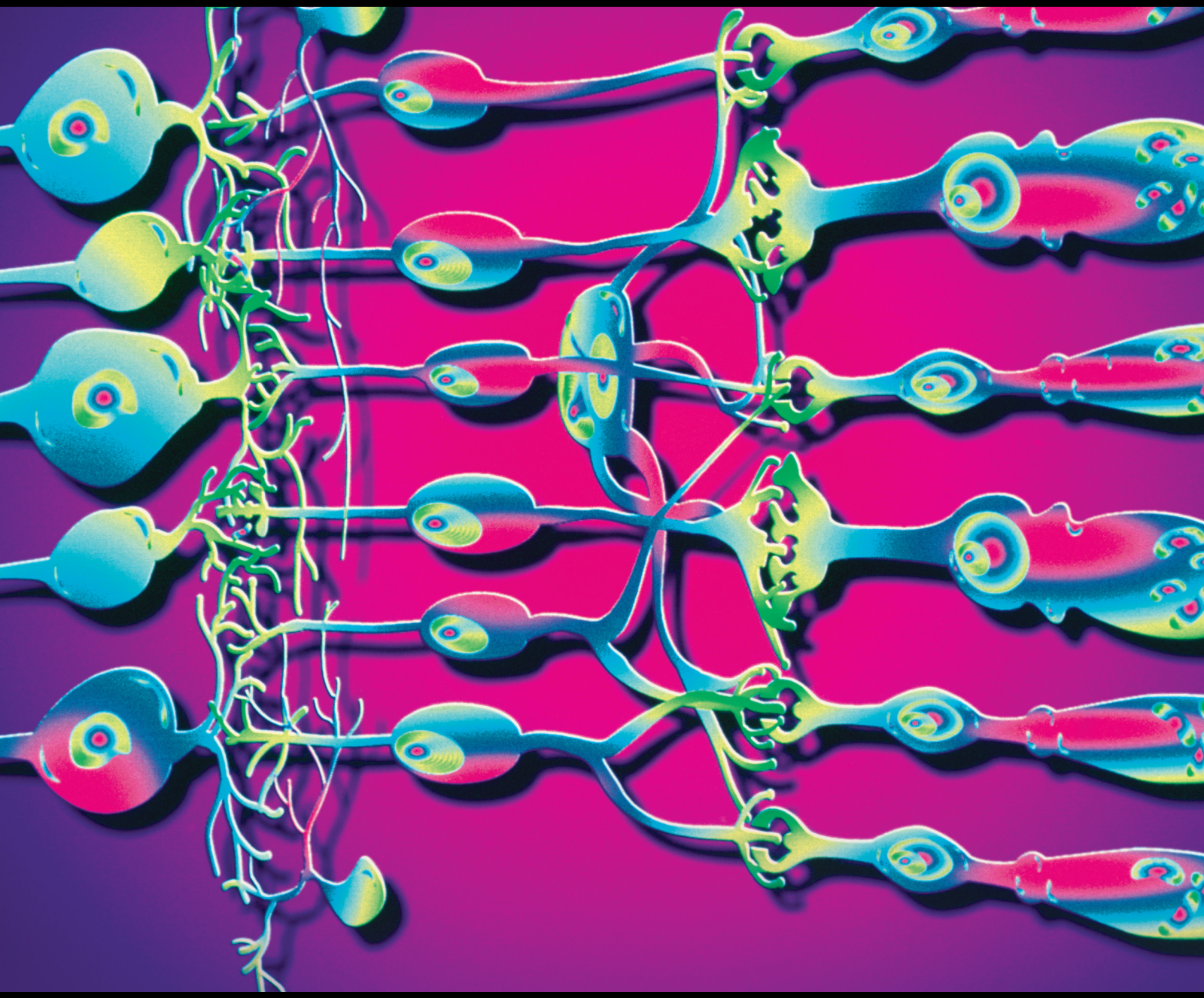

Retinitis Pigmentosa: Disease Mechanisms, Diagnosis, and Therapies

Journal of Ophthalmology

Retinitis Pigmentosa: Disease Mechanisms, Diagnosis, and Therapies

Guest Editors: Xinhua Shu, Ji-jing Pang, Houbin Zhang, and David Mansfield

Editorial Board

Contents

Hindawi Publishing Corporation
Journal of Ophthalmology
Volume 2015, Article ID 819452, 1 page
http://dx.doi.org/10.1155/2015/819452

Editorial

Retinitis Pigmentosa: Disease Mechanisms, Diagnosis, and Therapies

Xinhua Shu,[1] Ji-jing Pang,[2,3] Houbin Zhang,[4] and David Mansfield[5]

[1]*Department of Life Sciences, Glasgow Caledonian University, Glasgow G4 0BA, UK*
[2]*School of Ophthalmology & Optometry, The Eye Hospital, Wenzhou Medical University, Wenzhou, Zhejiang 325027, China*
[3]*Department of Ophthalmology, College of Medicine, University of Florida, Gainesville, FL 32610, USA*
[4]*Sichuan Provincial Key Laboratory for Disease Gene Study, Hospital of University of Electronic Science and Technology of China and Sichuan Provincial People's Hospital, Chengdu, Sichuan 610072, China*
[5]*Department of Ophthalmology, Inverclyde Royal Hospital, Greenock PA16 0XN, UK*

Correspondence should be addressed to Xinhua Shu; xinhua.shu@gcu.ac.uk

Received 29 April 2015; Accepted 29 April 2015

Retinitis pigmentosa (RP) is the most genetically and phenotypically heterogeneous disorder, characterized by the progressive death of photoreceptor cells. In recent years, huge advances have been made in understanding the disease mechanisms, identifying causal genes, and developing therapeutic strategies for this disorder. This special issue updates the knowledge of RP and presents original clinical and experimental research.

Photoreceptor cell death is known to be characterized at the early stage by caspase dependent or independent apoptosis and at late stage by necrosis, but the molecular mechanisms are not fully understood. In this special issue, S. R. Patnaik et al. review the functional role of RPGR protein complex in the pathogenesis of RP. Disease mechanisms are further elucidated in mouse (Q. Zheng et al.) and zebrafish models (Y. Liu et al. and S. Akhtar et al.). R. Migliorini et al. discuss RP associated syndromes, such as impaired ocular motility. E. Strobbe et al. report a correlation between ocular inflammation and endothelin (ET-1) plasma levels in early RP patients and suggest that anti-inflammatory therapy may slow the progression of RP.

With the development of new technologies such as next generation sequencing (NGS), more and more mutant genes that cause retinal degenerative diseases have been found. B. Gong et al. reported here a recessive RDH12 mutation identified by exome sequencing in severe early onset RP patients, which further verifies the application of NGS for molecular diagnosis of RP. Meanwhile, many naturally occurring or genetically engineered animal models have shown gene mutations and phenotypes similar to human inherited retinal diseases, which has led to the development of a variety of therapeutic strategies for those inherited diseases regarded traditionally as incurable.

Following the success of Leber congenital amaurosis 2 (LCA2) gene therapy clinical trials, more and more vector based gene therapy clinical trials have been performed on a variety of retinal conditions including RP with MERTK mutation. AAV-mediated gene replacement therapy shows great potential to treat patients in the early stage of the disease. Gene replacement therapy combined with other approaches like treatment with histone deacetylases inhibitors (reviewed by H. Zhang et al.) or antiapoptotic/inflammatory chemicals or natural products, which can extend the therapeutic window in middle to late stages of those patients, is a potentially promising strategy for improving photoreceptor function and significantly slowing the process of retinal degeneration. Cell replacement is a promising therapeutic strategy for RP. Successful cell replacement treatments have been done in RP animal models, providing hope for RP patients and their families. Chinese medicine has a long history in the treatment of RP; combinational treatment of Chinese medicine with Western medicine may further reduce the progression of RP (reviewed by J. Xu and Q. Peng).

Xinhua Shu
Ji-jing Pang
Houbin Zhang
David Mansfield

Hindawi Publishing Corporation
Journal of Ophthalmology
Volume 2015, Article ID 292615, 6 pages
http://dx.doi.org/10.1155/2015/292615

Research Article

ET-1 Plasma Levels, Aqueous Flare, and Choroidal Thickness in Patients with Retinitis Pigmentosa

Ernesto Strobbe, Mauro Cellini, Michela Fresina, and Emilio C. Campos

Ophthalmology Unit, Department of Experimental, Diagnostic, and Specialty Medicine, Alma Mater Studiorum, University of Bologna, Via Palagi 9, 40138 Bologna, Italy

Correspondence should be addressed to Ernesto Strobbe; strobern@gmail.com

Received 19 October 2014; Revised 9 December 2014; Accepted 15 December 2014

Academic Editor: Xinhua Shu

Purpose. To assess endothelin-1 (ET-1) plasma levels, choroidal thickness, and aqueous flare in patients with early stage retinitis pigmentosa (RP) and to search for possible correlations. *Methods*. We compared 24 RP patients with 24 healthy controls. Choroidal thickness and aqueous flare were measured, respectively, by using a spectral domain optical coherence tomography and a laser flare-cell meter, whereas plasma samples were obtained from each patient to evaluate ET-1 plasma levels. *Results*. Notably, RP subjects showed significantly increased ET-1 plasma levels and reduced choroidal thickness compared with controls: 2.143 ± 0.258 versus 1.219 ± 0.236 pg/mL, $P < 0.002$, and 226.75 ± 76.37 versus 303.9 ± 39.87 μm, $P < 0.03$, respectively. Higher aqueous flare values were also demonstrated in RP compared to controls: in detail, 10.51 ± 3.97 versus 5.66 ± 1.29 photon counts/ms, $P < 0.0001$. Spearman's correlation test highlighted that the increase of ET-1 plasma levels was related with the decrease of choroidal thickness ($r = -0.702$; $P < 0.023$) and the increase of aqueous flare ($r = 0.580$; $P < 0.007$). *Conclusions*. Early stage RP patients show a breakdown of blood-ocular barrier and increased ET-1 plasma levels and these findings may contribute to the reduction of choroidal thickness.

1. Introduction

Retinitis pigmentosa (RP) is a genetically heterogeneous hereditary disorder characterized by night blindness and progressive concentric visual field restriction, which may lead to severe central vision impairment due to degeneration and loss of photoreceptors and retinal pigment epithelium [1].

On the other hand, haemodynamic studies have demonstrated that RP patients show ocular blood flow disturbances, not only in retina and choroid but also in the retrobulbar vessels [2–4], and this finding may potentially contribute to the retinal damage. Moreover, increased endothelin-1 (ET-1) plasma levels have been described repeatedly in RP [5–7], and this increase might play a key role in determining vasoconstriction and ischemia, reducing ocular blood flow [8, 9], and leading to worsening of the abiotrophic process, as previously reported by our group in early stage RP [10].

Finally, alterations of the blood-ocular barrier and signs of intraocular inflammation, including cystoid macular edema, have been demonstrated in RP patients, by clinical examination and by fluorophotometric studies [11–13], and notably, Küchle and associates showed that RP eyes have increased aqueous flare values compared with controls that is strictly associated with cystoid macular edema [14].

In an attempt to establish better whether a relationship between ocular inflammation and haemodynamic alterations may exist and whether RP subjects may show some abnormalities in the choroid, we investigated the status of the blood-ocular barrier in early stage RP subjects by using the laser flare-cell meter and evaluated subfoveal choroidal thickness (SCT) by using spectral domain optical coherence tomography (SD-OCT).

2. Materials and Methods

The current study was an observational, case-control, single-center study performed in accordance with the tenets of the Declaration of Helsinki, was conducted between October 2012 and June 2014 at the S. Orsola-Malpighi Hospital in Bologna, and was reviewed and approved by the Institutional and Ethical Committee of University of Bologna.

Each patient signed an informed consent form, before being enrolled in the study, after a full explanation of the aim of the study and of the procedures.

24 patients aged 25 and 42 years, affected by early stage RP, were enrolled from a cohort of 58 RP subjects followed up by our center and compared with 24 age- and sex-matched healthy controls, aged between 28 and 45 years.

The diagnostic criteria for the early stage of RP we followed up are those described by Hamel in 2006 [15]: night blindness, peripheral visual field defects, normal or subnormal visual acuity, color vision and life habits, modest attenuation of retinal arterioles, normal or fairly pale optic disc, absent or rare peripheral bone spicule-shaped pigment deposits, and a decrease in maximum electroretinogram (ERG) amplitude. Thus, we selected only young RP patients with preserved visual function, nyctalopia, peripheral visual field defects, and decreased but not extinct ERG and excluded those who had systemic diseases, such as systemic hypertension, diabetes, and cardiovascular disease, were taking any medications, had cystoid macular edema demonstrated with SD-OCT and advanced posterior subcapsular cataract, or were syndromic RP patients.

All participants underwent a complete ophthalmological evaluation, including visual acuity, Goldmann applanation tonometry, and slit-lamp examination of anterior and posterior segment. A visual field test, an ERG, and assessment of choroidal thickness, aqueous flare, and ET-1 plasma levels were also performed.

2.1. Visual Field Test. Visual field test was performed by using standard automated perimetry with the Humphrey 740 field analyzer 30.2 full threshold program (Humphrey Instruments Inc., San Leandro, CA, USA), and both mean defect (MD) and pattern standard deviation (PSD) were obtained using Humphrey STATPAC software and were expressed in decibels (dB).

2.2. Electroretinogram. Electroretinogram (ERG) was recorded by using RETIMAX Plus Advanced (CSO Ophthalmic, Florence, Italy). After pupil dilation with 1% tropicamide and topical anesthesia of the cornea with 0.4% oxybuprocaine hydrochloride, HK-Loop ERG electrodes, a ground electrode, and the reference electrodes were applied, respectively, to the ocular surface, to the forehead, and to the temporal region. Electrical impedance was smaller than 5 kω for all electrodes. ERGs were recorded from both eyes simultaneously, according to International Society for Clinical Electrophysiology of Vision (ISCEV) standards [16], by using a standard flash strength of 2.5 cd·s·m^{-2}. Band-pass filter was between 0.3 Hz and 300 Hz with an amplification of 5 k while artifactual signals were automatically removed. The amplitudes of b-wave and a-wave were measured from the baseline and were expressed in microvolts (μV).

2.3. SD-OCT Image Acquisition and Analysis. SD-OCT is a noninvasive, objective technique that allows in vivo cross-sectional high resolution visualization of retina and choroid with a fast scanning speed [17]; however, to provide many details of the structure of the choroid, a new technique called enhanced depth imaging (EDI) has been developed in the recent years and described elsewhere [18, 19].

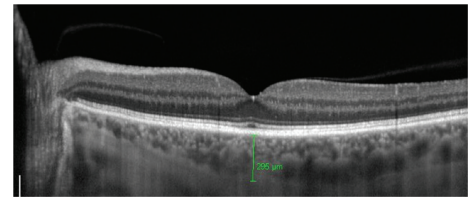

Figure 1: Representative enhanced depth imaging optical coherence tomography scan of a control subject. Choroidal thickness was measured as the distance between the hyperreflective line of the retinal pigment epithelium-Bruch's membrane complex and the innermost hyperreflective line of the choroid-sclera junction. For illustration purposes, the resultant images were reinverted.

We chose the horizontal scan running directly through the center of the fovea of both eyes of each patient by using SD-OCT (Heidelberg Engineering GmbH, Heidelberg, Germany) with the EDI technique and choroidal thickness was measured manually and was defined as the vertical distance from the hyperreflective line of the retinal pigment epithelium-Bruch's membrane complex to the innermost hyperreflective line of the choroidal scleral interface, exactly below the foveola. The values were expressed in micrometers (mμ) (Figure 1).

2.4. Endothelin-1 Determination. For ET-1 measurements the plasma samples were drawn from the antecubital vein and collected in a container with EDTA, cooled, and stored in ice. Subsequently, the samples were centrifuged at 4°C and frozen at −25°C. After centrifugation, the extraction was performed using a Sep-column containing C-18 (Peninsula Laboratories, Belmont, CA, USA) and ET-1 concentration was determined by using a commercial radioimmunoassay (RIA) kit (RIK-6901 Peninsula Laboratories, Belmont, CA, USA); after that samples and standards were firstly incubated with rabbit anti-ET-1 serum for 24 hours at 4°C. A second 24-hour incubation was performed after the addition of an iodinated tracer [^{125}I]-ET-1 (Peninsula Laboratories, Belmont, CA, USA). Free and bound radioligands were separated with centrifugation and radioactivity in the precipitate was counted with an automatic gamma-counter (Packard Industries, Boonton, NJ, USA). ET-1 concentration was expressed in picogram/milliliter (pg/mL).

2.5. Aqueous Flare Measurement. Examination of the aqueous humor by slit-lamp biomicroscopy is the primary method by which ophthalmologists evaluate the severity of anterior segment inflammation, by counting the number of cells and estimating "flare," that is, the amount of protein in the aqueous humor. Obviously, the ability to quantify inflammation relies on the experience of the examiner and this may result in substantial interobserver variability. For this reason, in the late 1980s, a laser flare-cell meter, an automated objective and noninvasive technique that enables rapid and reproducible

Table 1: Demographic, ocular parameters, and ET-1 plasma levels in patients with retinitis pigmentosa and healthy controls.

	Retinitis pigmentosa	Controls	$P < 0.05$
Age, years	33.8 ± 7.3	36.0 ± 6.8	0.155
Visual acuity, decimals	0.95 ± 0.07	0.97 ± 0.04	0.235
IOP, mmHg	15.8 ± 2.5	15.6 ± 2.3	0.81
SAP-PSD, dB	6.09 ± 4.22	1.98 ± 0.98	**0.001**
SAP-MD, dB	−7.90 ± 1.75	−1.95 ± 0.83	**0.006**
ERG b-wave, μV	45.08 ± 8.24	65.36 ± 9.84	**0.002**
ERG a-wave, μV	28.13 ± 5.77	38.16 ± 5.57	**0.019**
ET-1, pg/mL	2.143 ± 0.258	1.219 ± 0.236	**0.002**
Choroidal thickness, μm	226.75 ± 76.37	303.9 ± 39.87	**0.023**
Aqueous flare, pc/ms	10.51 ± 3.97	5.66 ± 1.29	**0.0001**

Note: values are presented as means ± SD; $n = 24$ per group.
IOP = intraocular pressure; SAP = standard automated perimetry; PSD = pattern standard deviation; MD = mean defect; dB = decibel; ERG = electroretinogram; μV = microvolt; ET-1 = endothelin-1; pg/mL = picogram/milliliter; μm = micrometer; pc/ms = photon counts/millisecond.

measurement of cells and flare in the aqueous humor [20, 21], by providing information about the status of the blood-aqueous barrier (BAB), and is able to identify small changes in aqueous humor proteins during the course of a disease that are not apparent clinically by slit-lamp biomicroscopy, was developed.

The device we used to assess intraocular inflammation was the laser flare-cell meter FC-500 (Kowa Company, Ltd, Tokyo, Japan), which uses a diode laser that is projected into the anterior chamber to scan a measurement window of 0.3 × 0.5 mm over 0.5 seconds [20], and the amount of backscattered light by protein particles in the aqueous humor, which is proportional to the concentration and size of proteins, is detected by a photomultiplier and processed by a computer. The average of signals coming from above and below the measurement window (background signals) is subtracted from the signal obtained from inside the scanned window to provide a laser flare photometry measurement.

The accuracy and reproducibility of the method have been shown in several studies by different groups [20, 22, 23], the coefficient of variation is less than 10%, and measurements are independent of the examiner using the instrument. Seven measurements for each eye were obtained and averaged, and those with artifacts were eliminated. The results were expressed as photon counts per millisecond (pc/ms).

2.6. Statistical Analysis. All data were expressed as the mean ± standard deviation (SD) and only 1 eye, for each subject, was randomly selected for statistical analysis. The statistical analysis was performed with MedCalc 10.9.1 statistical program (MedCalc Software, Ostend, Belgium), to assess the differences between RP patients and controls by using the Wilcoxon rank-sum test. Spearman's correlation test was used to evaluate the relationship between choroidal thickness and aqueous flare and the association between ET-1 plasma levels and both choroidal thickness and subclinical ocular inflammation. P values less than 0.05 were regarded as being statistically significant.

3. Results

A total of 48 eyes from 24 RP patients (male-to-female ratio, 14 : 10; mean age, 33.8 ± 7.3 years) and 24 healthy subjects (male-to-female ratio, 12 : 12; mean age, 36 ± 6.8 years) were examined in this study (Table 1).

As regards RP patients, the limits of visual field test parameters we considered for inclusion in the study were MD > −5 dB and PSD > 2.5 dB, whereas the limits of ERG were b-wave amplitude < 50 μV and a-wave amplitude < 35 μV (in our lab, normal range for a-wave and b-wave was 56.87–72.02 and 35.37–40.78 μV, resp.).

Clinically, no participants showed anterior chamber inflammatory reaction (cells and flare) or abnormalities in the lens and vitreous. Mild to modest attenuation of retinal arterioles, normal or fairly pale optic disc, and absent or rare peripheral bone spicule-shaped pigment deposits were also observed by slit-lamp biomicroscopic examination.

Age, best-corrected visual acuity, and intraocular pressure did not differ significantly between RP patients and healthy controls ($P > 0.05$), whereas there was a highly significant difference with regard to visual field parameters, MD ($P < 0.006$) and PSD ($P < 0.001$) and ERG; indeed, RP had peripheral visual field defects and decreased b-wave and a-wave amplitude compared to controls ($P < 0.002$ and $P < 0.019$, resp.). In addition, RP patients showed significantly higher ET-1 plasma levels and aqueous flare than controls, 2.143 ± 0.258 versus 1.219 ± 0.236 pg/mL ($P < 0.002$) and 10.51 ± 3.97 versus 5.66 ± 1.29 pc/ms ($P < 0.0001$), respectively, but also a significant reduction in choroidal thickness: 226.75 ± 76.37 versus 303.9 ± 39.87 μm ($P < 0.03$) (Table 1).

Furthermore, Spearman's correlation test highlighted that the increase of ET-1 plasma levels in RP was related with the decrease of choroidal thickness ($r = -0.702$; $P < 0.023$; Figure 2) and the increase of intraocular inflammation, represented by aqueous flare ($r = 0.580$; $P < 0.007$; Figure 3), whereas no statistically significant correlation between aqueous flare and choroidal thickness ($r = -0.308$; $P = 0.124$) was reported.

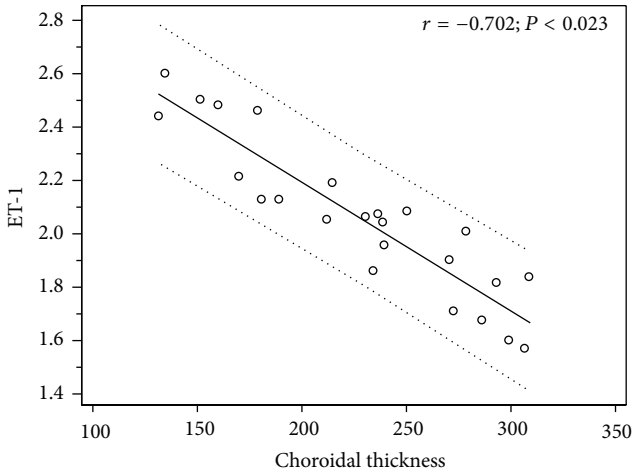

Figure 2: Scatterplot showing the correlation between ET-1 plasma levels (picogram/milliliter) and subfoveal choroidal thickness (micrometers) in patients with retinitis pigmentosa.

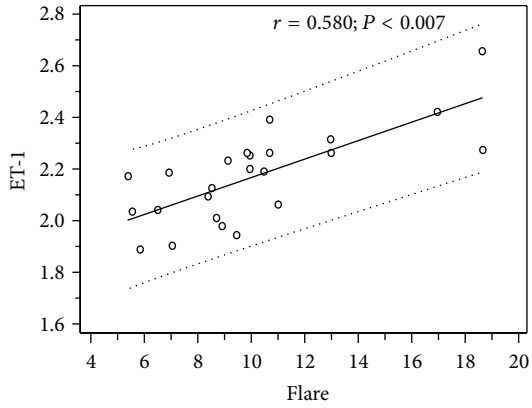

Figure 3: Scatterplot showing the correlation between ET-1 plasma levels (picogram/milliliter) and aqueous flare (photon counts/millisecond) in patients with retinitis pigmentosa.

4. Discussion

Retinitis pigmentosa is a group of inherited disorders characterized by progressive peripheral visual field loss, abnormal ERG responses and variable clinical presentation, severity, age of onset, and progression and may lead to central vision loss because it diffusely involves photoreceptors and retinal pigment epithelium (RPE) [1].

To the best of our knowledge, no data have been published concerning the relationship between intraocular inflammation and ET-1 plasma levels in RP patients.

Our results demonstrate that subjects affected by early stage RP with preserved central visual acuity have an 86% increase in aqueous flare values, a 34% decrease in choroidal thickness, and statistically significant higher ET-1 plasmatic levels compared with healthy controls.

The increase in aqueous flare reflects a disruption of the BAB, which allows leakage of serum proteins, as well as inflammatory molecules and cells, into the anterior segment, by causing a change in aqueous protein composition and concentration. By means of the noninvasive laser flare-cell meter that may provide an objective assessment of the status of the BAB [20], we showed that RP leads to a breakdown of the BAB that causes a local anterior subclinical inflammation that is not apparent clinically by slit-lamp biomicroscopy. This finding is in agreement with previous studies; indeed, fluorophotometric studies reported increased amount of fluorescein leakage into the vitreous of eyes with RP [12], whereas Küchle and associates [14] demonstrated that subjects affected by RP have higher aqueous flare values compared with healthy controls. Finally, Yoshida and coworkers [24] showed that aqueous flare is increased in RP patients and negatively correlates with visual function in phakic eyes.

The exact mechanism by which ocular inflammation occurs in RP patients is not clear, but two reasons may be postulated: firstly, most dystrophic and degenerative diseases are accompanied by low-grade inflammation; it is well known that increased retinal lipofuscin fluorophores in RP may determine damage, disturbed polarity, death of RPE, and apoptosis of photoreceptors [25].

In response to this stimulation, RPE synthesizes and releases a large variety of inflammatory molecules such as cytokines and chemokines [26], which, in turn, promote the recruitment of inflammatory cells that leak into the vitreous and may reach the aqueous, as there is no barrier separating the posterior from the anterior segment [27, 28], with a resulting enhanced aqueous flare. Secondly, as blood retinal barrier breakdown occurs both in retinal vessels and in RPE [29, 30], even BAB may be affected, leading to increased amount of proteins into the aqueous.

The thinnest choroidal thickness values we measured in RP patients compared with controls ($P = 0.03$), by using EDI SD-OCT, are in agreement with those already demonstrated by Dhoot et al. [31] with the same objective technique. It is possible that RPE and photoreceptor degeneration may result in choroidal thinning due to choriocapillaris atrophy [32, 33]; in animal models, it has been demonstrated that these cells are necessary for choroidal maintenance and thickness by producing several factors, such as vascular endothelial growth factor [34].

However, we reported choroidal thinning in patients with preserved visual acuity, suggesting that, probably, abnormalities in choroidal circulation and flow are the primum movens of photoreceptor degeneration. Indeed, both retinal and choroidal blood flow have previously been shown to be reduced in patients with RP, by using color Doppler imaging and laser Doppler flowmetry [2–4, 35, 36], and fluorescein angiography studies further support that choroidal circulation and volume are reduced and disturbed in RP [37–39].

Finally, these patients showed increased ET-1 plasma levels, and this finding was well related with the decrease of choroidal thickness and the increase of intraocular subclinical inflammation. Such an increase in ET-1 plasma levels in RP patients has been described in previous studies [5–7], but not confirmed by all researchers [40]. Different disease heterogeneity, stages of RP, race, sample size, and the method used for the ET-1 determination may justify contrasting results and different values reported in published data [7].

Currently, the exact mechanism why ET-1 levels are increased is not completely elucidated, but possible explanations may be formulated. Whether ET-1 is mainly produced by vascular endothelial cells, also several kinds of cells may synthetize and secrete ET-1 when they are under stress conditions, such as hypoxia and oxidative stress, and interestingly, it has been widely suggested that oxidative stress is a typical finding in RP and possibly contributes to its pathogenesis [41].

On the other hand, some authors have hypothesised a primary vascular dysregulation syndrome [42, 43] that might be the cause for the observed findings in blood flow reduction and increase in ET-1 and could explain all the signs and symptoms both in eye and in the body of RP patients. Indeed, Cellini and coworkers demonstrated, by using laser Doppler flowmetry, that blood flow abnormality in RP patients was not confined to the eye but also occurred in the peripheric circulatory system [5]. Thus, the observed increase of ET-1 plasma level might be secondary to vascular dysfunction and/or subclinical systemic inflammation.

Notably, we reported a negative association between choroidal thickness and ET-1 ($r = -0.702$; $P < 0.023$) and hypothesize that the reduction of choroidal thickness may be determined by the vasoconstrictive effect of ET-1, which may lead to vasospasms and unstable ocular blood supply, by altering the regulation of choroidal perfusion with a resulting relative ischemia.

There was also a significant positive correlation between aqueous flare and ET-1 plasmatic levels ($P < 0.007$) in RP patients. It is interesting to notice that RP subjects have an imbalance of the antioxidant-oxidant status in the peripheral blood [41] that leads to an increase in free radicals, chronic oxidative stress, and subclinical inflammation which may stimulate cells to secrete more ET-1, as in a vicious circle; on the other hand, increased ET-1 may, in turn, lead to vascular dysregulation and hypoxic stress with resulting activation of inflammatory pathways.

Independent of the cause of the ET-1 increase in the plasma, this increase has consequences on ocular blood impairment, and the thinned choroid reported in our patients may be a manifestation of this decreased flow.

In addition, choroidal thickness did not correlate with the extent of subclinical inflammation of the anterior chamber; this means that BAB breakdown does not directly influence the thinning of the choroid.

This study has some limitations. Firstly, the sample size was small because participants were accurately selected among young early stage RP patients, to limit confounding factors, such as age, systemic diseases, and different stages of RP, which could affect plasmatic ET-1 levels. Secondly, we did not evaluate intraocular ET-1 concentration for obvious ethical reasons. Thirdly, the retrospective nature of this study represents another limitation. Finally, we have no data on the systemic inflammatory status of the affected patients to strengthen our results. Larger evaluation of RP patients to investigate the correlation between vascular dysregulation and inflammation will help shed further light on the key role of these elements in RP.

5. Conclusions

To our knowledge, this is the first study that demonstrates a correlation between ocular inflammation and ET-1 plasma levels in early stage RP patients. This means that increased ET-1 plasma levels and subclinical inflammation may interact to play a key role in the impairment of choroidal blood flow, supply, and thickness which lead to an increase in free radicals and chronic oxidative stress.

Although our results require further confirmation and investigation, this study might provide reasonable data about the possibility to use antagonists of ET-1 and anti-inflammatory molecules together with antioxidants with the purpose of improving the ocular blood flow to ameliorate microvascular function and reduce the progression of the disease.

Conflict of Interests

The authors have no conflict of interests to disclose.

References

[1] Z.-Y. Li, D. E. Possin, and A. H. Milam, "Histopathology of bone spicule pigmentation in retinitis pigmentosa," *Ophthalmology*, vol. 102, no. 5, pp. 805–816, 1995.

[2] M. Cellini, R. Lodi, G. L. Possati, M. Sbrocca, D. Pelle, and N. Giubilei, "Color doppler ultrasonography in *Retinitis pigmentosa*. Preliminary study," *Journal Français d'Ophtalmologie*, vol. 20, no. 9, pp. 659–663, 1997.

[3] J. E. Grunwald, A. M. Maguire, and J. Dupont, "Retinal hemodynamics in retinitis pigmentosa," *The American Journal of Ophthalmology*, vol. 122, no. 4, pp. 502–508, 1996.

[4] M. E. Langham and T. Kramer, "Decreased choroidal blood flow associated with retinitis pigmentosa," *Eye*, vol. 4, no. 2, pp. 374–381, 1990.

[5] M. Cellini, E. Strobbe, C. Gizzi, and E. C. Campos, "ET-1 plasma levels and ocular blood flow in retinitis pigmentosa," *Canadian Journal of Physiology and Pharmacology*, vol. 88, no. 6, pp. 630–635, 2010.

[6] M. Cellini, L. Santiago, P. Versura, and R. Caramazza, "Plasma levels of endothelin-1 in retinitis pigmentosa," *Ophthalmologica*, vol. 216, no. 4, pp. 265–268, 2002.

[7] E. M. Vingolo, S. Lupo, P. L. Grenga et al., "Endothelin-1 plasma concentrations in patients with retinitis pigmentosa," *Regulatory Peptides*, vol. 160, no. 1–3, pp. 64–67, 2010.

[8] K. Polak, V. Petternel, A. Luksch et al., "Effect of endothelin and BQ123 on ocular blood flow parameters in healthy subjects," *Investigative Ophthalmology and Visual Science*, vol. 42, no. 12, pp. 2949–2956, 2001.

[9] K. Polak, A. Luksch, B. Frank, K. Jandrasits, E. Polska, and L. Schmetterer, "Regulation of human retinal blood flow by endothelin-1," *Experimental Eye Research*, vol. 76, no. 5, pp. 633–640, 2003.

[10] A. Finzi, M. Cellini, E. Strobbe, and E. C. Campos, "ET-1 plasma levels, choroidal thickness and multifocal electroretinogram in retinitis pigmentosa," *Life Sciences*, 2014.

[11] R. C. Pruett, "Retinitis pigmentosa: clinical observations and correlations," *Transactions of the American Ophthalmological Society*, vol. 81, pp. 693–735, 1983.

[12] G. A. Fishman, J. Cunha-Vaz, and T. Salzano, "Vitreous fluorophotometry in patients with retinitis pigmentosa," *Archives of Ophthalmology*, vol. 99, no. 7, pp. 1202–1207, 1981.

[13] Y. Ogura, J. G. Cunha-Vaz, and R. C. Zeimer, "Evaluation of vitreous body integrity in retinitis pigmentosa by vitreous fluorophotometry," *Archives of Ophthalmology*, vol. 105, no. 4, pp. 517–519, 1987.

[14] M. Küchle, N. X. Nguyen, P. Martus, K. Freissler, and R. Schalnus, "Aqueous flare in retinitis pigmentosa," *Graefe's Archive for Clinical and Experimental Ophthalmology*, vol. 236, no. 6, pp. 426–433, 1998.

[15] C. Hamel, "Retinitis pigmentosa," *Orphanet Journal of Rare Diseases*, vol. 1, p. 40, 2006.

[16] M. F. Marmor, A. B. Fulton, G. E. Holder, Y. Miyake, M. Brigell, and M. Bach, "ISCEV Standard for full-field clinical electroretinography (2008 update)," *Documenta Ophthalmologica*, vol. 118, no. 1, pp. 69–77, 2009.

[17] M. Wojtkowski, V. Srinivasan, J. G. Fujimoto et al., "Three-dimensional retinal imaging with high-speed ultrahigh-resolution optical coherence tomography," *Ophthalmology*, vol. 112, no. 10, pp. 1734–1746, 2005.

[18] R. F. Spaide, H. Koizumi, and M. C. Pozonni, "Enhanced depth imaging spectral-domain optical coherence tomography," *American Journal of Ophthalmology*, vol. 146, no. 4, pp. 496–500, 2008.

[19] R. Margolis and R. F. Spaide, "A pilot study of enhanced depth imaging optical coherence tomography of the choroid in normal eyes," *The American Journal of Ophthalmology*, vol. 147, no. 5, pp. 811–815, 2009.

[20] M. Sawa, Y. Tsurimaki, T. Tsuru, and H. Shimizu, "New quantitative method to determine protein concentration and cell number in aqueous in vivo," *Japanese Journal of Ophthalmology*, vol. 32, no. 2, pp. 132–142, 1988.

[21] J. G. Ladas, N. C. Wheeler, P. J. Morhun, S. O. Rimmer, and G. N. Holland, "Laser flare-cell photometry: methodology and clinical applications," *Survey of Ophthalmology*, vol. 50, no. 1, pp. 27–47, 2005.

[22] S. M. Shah, D. J. Spalton, and J. C. Taylor, "Correlations between laser flare measurements and anterior chamber protein concentrations," *Investigative Ophthalmology & Visual Science*, vol. 33, no. 10, pp. 2878–2884, 1992.

[23] T. Yoshitomi, A. S. Wong, E. Daher, and M. L. Sears, "Aqueous flare measurement with laser flare-cell meter," *Japanese Journal of Ophthalmology*, vol. 34, no. 1, pp. 57–62, 1990.

[24] N. Yoshida, Y. Ikeda, Y. Murakami et al., "Relationship between aqueous flare and visual function in retinitis pigmentosa," *ARVO Investigative Ophthalmology & Visual Science*, vol. 55, E-Abstract 1411, 2014.

[25] J. R. Sparrow, C. A. Parish, M. Hashimoto, and K. Nakanishi, "A2E, a lipofuscin fluorophore, in human retinal pigmented epithelial cells in culture," *Investigative Ophthalmology and Visual Science*, vol. 40, no. 12, pp. 2988–2995, 1999.

[26] G. M. Holtkamp, A. Kijlstra, R. Peek, and A. F. de Vos, "Retinal pigment epithelium-immune system interactions: cytokine production and cytokine-induced changes," *Progress in Retinal and Eye Research*, vol. 20, no. 1, pp. 29–48, 2001.

[27] D. M. Maurice, "Protein dynamics in the eye studied with labelled proteins," *American Journal of Ophthalmology*, vol. 47, no. 1, pp. 361–368, 1959.

[28] D. M. Maurice, "Flow of water between aqueous and vitreous compartments in the rabbit eye," *American Journal of Physiology—Renal Fluid and Electrolyte Physiology*, vol. 252, no. 1, pp. F104–F108, 1987.

[29] S. A. Vinores, M. Kuchle, N. L. Derevjanik et al., "Blood-retinal barrier breakdown in retinitis pigmentosa: light and electron microscopic immunolocalization," *Histology and Histopathology*, vol. 10, no. 4, pp. 913–923, 1995.

[30] R. B. Caldwell and B. J. McLaughlin, "Permeability of retinal pigment epithelial cell junctions in the dystrophic rat retina," *Experimental Eye Research*, vol. 36, no. 3, pp. 415–427, 1983.

[31] D. S. Dhoot, S. Huo, A. Yuan et al., "Evaluation of choroidal thickness in retinitis pigmentosa using enhanced depth imaging optical coherence tomography," *British Journal of Ophthalmology*, vol. 97, no. 1, pp. 66–69, 2013.

[32] T. Neuhardt, C. A. May, C. Wilsch, M. Eichhorn, and E. Lütjen-Drecoll, "Morphological changes of retinal pigment epithelium and choroid in rd- mice," *Experimental Eye Research*, vol. 68, no. 1, pp. 75–83, 1999.

[33] G. E. Korte, V. Reppucci, and P. Henkind, "PRE destruction causes choriocapillary atrophy," *Investigative Ophthalmology & Visual Science*, vol. 25, no. 10, pp. 1135–1145, 1984.

[34] M. Saint-Geniez, T. Kurihara, E. Sekiyama, A. E. Maldonado, and P. A. D'Amore, "An essential role for RPE-derived soluble VEGF in the maintenance of the choriocapillaris," *Proceedings of the National Academy of Sciences of the United States of America*, vol. 106, no. 44, pp. 18751–18756, 2009.

[35] B. Falsini, G. M. Anselmi, D. Marangoni et al., "Subfoveal choroidal blood flow and central retinal function in retinitis pigmentosa," *Investigative Ophthalmology and Visual Science*, vol. 52, no. 2, pp. 1064–1069, 2011.

[36] N. Akyol, S. Kükner, U. Celiker, H. Koyu, and C. Lüleci, "Decreased retinal blood flow in retinitis pigmentosa," *Canadian Journal of Ophthalmology*, vol. 30, no. 1, pp. 28–32, 1995.

[37] L. Hyvarinen, A. E. Maumenee, T. George, and G. W. Weinstein, "Fluorescein angiography of the choriocapillaris," *The American Journal of Ophthalmology*, vol. 67, no. 5, pp. 653–666, 1969.

[38] A. E. Krill, D. Archer, and F. W. Newell, "Fluorescein angiography in retinitis pigmentosa," *American Journal of Ophthalmology*, vol. 69, no. 5, pp. 826–835, 1970.

[39] G. W. Weinstein, A. E. Maumenee, and L. Hyvarinen, "On the pathogenesis of retinitis pigmentosa.," *Ophthalmologica*, vol. 162, no. 2, pp. 82–97, 1971.

[40] H. Ohguro, Y. Mashima, and M. Nakazawa, "Low levels of plasma endothelin-1 in patients with retinitis pigmentosa," *Clinical Ophthalmology*, vol. 4, no. 1, pp. 569–573, 2010.

[41] C. M.-F. de la Cámara, D. Salom, M. D. Sequedo et al., "Altered antioxidant-oxidant status in the aqueous humor and peripheral blood of patients with retinitis pigmentosa," *PLoS ONE*, vol. 8, no. 9, Article ID e74223, 2013.

[42] J. Flammer, K. Konieczka, and A. J. Flammer, "The primary vascular dysregulation syndrome: implications for eye diseases," *The EPMA Journal*, vol. 4, article 14, 2013.

[43] K. Konieczka, A. J. Flammer, M. Todorova, P. Meyer, and J. Flammer, "Retinitis pigmentosa and ocular blood flow," *EPMA Journal*, vol. 3, no. 1, p. 17, 2012.

Hindawi Publishing Corporation
Journal of Ophthalmology
Volume 2015, Article ID 250812, 9 pages
http://dx.doi.org/10.1155/2015/250812

Review Article

Histone Deacetylases Inhibitors in the Treatment of Retinal Degenerative Diseases: Overview and Perspectives

Hua Zhang,[1] Xufeng Dai,[1] Yan Qi,[1] Ying He,[1] Wei Du,[2] and Ji-jing Pang[1,2]

[1]*Eye Hospital, School of Ophthalmology and Optometry, Wenzhou Medical University, Wenzhou, Zhejiang 325027, China*
[2]*Department of Ophthalmology, University of Florida, Gainesville, FL, USA*

Correspondence should be addressed to Ji-jing Pang; jpang@ufl.edu

Received 6 August 2014; Accepted 9 September 2014

Academic Editor: Xinhua Shu

Retinal degenerative diseases are one of the important refractory ophthalmic diseases, featured with apoptosis of photoreceptor cells. Histone acetylation and deacetylation can regulate chromosome assembly, gene transcription, and posttranslational modification, which are regulated by histone acetyltransferases (HATs) and histone deacetylases (HDACs), respectively. The histone deacetylase inhibitors (HDACis) have the ability to cause hyperacetylation of histone and nonhistone proteins, resulting in a variety of effects on cell proliferation, differentiation, anti-inflammation, and anti-apoptosis. Several HDACis have been approved for clinical trials to treat cancer. Studies have shown that HDACis have neuroprotective effects in nervous system damage. In this paper, we will summarize the neuroprotective effects of common HDACis in retinal degenerative diseases and make a prospect to the applications of HDACis in the treatment of retinal degenerative diseases in the future.

1. Introduction

A nucleosome is the fundamental unit of eukaryotic chromosomes, whereas the core of the nucleosome is composed of histones (H2A, H2B, H3, and H4). Histone acetylation and deacetylation can regulate the binding of DNA and transcription complexes and further regulate chromosome assembly, gene expression, mitosis, and posttranslational modification [1, 2]. Histone acetylation and deacetylation are regulated by histone acetyltransferases (HATs) and histone deacetylases (HDACs), respectively. HATs and HDACs can regulate the dynamic acetylation equilibrium of histone and nonhistone proteins and play an important role in cell proliferation, apoptosis, differentiation, angiogenesis, cancer treatment, neuroprotection, and anti-inflammatory effects [2, 3].

The histone deacetylase inhibitor (HDACi) can interfere with the deacetylase function of HDACs, improve the acetylation level of histone and nonhistone proteins, and regulate gene transcription. Clinically, HDACis are effective drugs in the treatment of a variety of cancers, such as pancreatic, ovarian, breast, colon, prostate, and thyroid cancer [4–9]. Large amounts of data have shown that HDACis also have important neuroprotective effects in the treatment of diseases of the nervous system [10–13]. HDACis are known to reduce apoptosis, increase cell survival, regulate the expression of various neurotrophic factors, and enhance anti-inflammatory responses [10, 11, 14–16]. Apoptosis of retinal photoreceptor cells is a main feature of retinal degenerative diseases [17, 18], and neurotrophic factors have positive protective effects on retinal degenerative diseases [19, 20]. Thus, HDACis may have therapeutic potentials for retinal degenerative diseases. In this paper, we will focus on the progress of studies on using HDACis in the prevention and treatment of retinal degeneration.

2. Histone Deacetylase

There are 18 HDACs in human, and they are divided into four different classes based on their homology to yeast protein RPD3, Hda1, Sir2, and HOS3 (Table 1) [3]. Classes I, II, and IV HDACs are Zn^{2+}-dependent and homologous to the yeast RPD3, Hda1, and HOS3, respectively, whereas Class

Table 1: Class, homology, catalytic subunit, compound, and localization of HDACs.

Class	Homology	Catalytic subunit	Compound	Localization	References
I	RPD3	Zn^{2+}	HDACs 1–3 and 8	Nucleus	[3, 21]
IIa	Hda1	Zn^{2+}	HDACs 4, 5, 7, and 9	Nucleus/cytoplasm	[3, 21]
IIb	Hda1	Zn^{2+}	HDACs 6 and 10	Mostly cytoplasm	[3, 21]
III	Sir2	NAD^{+}	SIRT1–7	Nucleus/cytoplasm	[3, 21]
IV	HOS3	Zn^{2+}	HDAC 11	Nucleus/cytoplasm	[3, 21]

Table 2: Class, common compound, HDAC target, and main functions of HDACis.

Class	Compound	HDAC target	Function	References
Hydroxamic acids	TsA	Classes I and II	A, D, GA, P, CP, R, NG, and AI	[21, 22, 41, 42, 88]
	SAHA	Classes I and II	A, CP, S, TR, and AI	[21, 67, 69, 70, 74]
	LBH589	Classes I and II	A, GA, TR, and P	[21, 33, 89]
	PXD101	Classes I and II	A, GA, and TR	[21, 33]
Cyclic peptides	FK228	Class I	A, GA, D, and TR	[21, 33, 90]
Benzamides	MS-275	HDACs 1, 2, and 3	A, D, S, and GA	[21, 77]
	MGCD0103	Class I	A, TR, AI, and GA	[21, 91, 92]
Aliphatic acids	VPA	Classes I and IIa	A, AI, TR, S, D, and GA	[10, 11, 21, 51]
	PBA	Classes I and IIa	A, D, and GA	[21, 93, 94]
	NaB	Classes I and IIa	A, D, GA, AI, TR, S, and NG	[11, 15, 21, 57]

A: cell apoptosis/death; AI: anti-inflammatory effect; TR: transcriptional regulation; NG: neurogenesis; S: cell survival; CP: cell-cycle progression; P: proliferation; R: regeneration; D: differentiation; GA: growth arrest.

III HDACs are NAD^{+}-dependent and homologous to yeast Sir2. Class I HDACs include HDACs 1, 2, 3, and 8, which are localized in the nucleus [21]. Class I HDACs can regulate neurogenesis, cell senescence, proliferation, differentiation, and embryonic development [22–25]. HDACs 4, 5, 6, 7, 9, and 10 make up Class II HDACs, which are localized both in nucleus and in cytoplasm. Class II HDACs consist of two subclasses: Class IIa (HDACs 4, 5, 7, and 9) and Class IIb (HDACs 6 and 10). Compared to Class I HDACs, Class II has more tissue-specific functions, such as cardiac, microtubule, and chondrocyte differentiation defects [26–28]. Class III HADCs consist of sirtuins (SIRT1–7), whereas Class IV contains only HDAC11 and relatively little is studied about this subtype [3, 21]. In this paper, we introduce mainly the progress of Class I and II HDACs inhibitors in the treatment of retinal degenerative diseases.

3. Histone Deacetylase Inhibitor

According to the different chemical structures, HDACis can be divided into four classes, which include hydroxamic acids, cyclic peptides, benzamides, and aliphatic acids [21, 29] (Table 2). Hydroxamic acids can inhibit Class I and Class II HDACs, which include trichostatin A (TSA), vorinostat (SAHA), panobinostat (LBH589), and belinostat (PXD101) [30–33]. Cyclic peptides, romidepsin (FK228), have the most complex structure. Benzamides include entinostat (MS-275) and mocetinostat (MGCD0103). Common aliphatic acids include valproic acid (VPA), sodium butyrate (NaB), and phenylbutyrate (PBA) [34]. HDACis can cause hyperacetylation of histone and nonhistone proteins and further regulate transcription process, cellular microenvironment, and immune responses [35]. HDACis have an important role in the inhibition of tumor cell proliferation and in the induction of cell differentiation [36–38]. Studies have shown that HDACis can promote the transcription of retinal photoreceptor genes by histone acetylation, resulting in effectively reversing the course of retinal photoreceptor cell degeneration [39–41]. Several HDACis have been approved for clinical trials, such as SAHA, FK228, Mgcd0103, LBH589, PXD-101, and MS-275 [35]. Currently, the studies of HDACis focus mainly on cancer therapy, cell differentiation, neuroprotection, and heterochromatin fields, and as yet, research has just started in retinal degeneration.

4. Trichostatin A

TsA is a hydroxamic acid, a Class I and II HDACi, which is the first natural hydroxamic acid found to inhibit HDACs, and is one of the most studied HDACis, especially in the retina [31]. TsA has an important role in the prevention and treatment of neurodegenerative conditions [12, 42]. TsA can regulate the levels of apoptosis-related proteins and improve neurological performance in the rat permanent middle cerebral artery occlusion (pMCAO) model of stoke [11] (Table 3).

TsA suppressed TNF-α expression and signaling in retina from rat ischemic injury and changed the level of acetylated histone 3 (AcH3) and the secretion of

Table 3: Function and molecular targets of common HDACis in nervous system diseases.

HDACi	Function	Molecular targets	References
TSA	A	Bcl-2 and apaf-1	[11]
	AI	IL-6, TNF-α, and NF-kappaB	[42]
	TR	HSP70, AcH3, AcH4, PI3K/Akt, BDNF, and NF-κB	[11]
VPA	A	Caspase 3 and HSP70	[10, 11, 51, 52]
	AI	OX-42, ED-1, and iNOS	[11]
	TR	HSP70, AcH3, pERK, bcl-2, pCREB, pAkt, bcl-xl, NF-κB, and JNK	[10, 11, 51, 52]
NaB	AI	OX-42, ED-1, and iNOS	[11]
	N	BDNF-TrkB	[16]
	A	Caspase 3 and HSP70	[11]
	TR	HSP70, AcH3, AcH4, Sp1, p21, and p27	[11, 67]

A: cell apoptosis/death; AI: anti-inflammatory effect; TR: transcriptional regulation; N: neurogenesis.

Table 4: Function and molecular targets of common HDACis in retinal degenerative diseases.

HDACi	Function	Molecular targets	References
TsA	CP	Wnt signaling and notch signaling	[22]
	P	Notch signaling, cyclinD1, CDK, and p-Rb	[22]
	A	Caspase 3, apaf-1, and PARP	[41, 49]
	R	RARβ and AcH3K9	[46]
	AI	TNF-α	[43]
	TR	AcH3, TNF-α, MMP-1, and MMP-3	[43]
VPA	A	Caspase 3, Caspase 12, apaf-1, HSP70, and cytochrome C	[14, 56, 58, 59]
	S	Caspase 3, CREB, and pERK1/2	[14, 56, 58, 59]
	TR	HSP70, AcH3, cytochrome C, GRP78, CHOP, TrkB, and pERK1/2	[14, 56, 58, 59]
NaB	A	BDNF-TrkB and AcH3K14	[58]
	S	AcH3 and AcH4	[57]
	TR	AcH3, AcH4, Akt, and Erk	[57]

A: cell apoptosis/death; AI: anti-inflammatory effect; TR: transcriptional regulation; S: cell survival; CP: cell-cycle progression; P: proliferation; R: regeneration.

matrix metalloproteinase-1 (MMP-1) and MMP-3 [43]. TsA also improved the electroretinography (ERG) responses in ischemic injury retina [43, 44]. In the zebrafish retina, TsA can regulate cell-cycle progression and neurogenesis by Wnt and notch signaling pathways [22]. TsA also regulates the apoptotic process by upregulating the expression of apoptotic protease activating factor-1 (apaf-1) and caspase 3 in the developing mouse retina [41]. TsA treatment attenuated the downregulation of *Fem1c*^{R3}gene expression, delayed the progressive damage, and reduced apoptosis to retinal ganglion cells (RGCs) in aged DBA/2J mice [45]. TsA induced axonal regeneration by inducting expression of AcH3 and retinoic acid receptor β (RARβ) in adult rat RGCs [46], which play an important role in development and differentiation [47]. In *in vitro* retinal explants of retinal degeneration 1 (*rd1*) mice, TsA treatment decreased the rate of cells apoptosis, enhanced the photoreceptor cell survival, and prevented photoreceptor degeneration by suppressing poly(ADP-ribose) polymerase (PARP) activity, which promoted cell death of *rd1* retina [39, 48, 49]. However, in retinal explants of normal mice, TsA inhibited the expression of pro-rod transcription factors Otx2, Nrl, and Crx and the development of rod photoreceptor cells [40], which had the opposite effect compared with retinal degeneration mice. TsA treatment inhibited the proliferation and the TGF-β2-induced epithelial-mesenchymal transition (EMT) pathway by downregulating TGF-β/Akt, MAPK, ERK1/2, and notch signaling pathways in human retinal pigment epithelial (RPE) cells. This may have a clinical value in the prevention and treatment of proliferative vitreoretinopathy (PVR) [50] (Table 4).

5. Valproic Acid

As a short chain fatty acid, VPA is a broad-spectrum HDACi and is currently used widely as an anticonvulsant drug. Many studies have shown that VPA has neuroprotective effects against the damage of central nervous system (Table 3). VPA has been shown to reduce brain damage in a rat transient focal cerebral ischemia model and to improve functional outcome by reducing caspase 3 activation and increasing heat-shock protein 70 (Hsp70) levels [10]. In a rat pMCAO stoke model, VPA increased the anti-inflammatory effect by inhibiting inducible nitric-oxide synthase (iNOS) and OX-42, regulated the levels of apoptosis-related proteins, and improved neurological performance [11]. In rat intracerebral hemorrhage (ICH) model, VPA reduced perihematomal cell death and activities of caspases 3, 8, and 9 and alleviated inflammation by regulating transcriptional activation [51]. Under hypoxic conditions, VPA treatment prevented neuron apoptosis, increased levels of AcH3, activated NF-κB, and reduced JNK activation in the primary rat hippocampal and cortical cultures *in vitro* [52].

VPA has also an important role in protecting the RGCs (Table 4). In a rat ischemia/reperfusion (I/R) model, VPA prevented axon damage of RGCs [14, 53]. After I/R damage, VPA attenuated retinal neuron apoptosis by inhibiting the activation of caspase 3, upregulation of apaf-1, and release of cytochrome C. At the transcriptional level, VPA upregulated the expression of Hsp70 and enhanced acetylation of histone H3 and Hsp70 promoter [14]. VPA treatment prevented significantly the retinal histological damage and the loss of RGCs by reducing endoplasmic reticulum (ER) stress-induced apoptosis. VPA decreased the expression of C/EBP homologous protein (CHOP) and caspase 12 [53]. CHOP is a transcription factor involved in ER stress-induced apoptosis [54], whereas caspase 12 is a proapoptotic factor activated by ER stress [55]. After optic nerve crush (ONC) in rat, VPA has a neuroprotective effect by increasing RGCs survival and expression of pERK1/2, inhibiting caspase 3 activity, and inducing the DNA binding of cAMP response element binding protein (CREB) in the injured RGCs [56]. In purified rat RGCs, VPA enhanced cell survival and delayed spontaneous cell death [57]. In a rat model of ONC, VPA treatment can inhibit apoptosis of RGCs via the activation of brain-derived neurotrophic factor (BDNF) and tropomyosin-related kinase B (TrkB) signaling [58]. VPA can induce expression of HSP70 and attenuate the photoreceptor cell death induced by N-methyl-N-nitrosourea in mice [59]. In clinical trials of retinitis pigmentosa (RP), VPA may reduce the loss of photoreceptor cells. VPA has an effective therapeutic potential for RP, but efficacy and safety of VPA in the treatment of RP need to be assessed by further clinical trials [60].

6. Sodium Butyrate

Sodium butyrate (NaB) is a short chain fatty acid, which can increase histone acetylation levels, inhibit tumor cell proliferation, and promote tumor cell senescence and apoptosis [61–64]. NaB is widely used as an animal feed additive [65] and plays also an important role in the prevention and treatment of neurodegenerative conditions [12, 13] (Table 3). It has anti-inflammatory effects in rat brain-derived primary microglia cells [66]. In the ischemic brain of pMCAO rat, NaB stimulated neurogenesis and induced cell proliferation, migration, and differentiation by BDNF-TrkB signaling [15]. Like VPA, NaB also has anti-inflammatory effects and neuroprotective effects in the rat pMCAO stroke model [11]. NaB can induce the activation of BDNF promoter IV in the rat cortical neurons *in vitro* [16]. NaB can regulate G1-to-S cell cycle progression by cyclin-dependant kinase (cdk) inhibitors p21 and p27 in adult mouse neural stem cells (NSCs) [67].

In vitro, NaB can delay spontaneous cell death, enhance cell survival in purified rat RGCs, and increase levels of AcH3 and AcH4 [57]; it can also increase the level of AcH3 and induce morphological changes in Y79 cells, a retinoblastoma cell line [68]. After NaB treatment, original round morphology of Y79 cells changed into spindle or irregular morphology. After ONC injury in rat, NaB can promote survival of RGCs, increase ERG responses, upregulate phosphorylation of Akt and Erk, and increase hyperacetylation of histone H3K14 [58] (Table 4).

7. Other HDACis

SAHA, a hydroxamic acid derivative, is the first HDACi drug approved by the Food and Drug Administration (FDA) for the treatment of cancer in the United States [21]. In clinical trials, SAHA has been used to treat cutaneous T-cell lymphoma. Many studies have also shown that SAHA has neuroprotective effects [69–72]. Like NaB, SAHA can also regulate cell cycle progression by p21 and p27 in adult mouse NSCs [67] and SAHA also has a good protective effect in corneal haze and injury [73, 74]. SAHA can induce caspase-dependent apoptosis and reduce cell survival in human retinoblastoma (RB) cells [75, 76]. MS-275, a synthetic benzamide derivative, which selectively inhibits HDACs 1, 2, and 3, is also a HDACi drug used in cancer treatment in clinical trials. Ms-275 can protect RGCs differentiation and survival following optic nerve injury in Thy-1 CFP mice [77].

8. Discussion

Retinal degenerative diseases, such as RP, Leber congenital amaurosis (LCA2), achromatopsia, juvenile macular degeneration, and cone-rod dystrophy, are the major blinding fundus diseases, and the pathogenesis of these diseases is very complex. Apoptosis of photoreceptor cells is a common feature of retinal degeneration, and a variety of stimuli, such as tumor necrosis factor (TNF), Fas ligands (FasL), mitochondria, and ER stress, can lead to cell death. These stimuli can cause caspase cascade, activate firstly the initiator caspases (caspase 8, 9, 10, and 12), further activate downstream effector caspases (caspase 3, 6, and 7), and lead to apoptotic cell death [55], whereas antiapoptotic HSP70, B-cell lymphoma-2 (Bcl-2), and B-cell lymphoma-extra large (Bcl-xL) can inhibit this caspase cascade [11, 55]. HDACis can upregulate the expression of antiapoptotic HSP70 and Bcl-2 and downregulate the expression of proinflammatory TNF-α [11, 78, 79]. In retinal diseases, studies showed that HDACis treatment upregulated the expression of Hsp70, downregulated the expression of apaf-1 and caspase 3, inhibited the translocation of cytochrome C and activation of Akt and Erk, increased the rate of cell survival, and decreased the apoptosis process [14, 49, 58]. Akt and Erk signaling can inhibit apoptosis by preventing cytochrome C release [55]. VPA, NaB, and TsA regulate the activation of Akt and Erk signaling and further regulate the apoptosis process [50, 58].

Some factors, such as growth factors and cytokines, can activate PI3K/Akt, PKC, and Erk signaling, prevent the expression of antiapoptotic glycogen synthase kinase-3 (GSK-3), forkhead in rhabdomyosarcoma (FKHR), Bcl-2 antagonist of cell death (Bad), and Bcl-xL, and increase cell survival [55]. Neurotrophic factors also regulate the apoptosis of photoreceptor cells in the development of the visual system [55]. Ciliary neurotrophic factor (CNTF) can control photoreceptor differentiation in rat retina [80]. HDACis, VPA, NaB, and TSA increased the expression of glial cell

line-derived neurotrophic factor (GDNF) and BDNF in the rat astrocytes [81]. In *rd1* retinal explants, BDNF and CNTF activate the Erk, Akt, and CREB pathways to decrease the apoptosis of photoreceptor cells [82]. After ONC in rat, HDACis activate BDNF-TrkB signaling, upregulate the level of antiapoptotic Bcl-2, and downregulate the activation of caspase 3 [58]. These data suggest that HDACis have the potential to alter gene expression of neurotrophic factors and further regulate the apoptosis of photoreceptor cells in the retina.

Gene regulation is also an important function of HDACis in retinal degenerative diseases. Since the acetylation/deacetylation of histone and nonhistone proteins has extensive effects on gene regulation, upregulation of acetylation caused by HDACis would likely lead to significantly altered transcription of genes related to retinal degeneration. HDACis have been shown to inhibit the expression of FasL and proinflammatory cytokine interleukin-6 (IL-6), increase the acetylation of histone H3, activate the transcription of downstream genes Akt, Erk, CREB, and HSP70, and thus unregulated the levels of antiapoptotic proteins Bcl-2 and Bcl-xL, and eventually lead to the downregulation of caspase 3 [11, 51]. In retinal degenerative diseases, HDACis treatment can induce acetylation of histone H3, regulate Akt, Erk, CREB, and TrkB signaling, and further inhibit the activity of caspase 3 [14, 56, 58]. HDACis also can regulate the expression of neurotrophic factors [58].

Several factors can lead to the death of photoreceptor cells. In addition to spontaneous apoptosis and retinal degeneration, certain ocular adverse events, such as surgery and gene therapy, can also lead to the loss of photoreceptor cells. Gene therapy has broad application prospects and has achieved great success in the treatment of LCA2 [83]. It has been reported that gene therapy can restore visual function in animal models and clinical trials; but apoptosis of remaining photoreceptor cells could progress slowly and continuously in treated areas, and the restored visual function by gene therapy gradually weakens [83–86]. In addition to retinal detachment caused by subretinal injections and the release of toxic substances around the treated areas, continued photoreceptor loss is also related to photoreceptor cells having begun the irreversible apoptosis process before treatment [84, 87]. It is important to correct the negative effects of gene therapy that appeared in the ongoing clinical trial, and HDACis may be a good option. Considering the fact that HDACis can prevent death of photoreceptor cells and protect retinal damage, we hypothesize that HDACis may play a role in preventing the continuing death of photoreceptor cells after gene therapy and are conducting these experiments.

In this paper, we summarized the neuroprotective effects of common HDACis in retinal degenerative diseases (Figure 1). Currently, clinical trials of VPA in RP have been carried out. As in-depth studies of HDACis, more and more molecular mechanisms of HDACis on neuroprotective effects will be found in retinal degenerative diseases. HDACis can inhibit the apoptosis of photoreceptor cells during retinal damage process; therefore, HDACis may be a group of promising agents to be explored in the prevention of apoptosis of photoreceptors and in the treatment of retinal degenerative diseases.

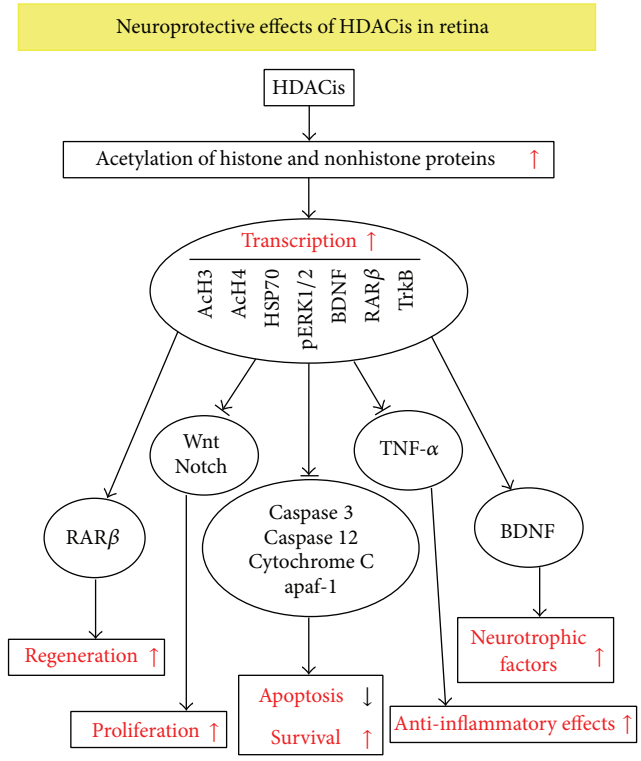

Figure 1: Possible mechanisms of HDACis in the prevention of retinal degenerative diseases. HDACis acetylate histone and nonhistone proteins, such as AcH3, AcH4, and HSP70, regulate transcription process. HDACis promote cell regeneration and proliferation, improve cell survival, enhance anti-inflammatory effects, attenuate cell apoptosis, and upregulate the expression of neurotrophic factors.

Conflict of Interests

All authors declare no potential conflict of interests related to this paper.

Authors' Contribution

Hua Zhang and Xufeng Dai contributed equally to the work presented here and should therefore be regarded as equivalent authors.

Acknowledgments

This work was supported by the National Natural Science Foundation of China (81371060), a retinal gene therapy study grant from Wenzhou Medical University, Wenzhou, China (QTJ11018), the scientific research foundation from Eye Hospital, School of Ophthalmology and Optometry, Wenzhou Medical University (KYQD130501), and the Jiangsu Province Foundation for Innovative Research Team and National Institutes of Health (NIH) grant (EY023543).

References

[1] C. Huang, E. A. Sloan, and C. F. Boerkoel, "Chromatin remodeling and human disease," *Current Opinion in Genetics and Development*, vol. 13, no. 3, pp. 246–252, 2003.

[2] C. Simone and A. Peserico, "Physical and functional HAT/HDAC interplay regulates protein acetylation balance," *Journal of Biomedicine and Biotechnology*, vol. 2011, Article ID 371832, 10 pages, 2011.

[3] G. Giannini, W. Cabri, C. Fattorusso, and M. Rodriquez, "Histone deacetylase inhibitors in the treatment of cancer: overview and perspectives," *Future Medicinal Chemistry*, vol. 4, no. 11, pp. 1439–1460, 2012.

[4] M.-J. Chuang, S.-T. Wu, S.-H. Tang et al., "The HDAC inhibitor LBH589 induces ERK-dependent prometaphase arrest in prostate cancer via HDAC6 inactivation and down-regulation," *PLoS ONE*, vol. 8, no. 9, Article ID e73401, 2013.

[5] W. Feng, B. Zhang, D. Cai, and X. Zou, "Therapeutic potential of histone deacetylase inhibitors in pancreatic cancer," *Cancer Letters*, vol. 347, no. 2, pp. 183–190, 2014.

[6] D. Khabele, "The therapeutic potential of class I selective histone deacetylase inhibitors in ovarian cancer," *Frontiers in Oncology*, vol. 4, article 111, 2014.

[7] M. A. Salvador, J. Wicinski, O. Cabaud et al., "The histone deacetylase inhibitor abexinostat induces cancer stem cells differentiation in breast cancer with low Xist expression," *Clinical Cancer Research*, vol. 19, no. 23, pp. 6520–6531, 2013.

[8] J. M. Mariadason, "HDACs and HDAC inhibitors in colon cancer," *Epigenetics*, vol. 3, no. 1, pp. 28–37, 2008.

[9] D. Russo, C. Durante, S. Bulotta et al., "Targeting histone deacetylase in thyroid cancer," *Expert Opinion on Therapeutic Targets*, vol. 17, no. 2, pp. 179–193, 2013.

[10] M. Ren, Y. Leng, M. Jeong, P. R. Leeds, and D.-M. Chuang, "Valproic acid reduces brain damage induced by transient focal cerebral ischemia in rats: potential roles of histone deacetylase inhibition and heat shock protein induction," *Journal of Neurochemistry*, vol. 89, no. 6, pp. 1358–1367, 2004.

[11] J. K. Hyeon, M. Rowe, M. Ren, J. S. Hong, P. S. Chen, and D. M. Chuang, "Histone deacetylase inhibitors exhibit anti-inflammatory and neuroprotective effects in a rat permanent ischemic model of stroke: multiple mechanisms of action," *Journal of Pharmacology and Experimental Therapeutics*, vol. 321, no. 3, pp. 892–901, 2007.

[12] D.-M. Chuang, Y. Leng, Z. Marinova, H.-J. Kim, and C.-T. Chiu, "Multiple roles of HDAC inhibition in neurodegenerative conditions," *Trends in Neurosciences*, vol. 32, no. 11, pp. 591–601, 2009.

[13] R. J. Ferrante, J. K. Kubilus, J. Lee et al., "Histone deacetylase inhibition by sodium butyrate chemotherapy ameliorates the neurodegenerative phenotype in Huntington's disease mice," *The Journal of Neuroscience*, vol. 23, no. 28, pp. 9418–9427, 2003.

[14] Z. Zhang, X. Qin, N. Tong et al., "Valproic acid-mediated neuroprotection in retinal ischemia injury via histone deacetylase inhibition and transcriptional activation," *Experimental Eye Research*, vol. 94, no. 1, pp. 98–108, 2012.

[15] H. J. Kim, P. Leeds, and D.-M. Chuang, "The HDAC inhibitor, sodium butyrate, stimulates neurogenesis in the ischemic brain," *Journal of Neurochemistry*, vol. 110, no. 4, pp. 1226–1240, 2009.

[16] S. Yasuda, M.-H. Liang, Z. Marinova, A. Yahyavi, and D.-M. Chuang, "The mood stabilizers lithium and valproate selectively activate the promoter IV of brain-derived neurotrophic factor in neurons," *Molecular Psychiatry*, vol. 14, no. 1, pp. 51–59, 2009.

[17] V. Marigo, "Programmed cell death in retinal degeneration: targeting apoptosis in photoreceptors as potential therapy for retinal degeneration," *Cell Cycle*, vol. 6, no. 6, pp. 652–655, 2007.

[18] J. Sancho-Pelluz, B. Arango-Gonzalez, S. Kustermann et al., "Photoreceptor cell death mechanisms in inherited retinal degeneration," *Molecular Neurobiology*, vol. 38, no. 3, pp. 253–269, 2008.

[19] M. M. LaVail, D. Yasumura, M. T. Matthes et al., "Protection of mouse photoreceptors by survival factors in retinal degenerations," *Investigative Ophthalmology & Visual Science*, vol. 39, no. 3, pp. 592–602, 1998.

[20] M. Frasson, S. Picaud, T. Léveillard et al., "Glial cell line-derived neurotrophic factor induces histologic and functional protection of rod photoreceptors in the rd/rd mouse," *Investigative Ophthalmology and Visual Science*, vol. 40, no. 11, pp. 2724–2734, 1999.

[21] M. Dokmanovic, C. Clarke, and P. A. Marks, "Histone deacetylase inhibitors: overview and perspectives," *Molecular Cancer Research*, vol. 5, no. 10, pp. 981–989, 2007.

[22] M. Yamaguchi, N. Tonou-Fujimori, A. Komori et al., "Histone deacetylase 1 regulates retinal neurogenesis in zebrafish by suppressing Wnt ad Notch signaling pathways," *Development*, vol. 132, no. 13, pp. 3027–3043, 2005.

[23] G. Lagger, D. O'Carroll, M. Rembold et al., "Essential function of histone deacetylase 1 in proliferation control and CDK inhibitor repression," *The EMBO Journal*, vol. 21, no. 11, pp. 2672–2681, 2002.

[24] D. Bandyopadhyay, J. L. Curry, Q. Lin et al., "Dynamic assembly of chromatin complexes during cellular senescence: Implications for the growth arrest of human melanocytic nevi," *Aging Cell*, vol. 6, no. 4, pp. 577–591, 2007.

[25] R. Brunmeir, S. Lagger, and C. Seiser, "Histone deacetylase 1 and 2-controlled embryonic development and cell differentiation," *International Journal of Developmental Biology*, vol. 53, no. 2-3, pp. 275–289, 2009.

[26] C. L. Zhang, T. A. McKinsey, S. Chang, C. L. Antos, J. A. Hill, and E. N. Olson, "Class II histone deacetylases act as signal-responsive repressors of cardiac hypertrophy," *Cell*, vol. 110, no. 4, pp. 479–488, 2002.

[27] Y. Xiong, K. Zhao, J. Wu, Z. Xu, S. Jin, and Y. Q. Zhang, "HDAC6 mutations rescue human tau-induced microtubule defects in Drosophila," *Proceedings of the National Academy of Sciences of the United States of America*, vol. 110, no. 12, pp. 4604–4609, 2013.

[28] R. B. Vega, K. Matsuda, J. Oh et al., "Histone deacetylase 4 controls chondrocyte hypertrophy during skeletogenesis," *Cell*, vol. 119, no. 4, pp. 555–566, 2004.

[29] I. Koutsounas, C. Giaginis, E. Patsouris, and S. Theocharis, "Current evidence for histone deacetylase inhibitors in pancreatic cancer," *World Journal of Gastroenterology*, vol. 19, no. 6, pp. 813–828, 2013.

[30] M. Yoshida, M. Kijima, M. Akita, and T. Beppu, "Potent and specific inhibition of mammalian histone deacetylase both in vivo and in vitro by trichostatin A," *Journal of Biological Chemistry*, vol. 265, no. 28, pp. 17174–17179, 1990.

[31] M. Rahman, A. Kukita, T. Kukita, T. Shobuike, T. Nakamura, and O. Kohashi, "Two histone deacetylase inhibitors, trichostatin A and sodium butyrate, suppress differentiation into osteoclasts but not into macrophages," *Blood*, vol. 101, no. 9, pp. 3451–3459, 2003.

[32] S. Belvedere, D. J. Witter, J. Yan, J. P. Secrist, V. Richon, and T. A. Miller, "Aminosuberoyl hydroxamic acids (ASHAs): a potent new class of HDAC inhibitors," *Bioorganic and Medicinal Chemistry Letters*, vol. 17, no. 14, pp. 3969–3971, 2007.

[33] S. K. Ghosh, S. P. Perrine, R. M. Williams, and D. V. Faller, "Histone deacetylase inhibitors are potent inducers of gene expression in latent EBV and sensitize lymphoma cells to nucleoside antiviral agents," *Blood*, vol. 119, no. 4, pp. 1008–1017, 2012.

[34] W. K. Rasheed, R. W. Johnstone, and H. M. Prince, "Histone deacetylase inhibitors in cancer therapy," *Expert Opinion on Investigational Drugs*, vol. 16, no. 5, pp. 659–678, 2007.

[35] H. M. Prince, M. J. Bishton, and S. J. Harrison, "Clinical studies of histone deacetylase inhibitors," *Clinical Cancer Research*, vol. 15, no. 12, pp. 3958–3969, 2009.

[36] P. A. Marks, "The clinical development of histone deacetylase inhibitors as targeted anticancer drugs," *Expert Opinion on Investigational Drugs*, vol. 19, no. 9, pp. 1049–1066, 2010.

[37] R. R. Rosato and S. Grant, "Histone deacetylase inhibitors in clinical development," *Expert Opinion on Investigational Drugs*, vol. 13, no. 1, pp. 21–38, 2004.

[38] A. Kretsovali, C. Hadjimichael, and N. Charmpilas, "Histone deacetylase inhibitors in cell pluripotency, differentiation, and reprogramming," *Stem Cells International*, vol. 2012, Article ID 184154, 10 pages, 2012.

[39] J. Sancho-Pelluz, M. V. Alavi, A. Sahaboglu et al., "Excessive HDAC activation is critical for neurodegeneration in the *rd1* mouse," *Cell Death and Disease*, vol. 1, no. 2, article e24, 2010.

[40] B. Chen and C. L. Cepko, "Requirement of histone deacetylase activity for the expression of critical photoreceptor genes," *BMC Developmental Biology*, vol. 7, article 78, 2007.

[41] D. M. Wallace, M. Donovan, and T. G. Cotter, "Histone deacetylase activity regulates Apaf-1 and caspase 3 expression in the developing mouse retina," *Investigative Ophthalmology and Visual Science*, vol. 47, no. 7, pp. 2765–2772, 2006.

[42] F. Niu, X. Zhang, L. Chang et al., "Trichostatin A enhances OGD-astrocyte viability by inhibiting inflammatory reaction mediated by NF-κB," *Brain Research Bulletin*, vol. 78, no. 6, pp. 342–346, 2009.

[43] C. E. Crosson, S. K. Mani, S. Husain, O. Alsarraf, and D. R. Menick, "Inhibition of histone deacetylase protects the retina from ischemic injury," *Investigative Ophthalmology and Visual Science*, vol. 51, no. 7, pp. 3639–3645, 2010.

[44] J. Fan, O. Alsarraf, M. Dahrouj et al., "Inhibition of HDAC2 protects the retina from ischemic injury," *Investigative Ophthalmology and Visual Science*, vol. 54, no. 6, pp. 4072–4080, 2013.

[45] H. R. Pelzel, C. L. Schlamp, M. Waclawski, M. K. Shaw, and R. W. Nickells, "Silencing of Fem1cR3 gene expression in the DBA/2J mouse precedes retinal ganglion cell death and is associated with histone deacetylase activity," *Investigative Ophthalmology and Visual Science*, vol. 53, no. 3, pp. 1428–1435, 2012.

[46] Y. Koriyama, K. Sugitani, K. Ogai, and S. Kato, "Neuritogenic activity of trichostatin a in adult rat retinal ganglion cells through acetylation of histone H3 lysine 9 and RARβ induction," *Journal of Pharmacological Sciences*, vol. 124, no. 1, pp. 112–116, 2014.

[47] Y. Koriyama, Y. Takagi, K. Chiba et al., "Requirement of retinoic acid receptor β for genipin derivative-induced optic nerve regeneration in adult rat retina," *PLoS ONE*, vol. 8, Article ID e71252, 2013.

[48] F. Paquet-Durand, J. Silva, T. Talukdar et al., "Excessive activation of poly(ADP-ribose) polymerase contributes to inherited photoreceptor degeneration in the retinal degeneration 1 mouse," *Journal of Neuroscience*, vol. 27, no. 38, pp. 10311–10319, 2007.

[49] J. Sancho-Pelluz and F. Paquet-Durand, "HDAC inhibition prevents Rd1 mouse photoreceptor degeneration," *Advances in Experimental Medicine and Biology*, vol. 723, pp. 107–113, 2012.

[50] W. Xiao, X. Chen, X. Liu, L. Luo, S. Ye, and Y. Liu, "Trichostatin A, a histone deacetylase inhibitor, suppresses proliferation and epithelial-mesenchymal transition in retinal pigment epithelium cells," *Journal of Cellular and Molecular Medicine*, vol. 18, no. 4, pp. 646–655, 2014.

[51] D.-I. Sinn, S.-J. Kim, K. Chu et al., "Valproic acid-mediated neuroprotection in intracerebral hemorrhage via histone deacetylase inhibition and transcriptional activation," *Neurobiology of Disease*, vol. 26, no. 2, pp. 464–472, 2007.

[52] Y. Li, Z. Yuan, B. Liu et al., "Prevention of hypoxia-induced neuronal apoptosis through histone deacetylase inhibition," *Journal of Trauma—Injury, Infection and Critical Care*, vol. 64, no. 4, pp. 863–870, 2008.

[53] Z. Zhang, N. Tong, Y. Gong et al., "Valproate protects the retina from endoplasmic reticulum stress-induced apoptosis after ischemia-reperfusion injury," *Neuroscience Letters*, vol. 504, no. 2, pp. 88–92, 2011.

[54] M. Shimazawa, Y. Inokuchi, Y. Ito et al., "Involvement of ER stress in retinal cell death," *Molecular Vision*, vol. 13, pp. 578–587, 2007.

[55] E. Vecino, M. Hernández, and M. García, "Cell death in the developing vertebrate retina," *International Journal of Developmental Biology*, vol. 48, no. 8-9, pp. 965–974, 2004.

[56] J. Biermann, P. Grieshaber, U. Goebel et al., "Valproic acid-mediated neuroprotection and regeneration in injured retinal ganglion cells," *Investigative Ophthalmology & Visual Science*, vol. 51, no. 1, pp. 526–534, 2010.

[57] J. Biermann, J. Boyle, A. Pielen, and W. A. Lagrèze, "Histone deacetylase inhibitors sodium butyrate and valproic acid delay spontaneous cell death in purified rat retinal ganglion cells," *Molecular Vision*, vol. 17, pp. 395–403, 2011.

[58] Z. Z. Zhang, Y. Y. Gong, Y. H. Shi, W. Zhang, X. H. Qin, and X. W. Wu, "Valproate promotes survival of retinal ganglion cells in a rat model of optic nerve crush," *Neuroscience*, vol. 224, pp. 282–293, 2012.

[59] Y. Koriyama, K. Sugitani, K. Ogai et al., "Heat shock protein 70 induction by valproic acid delays photoreceptor cell death by N-methyl-N-nitrosourea in mice," *Journal of Neurochemistry*, vol. 130, no. 5, pp. 707–719, 2014.

[60] C. M. Clemson, R. Tzekov, M. Krebs, J. M. Checchi, C. Bigelow, and S. Kaushal, "Therapeutic potential of valproic acid for retinitis pigmentosa," *British Journal of Ophthalmology*, vol. 95, no. 1, pp. 89–93, 2011.

[61] J. S. Chen, D. V. Faller, and R. A. Spanjaard, "Short-chain fatty acid inhibitors of histone deacetylases: promising anticancer therapeutics?" *Current Cancer Drug Targets*, vol. 3, no. 3, pp. 219–236, 2003.

[62] R. Kuefer, M. D. Hofer, V. Altug et al., "Sodium butyrate and tributyrin induce in vivo growth inhibition and apoptosis in human prostate cancer," *British Journal of Cancer*, vol. 90, no. 2, pp. 535–541, 2004.

[63] H. Kamitani, S. Taniura, K. Watanabe, M. Sakamoto, T. Watanabe, and T. Eling, "Histone acetylation may suppress human

glioma cell proliferation when p21WAF/Cip1 and gelsolin are induced," *Neuro-Oncology*, vol. 4, no. 2, pp. 95–101, 2002.

[64] X. X. Cao, I. Mohuiddin, F. Ece, D. J. McConkey, and W. R. Smythe, "Histone deacetylase inhibitor downregulation of bcl-xl gene expression leads to apoptotic cell death in mesothelioma," *American Journal of Respiratory Cell and Molecular Biology*, vol. 25, no. 5, pp. 562–568, 2001.

[65] R. Claus, D. Günthner, and H. Letzguss, "Effects of feeding fat-coated butyrate on mucosal morphology and function in the small intestine of the pig," *Journal of Animal Physiology and Animal Nutrition*, vol. 91, no. 7-8, pp. 312–318, 2007.

[66] J. Huuskonen, T. Suuronen, T. Nuutinen, S. Kyrylenko, and A. Salminen, "Regulation of microglial inflammatory response by sodium butyrate and short-chain fatty acids," *British Journal of Pharmacology*, vol. 141, no. 5, pp. 874–880, 2004.

[67] Q. Zhou, C. L. Dalgard, C. Wynder, and M. L. Doughty, "Histone deacetylase inhibitors SAHA and sodium butyrate block G1-to-S cell cycle progression in neurosphere formation by adult subventricular cells," *BMC Neuroscience*, vol. 12, article 50, 2011.

[68] Y. Karasawa and S. Okisaka, "Inhibition of histone deacetylation by butyrate induces morphological changes in Y79 retinoblastoma cells," *Japanese Journal of Ophthalmology*, vol. 48, no. 6, pp. 542–551, 2004.

[69] G. Faraco, T. Pancani, L. Formentini et al., "Pharmacological inhibition of histone deacetylases by suberoylanilide hydroxamic acid specifically alters gene expression and reduces ischemic injury in the mouse brain," *Molecular Pharmacology*, vol. 70, no. 6, pp. 1876–1884, 2006.

[70] S. H. Chen, H. M. Wu, B. Ossola et al., "Suberoylanilide hydroxamic acid, a histone deacetylase inhibitor, protects dopaminergic neurons from neurotoxin-induced damage," *British Journal of Pharmacology*, vol. 165, no. 2, pp. 494–505, 2012.

[71] J. P. Dompierre, J. D. Godin, B. C. Charrin et al., "Histone deacetylase 6 inhibition compensates for the transport deficit in Huntington's disease by increasing tubulin acetylation," *Journal of Neuroscience*, vol. 27, no. 13, pp. 3571–3583, 2007.

[72] N. Agrawal, J. Pallos, N. Slepko et al., "Identification of combinatorial drug regimens for treatment of Huntington's disease using Drosophila," *Proceedings of the National Academy of Sciences of the United States of America*, vol. 102, no. 10, pp. 3777–3781, 2005.

[73] A. Tandon, J. C. K. Tovey, M. R. Waggoner et al., "Vorinostat: a potent agent to prevent and treat laser-induced corneal haze," *Journal of Refractive Surgery*, vol. 28, no. 4, pp. 285–290, 2012.

[74] X. Li, Q. Zhou, J. Hanus et al., "Inhibition of multiple pathogenic pathways by histone deacetylase inhibitor SAHA in a corneal alkali-burn injury model," *Molecular Pharmaceutics*, vol. 10, no. 1, pp. 307–318, 2013.

[75] V. Poulaki, C. S. Mitsiades, V. Kotoula et al., "Molecular sequelae of histone deacetylase inhibition in human retinoblastoma cell lines: Clinical implications," *Investigative Ophthalmology and Visual Science*, vol. 50, no. 9, pp. 4072–4079, 2009.

[76] C. L. Dalgard, K. R. van Quill, and J. M. O'Brien, "Evaluation of the in vitro and in vivo antitumor activity of histone deacetylase inhibitors for the therapy of retinoblastoma," *Clinical Cancer Research*, vol. 14, no. 10, pp. 3113–3123, 2008.

[77] P. Chindasub, J. D. Lindsey, K. Duong-Polk, C. K. Leung, and R. N. Weinreb, "Inhibition of histone deacetylases 1 and 3 protects injured retinal ganglion cells," *Investigative Ophthalmology and Visual Science*, vol. 54, no. 1, pp. 96–102, 2013.

[78] M. A. Yenari, J. Liu, Z. Zheng, Z. S. Vexler, J. E. Lee, and R. G. Giffard, "Antiapoptotic and anti-inflammatory mechanisms of heat-shock protein protection," *Annals of the New York Academy of Sciences*, vol. 1053, pp. 74–83, 2005.

[79] T. Ichiyama, K. Okada, J. M. Lipton, T. Matsubara, T. Hayashi, and S. Furukawa, "Sodium valproate inhibits production of TNF-α and IL-6 and activation of NF-κB," *Brain Research*, vol. 857, no. 1-2, pp. 246–251, 2000.

[80] M. Kirsch, S. Schulz-Key, A. Wiese, S. Fuhrmann, and H. D. Hofmann, "Ciliary neurotrophic factor blocks rod photoreceptor differentiation from postmitotic precursor cells in vitro," *Cell and Tissue Research*, vol. 291, no. 2, pp. 207–216, 1998.

[81] X. Wu, P. S. Chen, S. Dallas et al., "Histone deacetylase inhibitors up-regulate astrocyte GDNF and BDNF gene transcription and protect dopaminergic neurons," *The International Journal of Neuropsychopharmacology*, vol. 11, no. 8, pp. 1123–1134, 2008.

[82] S. Azadi, L. E. Johnson, F. Paquet-Durand et al., "CNTF + BDNF treatment and neuroprotective pathways in the rd1 mouse retina," *Brain Research*, vol. 1129, no. 1, pp. 116–129, 2007.

[83] A. V. Cideciyan, T. S. Aleman, S. L. Boye et al., "Human gene therapy for RPE65 isomerase deficiency activates the retinoid cycle of vision but with slow rod kinetics," *Proceedings of the National Academy of Sciences of the United States of America*, vol. 105, no. 39, pp. 15112–15117, 2008.

[84] S. G. Jacobson, A. V. Cideciyan, R. Ratnakaram et al., "Gene therapy for leber congenital amaurosis caused by RPE65 mutations: safety and efficacy in 15 children and adults followed up to 3 years," *Archives of Ophthalmology*, vol. 130, no. 1, pp. 9–24, 2012.

[85] J. W. B. Bainbridge, A. J. Smith, S. S. Barker et al., "Effect of gene therapy on visual function in Leber's congenital amaurosis," *The New England Journal of Medicine*, vol. 358, no. 21, pp. 2231–2239, 2008.

[86] X. Li, W. Li, X. Dai et al., "Gene therapy rescues cone structure and function in the 3-month-old rd12 mouse: a model for midcourse RPE65 leber congenital amaurosis," *Investigative Ophthalmology and Visual Science*, vol. 52, no. 1, pp. 7–15, 2011.

[87] A. V. Cideciyan, S. G. Jacobson, W. A. Beltran et al., "Human retinal gene therapy for Leber congenital amaurosis shows advancing retinal degeneration despite enduring visual improvement," *Proceedings of the National Academy of Sciences of the United States of America*, vol. 110, no. 6, pp. E517–E525, 2013.

[88] B. R. Schwechter, L. E. Millet, and L. A. Levin, "Histone deacetylase inhibition-mediated differentiation of RGC-5 cells and interaction with survival," *Investigative Ophthalmology and Visual Science*, vol. 48, no. 6, pp. 2845–2857, 2007.

[89] X. Song, J. Wang, T. Zheng et al., "LBH589 Inhibits proliferation and metastasis of hepatocellular carcinoma via inhibition of gankyrin/stat3/akt pathway," *Molecular Cancer*, vol. 12, no. 1, article 114, 2013.

[90] J. Savickiene, G. Treigyte, V. Borutinskaite, R. Navakauskiene, and K.-E. Magnusson, "The histone deacetylase inhibitor FK228 distinctly sensitizes the human leukemia cells to retinoic acid-induced differentiation," *Annals of the New York Academy of Sciences*, vol. 1091, pp. 368–384, 2006.

[91] E.-S. K. Assem, K. H. Peh, B. Y. C. Wan, B. J. Middleton, J. Dines, and C. M. Marson, "Effects of a selection of histone deacetylase inhibitors on mast cell activation and airway and colonic smooth muscle contraction," *International Immunopharmacology*, vol. 8, no. 13-14, pp. 1793–1801, 2008.

[92] P. Kumar, S. Tripathi, and K. N. Pandey, "Histone deacetylase inhibitors modulate the transcriptional regulation of guanylyl

cyclase/natriuretic peptide receptor-a gene: interactive roles of modified histones, histone acetyltransferase, p300, and Sp1," *Journal of Biological Chemistry*, vol. 289, no. 10, pp. 6991–7002, 2014.

[93] I. Svechnikova, P. M. Almqvist, and T. J. Ekström, "HDAC inhibitors effectively induce cell type-specific differentiation in human glioblastoma cell lines of different origin," *International Journal of Oncology*, vol. 32, no. 4, pp. 821–827, 2008.

[94] Z. Khan, M. Akhtar, and T. J. Ekström, "HDAC inhibitor 4-phenylbutyrate preserves immature phenotype of human embryonic midbrain stem cells: implications for the involvement of DNA methyltransferase," *International Journal of Molecular Medicine*, vol. 28, no. 6, pp. 977–983, 2011.

Hindawi Publishing Corporation
Journal of Ophthalmology
Volume 2015, Article ID 816329, 7 pages
http://dx.doi.org/10.1155/2015/816329

Research Article

Knocking Down *Snrnp200* Initiates Demorphogenesis of Rod Photoreceptors in Zebrafish

Yuan Liu,[1] Xue Chen,[1] Bing Qin,[2] Kanxing Zhao,[3] Qingshun Zhao,[4] Jonathan P. Staley,[5] and Chen Zhao[1]

[1]*Department of Ophthalmology, The First Affiliated Hospital of Nanjing Medical University and State Key Laboratory of Reproductive Medicine, Nanjing Medical University, Nanjing 210029, China*
[2]*Department of Ophthalmology, The First People's Hospital of Suqian, Suqian 223000, China*
[3]*Department of Ophthalmology, Tianjin Medical University, Tianjin Eye Hospital, Tianjin Key Laboratory of Ophthalmology and Visual Science, Tianjin 300040, China*
[4]*Model Animal Research Center, MOE Key Laboratory of Model Animal for Disease Study, Nanjing University, Nanjing 210061, China*
[5]*Department of Molecular Genetics and Cell Biology, University of Chicago, 920 E. 58th Street, Chicago, IL 60637, USA*

Correspondence should be addressed to Chen Zhao; dr_zhaochen@163.com

Received 31 October 2014; Revised 17 December 2014; Accepted 29 December 2014

Academic Editor: Patrik Schatz

Purpose. The small nuclear ribonucleoprotein 200 kDa (*SNRNP200*) gene is a fundamental component for precursor message RNA (pre-mRNA) splicing and has been implicated in the etiology of autosomal dominant retinitis pigmentosa (adRP). This study aims to determine the consequences of knocking down *Snrnp200* in zebrafish. *Methods*. Expression of the *Snrnp200* transcript in zebrafish was determined via whole mount *in situ* hybridization. Morpholino oligonucleotide (MO) aiming to knock down the expression of *Snrnp200* was injected into zebrafish embryos, followed by analyses of aberrant splicing and expression of the U4/U6-U5 tri-small nuclear ribonucleoproteins (snRNPs) components and retina-specific transcripts. Systemic changes and retinal phenotypes were further characterized by histological study and immunofluorescence staining. *Results*. *Snrnp200* was ubiquitously expressed in zebrafish. Knocking down *Snrnp200* in zebrafish triggered aberrant splicing of the *cbln1* gene, upregulation of other U4/U6-U5 tri-snRNP components, and downregulation of a panel of retina-specific transcripts. Systemic defects were found correlated with knockdown of *Snrnp200* in zebrafish. Only demorphogenesis of rod photoreceptors was detected in the initial stage, mimicking the disease characteristics of RP. *Conclusions*. We conclude that knocking down *Snrnp200* in zebrafish could alter regular splicing and expression of a panel of genes, which may eventually trigger rod defects.

1. Introduction

Retinitis pigmentosa (RP (MIM 268000)) is the most common form of inherited retinal dystrophies (IRDs) with a prevalence ranging from 1/3500 to 1/5000 among different populations [1–3]. RP presents significant clinical and genetic heterogeneities [4]. In the disease course of RP, rod photoreceptors will initially be affected followed by degeneration of cone photoreceptors and retinal pigment epithelium (RPE). The clinical hallmarks of RP include initial symptom of nyctalopia, subsequent constricted visual fields (VFs), and eventual loss of central vision. Hitherto, mutations in 64 genes have been found as RP causative (RetNet). Of those, 24 were autosomal dominant RP (adRP) relevant genes and they include seven ubiquitously expressed precursor messenger RNA (pre-mRNA) splicing genes, namely, *PRPF8* (MIM 607300) [5], *PRPF31* (MIM 606419) [6], *PRPF3* (MIM 607331) [7], PIM1-associated protein (*RP9* (MIM 607331)) [8], small nuclear ribonucleoprotein 200 kDa (*SNRNP200* (MIM 601664)) [9, 10], *PRPF6* (MIM 613979) [11], and *PRPF4* (MIM 607795) [12].

Recent genetic and functional studies have revealed the important role of pre-mRNA splicing in RP etiology and has shed light on the splicing process itself, a fundamental

biological process [9, 12–14]. Pre-mRNA splicing is predominantly regulated by the spliceosome, a large complex that recognizes the pre-mRNA splice sites, removes the introns, and ligates the flanking exons accurately [15]. Notably, six of the seven identified adRP causative pre-mRNA splicing genes encode proteins embodied in the U4/U6-U5 tri-small nuclear ribonucleoproteins (snRNPs), a dynamic entity critical for the assembly and catalytic activation of the spliceosome, suggesting the important role of U4/U6-U5 tri-snRNP defects in the etiology and pathogenesis of RP [13]. The six genes can be further divided into two groups: U4/U6-specific genes including *PRPF3*, *PRPF4*, and *PRPF31* and U5-specific genes including *PRPF6*, *PRPF8*, and *SNRNP200*. How RP mutations in these ubiquitously expressed genes lead to retinopathy is currently under debate [12].

SNRNP200, located on 2q11.2 (RP33 locus), encodes the RNA helicase hBrr2, a U5-specific protein that contains 2136 amino acids and catalyzes the U4/U6 unwinding [16]. We have previously established that *SNRNP200* mutations do not compromise triple snRNP assembly but do compromise U4/U6 unwinding [9]. However, the retinal phenotypes and mRNA metabolism induced by knocking down *SNRNP200* in animal models have never been characterized. Therefore, to reveal the potential link between knockdown of *SNRNP200* and its relevant consequences, we studied the biochemical and morphological changes caused by knockdown of *Snrnp200* in a zebrafish model.

2. Materials and Methods

2.1. Whole Mount In Situ Hybridization in Zebrafish. All animal experiments were conducted in accordance with the Institutional Animal Care and Use Committee (IACUC) approved protocol and were approved and reviewed by the Institutional Committee of Nanjing Medical University. Zebrafish rearing and husbandry were maintained at 28.5°C with a 14-hour (hr) light/10 hr dark cycle. Digoxigenin-labeled antisense RNA probes were generated with cDNA of *Snrnp200* (NM_001123257.1), analogous of human *Snrnp200* in zebrafish, per the manufacturer's directions (Roche Applied Science, Mannheim, Germany). Whole mount *in situ* hybridization was conducted on 6 zebrafish for each developmental stage using a previously described modified protocol [17, 18]. Primer information is detailed in Supplementary Table S1 (in Supplementary Material available online at http://dx.doi.org/10.1155/2015/816329).

2.2. Morpholino Oligos and Knockdown of Snrnp200 in Zebrafish. Standard control morpholino oligos (control-MO: 5′-CCTCTTACCTCAGTTACAATTTATA-3′) and zebrafish *Snrnp200* splicing-blocking MO targeting exon 25 (*Snrnp200*-MO: 5′-TCAACATCAAGACAACTCACATCC-T-3′) were purchased from Gene Tools (Philomath, OR, USA). MO has been widely used to interfere in the transcription or translation of a targeted gene resulting in loss-of-function of the gene [19, 20]. Zebrafish embryos were injected at the 1- or 2-cell stage (0 day postfertilization (dpf)) with ~1 nL of purified MOs dissolved in water. To get the best adjusted dosage for *Snrnp200*-MO, zebrafish embryos were divided into three groups and injected with 2 ($n = 67$), 4 ($n = 68$), and 8 ng ($n = 65$) of MOs, respectively. Another two groups were further obtained and were injected with control-MO (4 ng; $n = 72$) and *Snrnp200*-MO (4 ng; $n = 68$), respectively. The counting and the percentage calculation of deformation and death in each injected group were conducted from 2 to 4 dpf as described previously [12]. Embryos that died within 24 hr postfertilization were excluded because such death likely resulted from unspecific causes. At 4 dpf, embryos with relatively normal appearance were collected from each injected group for further investigations.

2.3. RT-PCR and Q-PCR. RNA was isolated from 10 zebrafish embryos from each injection group, followed by reverse-transcriptase polymerase chain reaction (RT-PCR) to generate cDNA templates [9, 21]. PCR was subsequently conducted on the obtained cDNA to verify the effectiveness of *Snrnp200*-MO and amplify the targeted region of the *cbln1* gene with primers detailed in Supplementary Table S1 using a previously defined protocol [9, 21]. Quantitative real-time PCR (Q-PCR) was further performed using FastStart Universal SYBR Green Master (ROX; Roche, Basel, Switzerland) with the StepOnePlus Real-Time PCR System (Applied Biosystems, Darmstadt, Germany) per manufacturer's protocol. Expression analyses were conducted as described previously [22]. Primer information for Q-PCR was detailed in Supplementary Table S1.

2.4. Immunofluorescence Staining and Antibodies. Twelve embryos from the uninjected group, 11 from the control-MO injected group, and 14 from the *Snrnp200*-MO injected group were harvested and cryopreserved per standard procedures. They were fixed in 4% paraformaldehyde, incubated with 30% sucrose, embedded with optimal cutting temperature solution, and frozen in liquid nitrogen for sectioning at 5 μm using a Leica CM1900 cryostat (Leica, Wetzlar, Germany). Rod and cone photoreceptors were further visualized through immunofluorescence staining as indicated previously [12]. Briefly, cryosections were incubated with designated primary antibodies, including antirhodopsin (Mouse, 1 : 250; Abcam, Cambridge, UK) and zpr-1 antibodies (Mouse, 1 : 250; ZRIC, USA), to label rod and cone photoreceptors, respectively. The cryosections were then treated with fluorescence-conjugated secondary antibodies (Invitrogen, Carlsbad, CA, USA) for another 1 hr at room temperature and finally counterstained by 4′,6-diamidino-2-phenylindole (DAPI; Sigma, USA) for cell nuclei staining. Images were taken with an Olympus IX70 confocal laser-scanning microscope (Olympus, Tokyo, Japan).

2.5. Statistics. GraphPad Prism (version 4.0; GraphPad Software, San Diego, CA, USA) was applied for statistical analysis. We also use one-way ANOVA or Student's t-test for comparisons among different groups. Data was presented as mean ± standard deviation (SD), and $P < 0.05$ was taken as statistically significant.

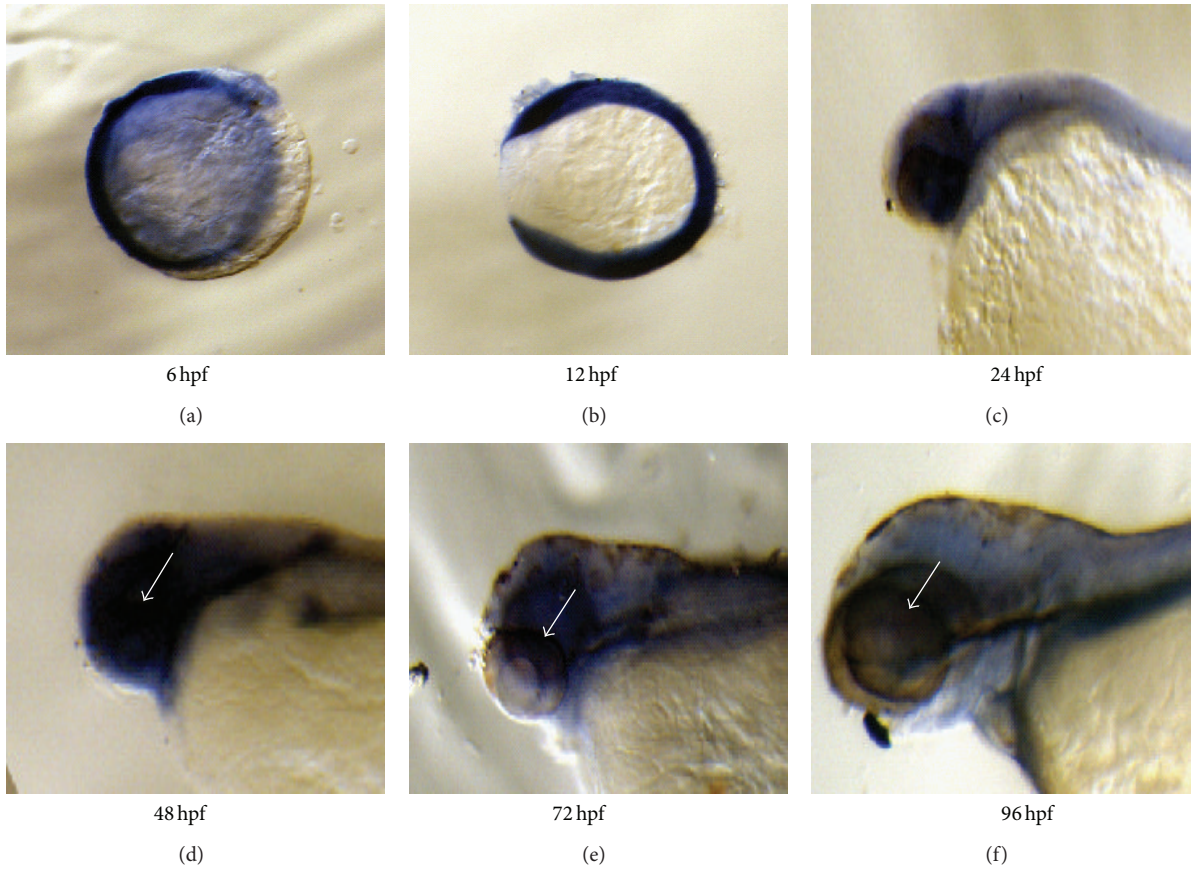

Figure 1: Whole mount *in situ* hybridization revealed a ubiquitous expression of the *Snrnp200* gene in all developmental stages of zebrafish. The 6 time points include 6 hours postfertilization (hpf) (a), 12 hpf (b), 24 hpf (c), 48 hpf (d), 72 hpf (e), and 96 hpf (f). Six embryos from each time point were collected for the experiment, and the *Snrnp200* signal in retina was indicated by white arrows (d–f).

3. Results

3.1. Ubiquitous Expression of Snrnp200 in Zebrafish. We have previously showed a ubiquitous expression of *SNRNP200* in multiple human and murine tissues [9]. Whole mount *in situ* hybridization revealed overall expression of *Snrnp200* in zebrafish among all developmental stages (Figure 1).

3.2. Knocking Down Snrnp200 Induces Aberrant Splicing in cbln1. The efficacy of *Snrnp200*-MO was confirmed by RT-PCR (Figure S1A) and the optimized condition for tissue-specific effects by *Snrnp200*-MO injection was defined with graded levels of concentration (Figures S1B and S1C). Injection of *Snrnp200*-MO at 4 ng in zebrafish was proved as the optimization dosage for an effective knockdown of the *Snrnp200* gene with moderate mortality (18%) and aberration (41.5%) rates (Figures 2(a), 3(a), and S1C). Previous studies demonstrated that patients with mutations in *PRPF31*, *PRPF3*, *PRPF8*, and *PRPF6* failed to correctly remove the intron between the first and the second exons of the *cbln1* gene [11]. Herein, the aberrantly spliced product (589 bp) containing the first intron of the *cbln1* gene was also detected in zebrafish injected with *Snrnp200*-MO (Figure 2(b)).

3.3. Knocking Down Snrnp200 Triggers Upregulation of U4/U6-U5 Tri-snRNP Components and Downregulation of Retinal Transcripts. Knocking down a pre-mRNA splicing gene, like *sart3*, *prpf31*, or *prpf4*, in zebrafish can trigger compensatory responses by upregulating itself and other relevant splice components [12, 14, 23]. To test whether knocking down *Snrnp200* will have similar effects, we performed Q-PCR on the cDNA templates obtained from zebrafish injected with control-MO or *Snrnp200*-MO, respectively. Increased expressions of *prpf3* (NM_205748.1), *prpf31* (NM_200504.1), *prpf6* (NM_212655.1), and *prpf8* (NM_200976.2) were found in embryos injected with *Snrnp200*-MO when compared with those injected with control-MO, suggesting that other splicing components will show compensatory responses to *Snrnp200* deficiency in zebrafish (Figure 2(c)). In addition, consistent with previous findings in zebrafish with *prpf31* and *prpf4* knocked down [12, 14], Q-PCR revealed that the expression levels of several important retinal transcripts including *opn1lw1* (NM_131175.1), *gnat2* (NM_131869.2), *rs1* (NM_001003438.2), and *rho* (NM_131084.1) were decreased in *Snrnp200* morphants when compared with the control group (Figure 2(d)).

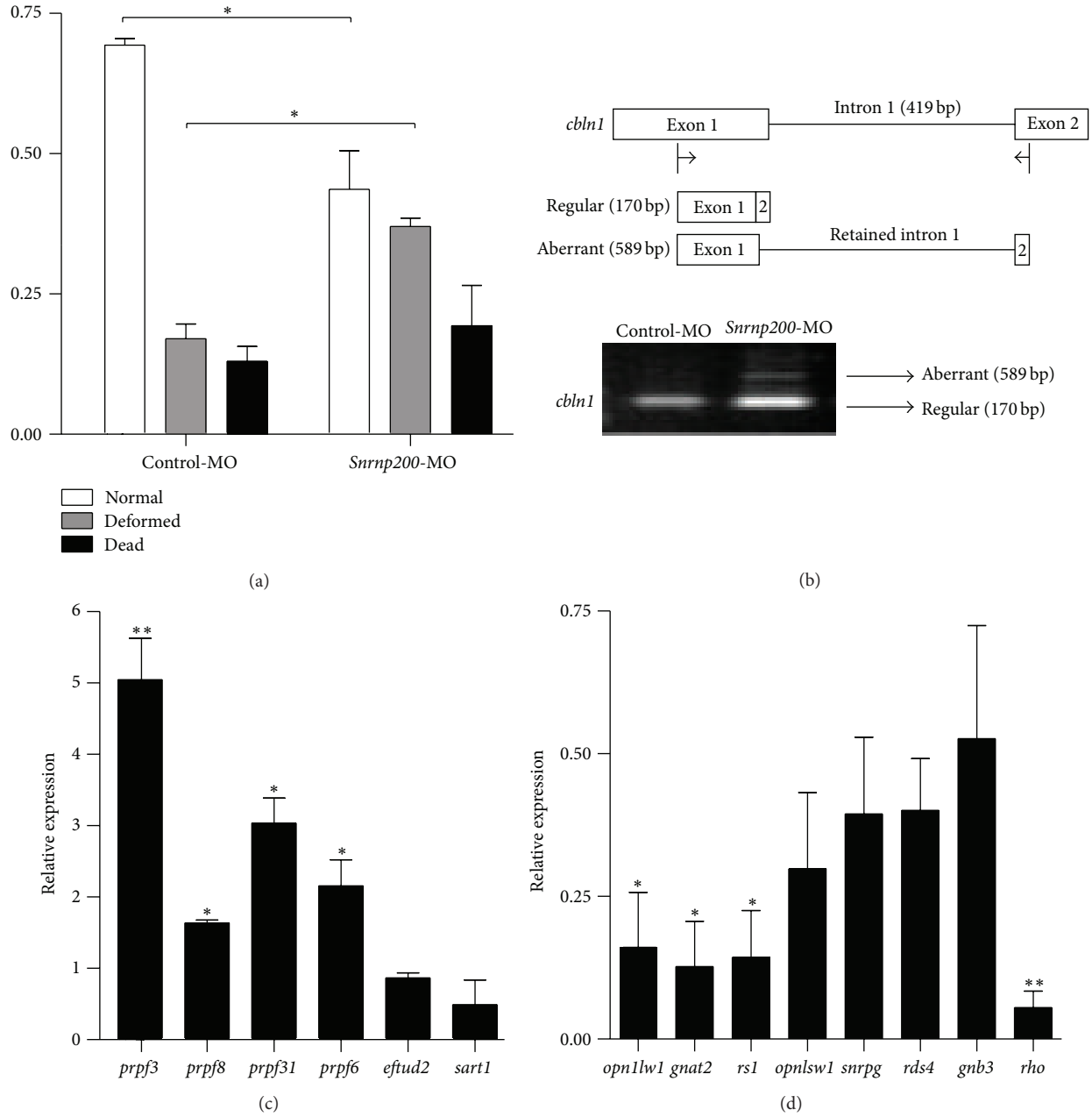

FIGURE 2: (a) Quantification of normal, deformed, and dead zebrafish injected with control morpholinos (control-MO) ($n = 72$) or *Snrnp200*-MO ($n = 68$) from 2 to 4 days postfertilization (dpf). (b) The upper panel presents the regular and aberrant cDNA structures of the *cbln1* gene, while the below panel indicates the aberrant splicing detected in the *cbln1* gene in zebrafish injected with *Snrnp200*-MO. The first intron of the *cbln1* gene was retained. (c) The relative expressions of splicing components, including *prpf3* ($P = 0.007$), *prpf8* ($P = 0.011$), *prpf31* ($P = 0.032$), *prpf6* ($P = 0.048$), *eftud2* ($P = 0.086$), and *sartl* ($P = 0.125$), were upregulated in zebrafish injected with *Snrnp200*-MO when compared with those injected with control-MO. (d) The relative expressions of retina specific transcripts, including *opn1lw1* ($P = 0.013$), *gnat2* ($P = 0.011$), *rs1* ($P = 0.011$), *opnlswl* ($P = 0.060$), *snrpg* ($P = 0.068$), *rds4* ($P = 0.056$), *gnb3* ($P = 0.158$), and *rho* ($P = 0.002$), were downregulated in zebrafish injected with *Snrnp200*-MO when compared with those injected with control-MO. Data in (a), (c), and (d) are presented as mean ± standard deviation (SD) for technical triplicates. $^{*}P < 0.05$; $^{**}P < 0.01$.

3.4. Demorphogenesis of Rod Photoreceptors in Snrnp200 Morphants. We further analyzed whether knocking down *Snrnp200* in zebrafish will lead to primary damages on retina, especially defects in rod and cone photoreceptors. Retinal phenotypes were investigated on zebrafish injected with control-MO or *Snrnp200*-MO at 4 dpf. To confirm the integrity of the eyeballs, thus minimizing the possibility for false positive results, we only include larvae with relatively normal systemic appearances from each injected group to visualize the morphology of cone and rod photoreceptors. Larvae with severely general morphological defects, including malformed brains, short trunks, cardiac edema, and

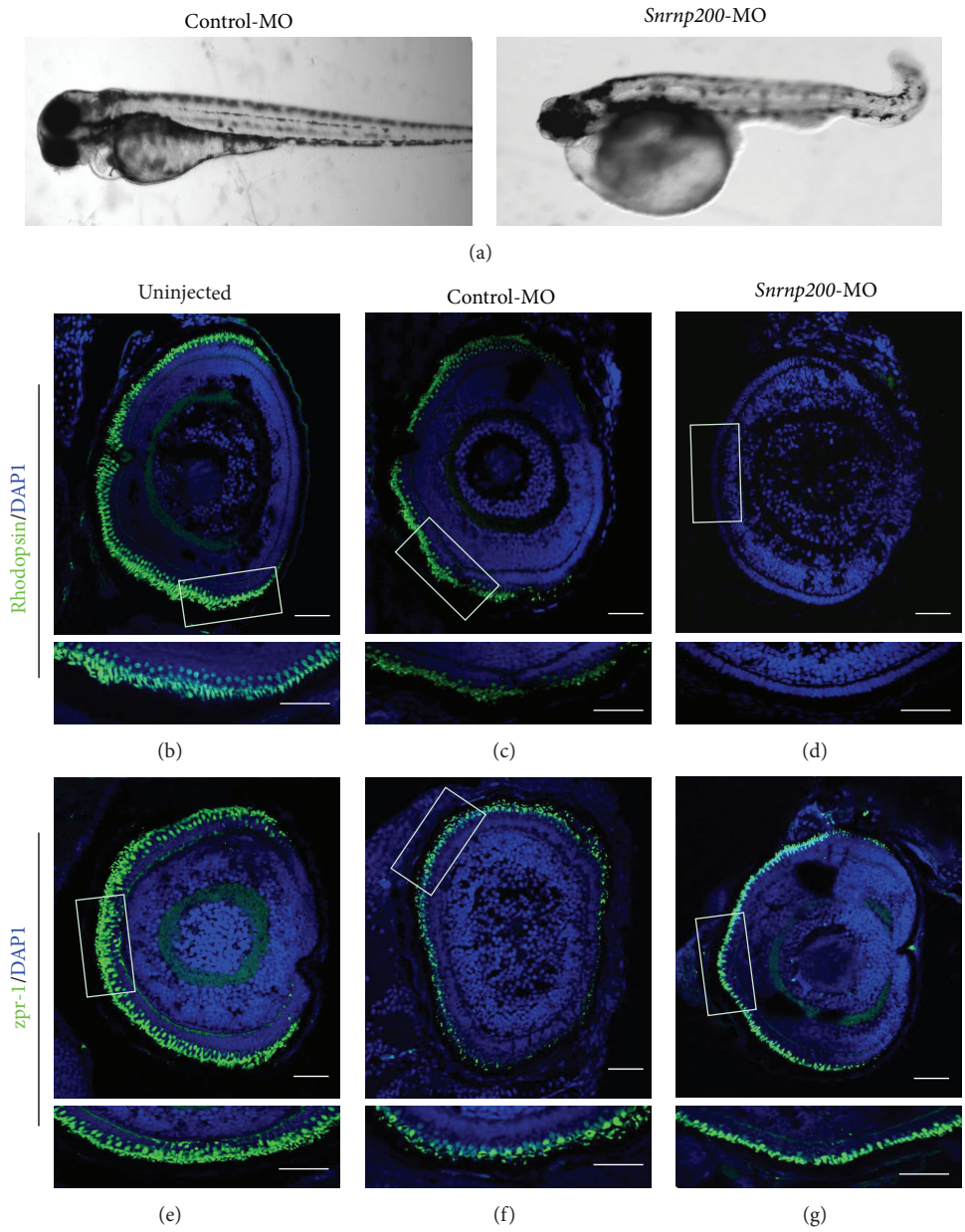

Figure 3: (a) Morphological changes in zebrafish injected with control morpholinos (control-MO) (left) or *Snrnp200*-MO (right) at 4 days postfertilization (dpf). *Snrnp200*-MO injection would result in morphological changes like malformed brains, short trunks, cardiac edema, and curved body axis, comparing with control-MO injection. (b–g) Retinal frozen sections of uninjected zebrafish (b and e) (n = 12) and zebrafish injected with control MO (c and f) (n = 11) and with *Snrnp200*-MO (d and g) (n = 14) were immunostained for rhodopsin (b–d) or zpr-1 (e–g).

curved body axis, were excluded. The rhodopsin activity was significantly reduced in *Snrnp200*-morphants (Figures 3(b)–3(d)), while no significant divergence was shown concerning the morphology of the cone photoreceptors between the control and the morphant eyes (Figures 3(e)–3(g)).

4. Discussion

Mutations in the ubiquitously expressed pre-mRNA splicing genes have long been implicated in the etiology of RP, while the specific mechanisms underlying how such mutations would cause retina-specific phenotypes have not been fully elucidated. Previous studies suggest that reduced expression levels of *prpf31* and *prpf4* in zebrafish would selectively affect gene expression, in particular, retina-specific genes [12, 14]. However, both *prpf31* and *prpf4* are U4/U6-specific genes, and whether knocking down U5-specific genes will have similar impacts is still unknown. In the present study, we for the first time used a zebrafish model to characterize the retinal phenotypes and mRNA metabolism induced by knockdown

of *Snrnp200*. Our findings in zebrafish indicate that knocking down of *Snrnp200* would cause systemic defects, retinal phenotypes, and splicing anomalies.

Similar to findings in zebrafish with *sart3*, *prpf31*, or *prpf4* knocked down [12, 14, 23], upregulation of other U4/U6-U5 tri-snRNP components was detected in *Snrnp200* morphants suggesting compensatory responses of other splicing components. Retinal phenotypes in the *Snrnp200* morphants were also similar to previous findings in *prpf31* and *prpf4* morphants [12, 14]. The expression levels of retina-specific transcripts were significantly reduced, and rod loss/demorphogenesis was predominantly detected in *Snrnp200* morphants, mimicking the RP phenotypes in patients. In addition, consistent with previous finding in patients carrying mutations in *PRPF31*, *PRPF3*, *PRPF8*, and *PRPF6*, aberrant splicing of the *cbln1* gene with retaining of its first intron was revealed in zebrafish injected with *Snrnp200*-MO [11]. Our result implies that defects in *SNRNP200* and other pre-mRNA splicing genes would share common splicing abnormalities.

The hBrr2 protein is critical for the proofreading of pre-mRNA splicing [9]. Thus, *SNRNP200* defects may interfere with the fidelity of retinal transcripts and further generate aberrantly spliced products toxic to the retina. Therefore, transcriptome analyses are needed for the detection of downstream target genes, particularly, retina-specific genes, of *SNRNP200* mutations and mutations in other adRP-associated splicing genes. Identification of such target genes will definitely provide us with a better insight into the molecular mechanisms for pre-mRNA splicing defects and could lead to discovery of new pathways for RP, which would assist in genetic counseling and direct future gene therapy for the patients with pre-mRNA splicing deficiency.

Taken together, our data suggest the potential pathogenesis shared by defects in pre-mRNA splicing genes, in particular, defects in *SNRNP200*, *PRPF31*, and *PRPF4*. Mutations in *PRPF31* have been reported to induce RP through haploinsufficiency [12], while *PRPF4* mutations are found as RP causative in a dominant negative manner [12]. Therefore, we highly hypothesize that *SNRNP200* mutations will cause RP eventually via loss-of-function, and investigations on the definite pathogenesis underlying *SNRNP200* mutations will be part of our future work. Elucidating the pathogenesis for *SNRNP200* mutations would aid in the development of novel therapeutics for retinitis pigmentosa. If haploinsufficiency mechanism is responsible for *SNRNP200* defects, the primary aim should be restoration of the normal levels of wild-type hBrr2 proteins. On the other hand, if the dominant negative gain-of-function toxicity mechanism plays an important role in photoreceptor loss, then enhancing the clearance of the toxic mutant hBrr2 protein would be of therapeutic value if implemented early.

Conflict of Interests

The authors declare that there is no conflict of interests regarding the publication of this paper.

Authors' Contribution

Yuan Liu and Xue Chen contributed equally to the work and should therefore be regarded as equivalent authors.

Acknowledgments

This work was supported by National Key Basic Research Program of China (973 Program, 2013CB967500), National Natural Science Foundation of China (81222009 and 81170856), Thousand Youth Talents Program of China (to Chen Zhao), Jiangsu Outstanding Young Investigator Program (BK2012046), Jiangsu Province's Key Provincial Talents Program (RC201149), the Fundamental Research Funds of the State Key Laboratory of Ophthalmology (to Chen Zhao), Jiangsu Province's Scientific Research Innovation Program for Postgraduates (CXZZ13_0590 to Xue Chen), and a project funded by the Priority Academic Program Development of Jiangsu Higher Education Institutions (PAPD). The funders had no role in study design, data collection and analysis, decision to publish, or preparation of the paper.

References

[1] J. Carrillo, P. Martínez, J. Solera et al., "High resolution melting analysis for the identification of novel mutations in DKC1 and TERT genes in patients with dyskeratosis congenita," *Blood Cells, Molecules, and Diseases*, vol. 49, no. 3-4, pp. 140–146, 2012.

[2] M. Chizzolini, A. Galan, E. Milan, A. Sebastiani, C. Costagliola, and F. Parmeggiani, "Good epidemiologic practice in retinitis pigmentosa: from phenotyping to biobanking," *Current Genomics*, vol. 12, no. 4, pp. 260–266, 2011.

[3] R. W. J. Collin, C. Safieh, K. W. Littink et al., "Mutations in C2ORF71 cause autosomal-recessive retinitis pigmentosa," *The American Journal of Human Genetics*, vol. 86, no. 5, pp. 783–788, 2010.

[4] D. T. Hartong, E. L. Berson, and T. P. Dryja, "Retinitis pigmentosa," *The Lancet*, vol. 368, no. 9549, pp. 1795–1809, 2006.

[5] A. B. McKie, J. C. McHale, T. J. Keen et al., "Mutations in the pre-mRNA splicing factor gene PRPC8 in autosomal dominant retinitis pigmentosa (RP13)," *Human Molecular Genetics*, vol. 10, no. 15, pp. 1555–1562, 2001.

[6] E. N. Vithana, L. Abu-Safieh, M. J. Allen et al., "A human homolog of yeast pre-mRNA splicing gene, *PRP31*, underlies autosomal dominant retinitis pigmentosa on chromosome 19q13.4 (*RP11*)," *Molecular Cell*, vol. 8, no. 2, pp. 375–381, 2001.

[7] C. F. Chakarova, M. M. Hims, H. Bolz et al., "Mutations in HPRP3, a third member of pre-mRNA splicing factor genes, implicated in autosomal dominant retinitis pigmentosa," *Human Molecular Genetics*, vol. 11, no. 1, pp. 87–92, 2002.

[8] T. J. Keen, M. M. Hims, A. B. McKie et al., "Mutations in a protein target of the Pim-1 kinase associated with the RP9 form of autosomal dominant retinitis pigmentosa," *European Journal of Human Genetics*, vol. 10, no. 4, pp. 245–249, 2002.

[9] C. Zhao, D. L. Bellur, S. Lu et al., "Autosomal-dominant retinitis pigmentosa caused by a mutation in *SNRNP200*, a gene required for unwinding of U4/U6 snRNAs," *American Journal of Human Genetics*, vol. 85, no. 5, pp. 617–627, 2009.

[10] N. Li, H. Mei, I. M. MacDonald, X. Jiao, and J. F. Hejtmancik, "Mutations in ASCC3L1 on 2q11.2 are associated with autosomal

dominant retinitis pigmentosa in a chinese family," *Investigative Ophthalmology and Visual Science*, vol. 51, no. 2, pp. 1036–1043, 2010.

[11] G. Tanackovic, A. Ransijn, C. Ayuso, S. Harper, E. L. Berson, and C. Rivolta, "A missense mutation in *PRPF6* causes impairment of pre-mRNA splicing and autosomal-dominant retinitis pigmentosa," *American Journal of Human Genetics*, vol. 88, no. 5, pp. 643–649, 2011.

[12] X. Chen, Y. Liu, X. Sheng et al., "PRPF4 mutations cause autosomal dominant retinitis pigmentosa," *Human Molecular Genetics*, vol. 23, no. 11, Article ID ddu005, pp. 2926–2939, 2014.

[13] S. Liu, R. Rauhut, H.-P. Vornlocher, and R. Lührmann, "The network of protein-protein interactions within the human U4/U6.U5 tri-snRNP," *RNA*, vol. 12, no. 7, pp. 1418–1430, 2006.

[14] B. Linder, H. Dill, A. Hirmer et al., "Systemic splicing factor deficiency causes tissue-specific defects: a zebrafish model for retinitis pigmentosa," *Human Molecular Genetics*, vol. 20, no. 2, Article ID ddq473, pp. 368–377, 2011.

[15] M. C. Wahl, C. L. Will, and R. Lührmann, "The spliceosome: design principles of a dynamic RNP machine," *Cell*, vol. 136, no. 4, pp. 701–718, 2009.

[16] J. Lauber, P. Fabrizio, S. Teigelkamp, W. S. Lane, E. Hartmann, and R. Lührmann, "The HeLa 200 kDa U5 snRNP-specific protein and its homologue in *Saccharomyces cerevisiae* are members of the DEXH-box protein family of putative RNA helicases," *The EMBO Journal*, vol. 15, no. 15, pp. 4001–4015, 1996.

[17] D. Liang, M. Zhang, J. Bao et al., "Expressions of Raldh3 and Raldh4 during zebrafish early development," *Gene Expression Patterns*, vol. 8, no. 4, pp. 248–253, 2008.

[18] Q. Zhao, B. Dobbs-McAuliffe, and E. Linney, "Expression of cyp26b1 during zebrafish early development," *Gene Expression Patterns*, vol. 5, no. 3, pp. 363–369, 2005.

[19] B. W. Draper, P. A. Morcos, and C. B. Kimmel, "Inhibition of zebrafish fgf8 pre-mRNA splicing with morpholino oligos: a quantifiable method for gene knockdown," *Genesis*, vol. 30, no. 3, pp. 154–156, 2001.

[20] S. C. Ekker, "Morphants: a new systematic vertebrate functional genomics approach," *Yeast*, vol. 17, no. 4, pp. 302–306, 2000.

[21] C. Zhao, S. Lu, X. Zhou, X. Zhang, K. Zhao, and C. Larsson, "A novel locus (RP33) for autosomal dominant retinitis pigmentosa mapping to chromosomal region 2cen-q12.1," *Human Genetics*, vol. 119, no. 6, pp. 617–623, 2006.

[22] K. J. Livak and T. D. Schmittgen, "Analysis of relative gene expression data using real-time quantitative PCR and the $2^{-\overline{\Delta\Delta C}}$T method," *Methods*, vol. 25, no. 4, pp. 402–408, 2001.

[23] N. S. Trede, J. Medenbach, A. Damianov et al., "Network of coregulated spliceosome components revealed by zebrafish mutant in recycling factor p110," *Proceedings of the National Academy of Sciences of the United States of America*, vol. 104, no. 16, pp. 6608–6613, 2007.

Hindawi Publishing Corporation
Journal of Ophthalmology
Volume 2015, Article ID 918473, 8 pages
http://dx.doi.org/10.1155/2015/918473

Research Article

iTRAQ-Based Proteomic Analysis of Visual Cycle-Associated Proteins in RPE of *rd12* Mice before and after *RPE65* Gene Delivery

Qinxiang Zheng,[1] Yueping Ren,[1] Radouil Tzekov,[2,3] Shanshan Hua,[1] Minghan Li,[1] Jijing Pang,[1] Jia Qu,[1] and Wensheng Li[1,4]

[1]*School of Ophthalmology and Optometry, Wenzhou Medical University, Zhejiang 325027, China*
[2]*The Roskamp Institute, Sarasota, FL 34243, USA*
[3]*Department of Ophthalmology, University of South Florida, Tampa, FL 33612, USA*
[4]*Xiamen Eye Center of Xiamen University, Xiamen, Fujian 361005, China*

Correspondence should be addressed to Jia Qu; jqu@wzmc.net and Wensheng Li; drlws@qq.com

Received 10 December 2014; Accepted 6 January 2015

Academic Editor: Xinhua Shu

Purpose. To investigate the iTRAQ-based proteomic changes of visual cycle-associated proteins in RPE of *rd12* mice before and after *RPE65* gene delivery. *Mehtods*. The right eyes of *rd12* mice underwent *RPE65* gene delivery by subretinal injection at P14, leaving the left eyes as control. C57BL/6J mice were served as a wide-type control group. ERGs were recorded at P42, and RPE-choroid-sclera complex was collected to evaluate the proteomic changes in visual cycle-associated proteins by iTRAQ-based analysis. Western blot was used to confirm the changes in the differentially expressed proteins of interest. *Results*. ERG parameters improved dramatically at P42 after *RPE65* delivery. The proteomics analysis identified a total 536 proteins with a global false discovery rate of 0.21%, out of which 7 were visual cycle-associated proteins. RALBP-1, RBP-1, and IRBP were reduced in the untreated *rd12* eyes and the former two were improved after gene therapy, confirmed by Western blot analysis. *Conclusions*. *RPE65* gene delivery restored retinal function at P42 and modified the expression of other functional proteins implicated in the visual cycle. The level of RALBP-1 was still below the normal level after gene therapy in *rd12* mice, which may explain the delayed dark adaption in LCA patients undergoing similar therapy.

1. Introduction

Vertebrate vision is initiated by the activation of the phototransduction cascade in rod and cone photoreceptor cells of the retina when photons are absorbed by the ubiquitous chromophore 11-*cis*-retinal and converted to its all-*trans*-isomer [1]. Continued function of photoreceptors requires removal of the all-*trans*-retinal and resupply with chromophore [2]. The classical visual cycle regeneration pathway takes place mostly in the retinal pigment epithelium (RPE) and uses a key enzyme, retinoid isomerase, to supply 11-*cis*-retinal for both rod and cone photoreceptors using all-*trans*-retinoid substrates either recycled from photoreceptors as vision byproducts or originating from the choroidal blood supply [3]. The RPE65 protein is the indispensable retinoid isomerase of the canonical RPE visual cycle and it is highly and preferentially expressed in the RPE cells [4–7]. Mutations in the *RPE65* gene cause Leber's congenital amaurosis (LCA), a hereditary retinal degeneration most often transmitted with an autosomal recessive pattern of inheritance [8, 9]. LCA is a blinding disease with an estimated prevalence of about 1 : 80,000 [10]; mutations in more than a dozen genes can cause LCA and RPE65-LCA is thought to represent about 6% of all LCA cases [11].

Retinal degeneration 12 (*rd12*) mouse model is an LCA animal model with a nonfunctional RPE65 protein because of a mutation in the *RPE65* gene [12, 13]. The absence of a functional RPE65 protein interferes with the visual cycle

and leads to substantial reduction in 11-*cis*-retinal levels and accumulation of retinyl esters in RPE, which gradually exerts a toxic effect on the retinal photoreceptors and severely affects the visual function. However, histologically *rd12* mice show predominantly cone degeneration while rods appear to be intact with normal expression of rhodopsin and rod transducin at early ages, indicating that it might be the lack of the chromophore 11-*cis*-retinal that leads to a nonrecordable rod ERG response at the early stages of the disease [14]. RPE65-associated LCA recently gained recognition due to the apparent early success achieved in three clinical trials using gene therapy and recombinant adenoassociated virus (AAV) vectors [15–17]. Nine LCA patients received a subretinal injection with an AAV vector and demonstrated partially restored local visual function, with local visual sensitivity improved by ~50-fold in cones and ~63000-fold in rods [15–17]. However, this reconstituted vision cycle was not completely normal but showed slow rod kinetics, resulting in prolonged course of dark-adaptation and decreased visual ability after photobleaching, indicating that the recycling of the retinal chromophore was still abnormal [17]. Currently, most studies are focused on changes in the RPE65 protein, but that may be insufficient to explain this problem. There are several proteins implicated in visual chromophore recycling, but currently there are no reports of changes in these visual cycle-associated proteins as a result of gene therapy.

The present study aims to explore the changes in these proteins after *RPE65* gene delivery, using *rd12* mice, an LCA model caused by a mutation in the *RPE65* gene. In our previous work, we used the same model to explore the proteomic differences occurring in the retina after gene therapy using two-dimensional electrophoresis (2-DE) and mass spectrometry [18]. In this study, we collected tissue samples containing RPE (retina-pigment epithelium-choroid-sclera complex, RPE/Ch/Sc) in *rd12* mice at P42, 4 weeks after AAV subretinal injection. This enabled us to do quantified proteomic study of visual cycle-associated proteins in the RPE, using a more accurate and sensitive technique in protein quantification, the isobaric tagging for relative and absolute protein quantification (iTRAQ) [19, 20]. Seven visual cycle-associated proteins were identified in *rd12* mice. Three of them, RALBP-1, RBP-1, and IRBP, were differentially expressed before and after gene therapy.

2. Materials and Methods

2.1. Animals. Twelve *rd12* mice (*Rpe65 rd12* or B6(A)-*Rpe65 rd12/J*) were purchased from the Jackson Laboratory (Bar Harbor, ME), and 6 age-matched C57BL/6J mice were obtained from Animal Center of Wenzhou Medical University. All mice were bred and maintained in the Animal Facilities of Wenzhou Medical University. They were kept in a 12-hour light-12-hour dark cycle with an ambient light intensity of 18 lux. All experiments were approved by the Wenzhou Medical University's Institutional Review Board and were conducted in accordance with the ARVO Statement for the Use of Animals in Ophthalmic and Vision Research. Three groups were assigned in the experiment: the treated right eyes of *rd12* mice were set as the treated *rd12* group, the contralateral untreated left eyes were untreated *rd12* group, and both eyes of age-matched wide-type C57BL/6J mice were the normal control group.

2.2. Gene Therapy. The scAAV5-smCBA-hRPE65 vector as used in previous studies was used to deliver *RPE65* gene in *rd12* mice, with the same method of subretinal injections at age P14 [18, 21, 22]. Animals were prepared with pupil dilation and general anesthesia. A 30.5-gauge disposable needle was used to make a small incision in the cornea within the pupil area. Then a 33-gauge, unbeveled, blunt needle mounted on a 5 μL syringe (Hamilton Co., Reno, NV) was introduced through the corneal incision to reach the subretinal space in the inferior central region, avoiding touching the lens and penetrating the neuroretina. One microliter of vector suspension (1×10^{13} genome containing particles/mL) containing 1% fluorescein was injected slowly in the subretinal space in the right eye of *rd12* mice. The injected retinal area was visualized by fluorescein positive subretinal blebs demarking the retinal detachment and more than 95% retinal detachment indicates successful injection. After injection, 1% atropine eye drops and 0.3% tobramycin-dexamethasone eye ointment (Alcon Laboratories Inc., Fort Worth, TX) were given 3 times a day for 3 days. Animals with any complications, including iris-cornea adhesion, iris or retinal hemorrhage, and lens injury, were excluded from the experiment.

2.3. Electroretinograms. Scotopic and photopic ERGs at ages P14 and P42 were recorded. Full-field ERGs were recorded with a custom-built Ganzfeld dome connecting to a computer based system (Q450SC UV; Roland Consult, Wiesbaden, Germany). Six LED stimuli intensities of −35, −25, −15, −5, 5, and 15 cd·s/m^2 were applied under scotopic conditions, and 2 white LED stimuli intensities (1 cd·s/m^2, 1.96 cd·s/m^2) with a background of 30 cd/m^2 were used under photopic conditions. After dark adaption overnight, scotopic ERG was always recorded between 8 AM and 11 AM, followed by photopic ERG. All testing was performed in a climate-controlled, electrically isolated dark room under dim red light illumination. Systemic anesthesia was achieved by the intraperitoneal administration of a mixture of ketamine (72 mg/kg) and xylazine (4 mg/kg) and 0.5% proparacaine hydrochloride used to ensure full corneal anesthesia. A small amount of 2.5% methylcellulose gel was applied to the eye, and a special Ag/AgCl wire loop electrode was placed over the cornea as an active electrode. Needle reference and ground electrodes were inserted into the cheek and tail, respectively. Recordings were started from the dimmest light intensity to the brightest. Body temperature was maintained by placing the animals on a 37°C warming pad during the experiment.

2.4. Protein Sample Preparation. After retinas were dissected from enucleated eyes, the RPE/Ch/Sc complex was extracted, homogenated, and then mixed with 100 μL ice-cold lysis buffer (7 M urea, 2 M thiourea, 4% CHAPS, 2 M TBP, 20 mM Tris-HCL, 1% IEF buffer, 1 mM PMSF, 100 μg/mL DNase, and 100 μg/mL RNase). The supernatant was obtained after

centrifugation at 15,000 rpm for 15 minutes at 4°C. Protein concentrations were determined by BCA assay. Equal protein amount (100 μg) in each group sample was applied to conduct the subsequent iTRAQ.

2.5. iTRAQ Labeling and Strong Cationic Exchange (SCX) Fractionation. Following the iTRAQ protocol (Applied Biosystems, Foster City, CA), each 100 μg protein was digested with 0.2 mL of a 50 μg/mL trypsin (Promega, Madison, WI, USA) at 37°C for 16 h. Peptides were labeled with isobaric tags 118 (normal control group), 119 (untreated *rd12* group), and 121 (treated *rd12* group) and incubated at room temperature for 2 h. Then the labeled mixtures were dried by vacuum centrifugation, desalted with Sep-Pak Vac C18 cartridge 1 cm^3/50 mg (Waters, USA), and fractionated using a ShimazuLC-20AB HPLC Pump system (Shimazu, Japan) connected to a strong cation exchange (SCX) column (polysulfoethyl column, 2.1 mm × 100 mm, 5 μm, 200 Å, The Nest Group, Inc. USA). SCX separation was performed using a linear binary gradient of 0–45% buffer B (350 mM KCl, 10 mM KH2PO4 in 25% ACN, pH 2.6) in buffer A (10 mM KH2PO4 in 25% ACN, pH2.6) at a flow rate of 200 μL/min for 90 min, and 30 fractions were collected every 3 min. Each fraction was dried down and redissolved in buffer C (5% (v/v) acetonitrile and 0.1% formic acid solution), and the fractions with high KCl concentration were desalted with PepClean C-18 spin Column (Pierce, USA).

2.6. LC-ESI-MS/MS Analysis. Each fraction was resuspended in buffer A (2% ACN, 0.1% FA) and centrifuged at 20,000 ×g for 10 min. In each fraction, the final concentration of peptides was approximately 0.25 μg/μL. Using an autosampler, 20 μL of supernatant was loaded onto a 2 cm C18 trap column (inner diameter 200 μm) on a Shimadzu LC-20AD nanoHPLC. Peptides were eluted onto a resolving 10 cm analytical C18 column (inner diameter 75 μm) that was assembled in-house. The samples were loaded at 15 μL/min for 4 min and eluted with a 44 min gradient at 400 nL/min from 2 to 35% B (98% ACN, 0.1% FA), followed by a 2 min linear gradient to 80% B, maintenance at 80% B for 4 min, and finally a return to 2% B over 1 min.

The peptides were subjected to nanoelectrospray ionization followed by tandem mass spectrometry (MS/MS) in an LTQ OrbitrapVelos (Thermo) coupled in-line to the HPLC. Intact peptides were detected in the Orbitrap. Peptides were selected for MS/MS using the high-energy collision dissociation (HCD) operating mode with a normalized collision energy setting of 45%. Ion fragments were detected in the LTQ. A data-dependent procedure that alternated between one MS scan followed by eight MS/MS scans was applied for the eight most abundant precursor ions above a threshold ion count of 5,000 in the MS survey scan with the following Dynamic Exclusion settings: repeat counts: 2; repeat duration: 30 s; and exclusion duration: 120 s. The applied electrospray voltage was 1.5 kV. Automatic gain control (AGC) was used to prevent overfilling of the ion trap; 1×10^4 ions were accumulated in the ion trap to generate HCD spectra. For MS scans, the m/z scan range was 350 to 2,000 Da.

2.7. Database Search and Bioinformatics. The resulting MS/MS spectra were searched against the International Protein Index (IPI) mouse sequence databases (version 3.45) with MASCOT software (Matrix Science, London, UK; version 2.2). Protein identification and quantification for iTRAQ experiments were carried out using the ProteinPilot software v3.0 (Applied Biosystems, USA). The Paragon algorithm in ProteinPilot software was used as the default search program with trypsin as the digestion agent and cysteine modification of methyl methanethiosulfonate. The search also included the possibility of more than 80 biological modifications and amino acid substitutions of up to two substitutions per peptide using the BLOSUM 62 matrix. Only proteins identified with at least 95% confidence, or a ProtScore of 1.3, were reported. A 1.3-fold change was used as the benchmark. All proteins that showed significantly altered expression levels went through Ingenuity Pathway Analysis software (IPA) for pathway and network analysis.

2.8. Western Blot Validation. Western blot analyses were performed to validate the differentially expressed proteins. Every two samples in each group were mixed in one Western blot experiment, which was repeated for three times. Protein was extracted with lysis buffer and centrifuged to obtain the supernatant and determine the protein content by BCA assay. Each of the protein samples (30 μg) was subjected to SDS-PAGE and then transferred to polyvinylidene difluoride (PVDF) membranes (Bio-Rad, Hercules, CA). The membranes were blocked for 1 h at room temperature with 5% nonfat dried milk in Tris-buffered saline containing 0.1% Tween 20 (TBST, Applygen Gene Technology Corp). Then they were probed overnight with primary anti-RALBP-1 (ab166655, Abcam, MA, USA, 1 : 1000) and anti-RBP-1 (ab154881, Abcam, MA, USA, 1 : 2000), followed by incubation with horse radish peroxidase (HRP) conjugated goat anti-mouse IgG (Santa Cruz Biotechnology, Santa Cruz, CA, 1 : 2500). Then they were developed with an enhanced chemiluminescence detection kit (Pierce Biotechnology, Inc., Rockford, IL). β-actin was used as a loading control.

2.9. Statistical Analysis. Results for continuous variables with normal distributions are presented as means ± standard deviations (SD). Nonpaired Student's t-test was used to compare means between two groups. Statistical analyses were conducted with SPSS 18.0 (SPSS, Chicago, IL, USA), and a two-tailed $P < 0.05$ was considered significant.

3. Results

3.1. Electroretinography (ERG) Responses. The untreated *rd12* eyes showed extremely low or even undetectable a-wave and b-wave peaks under scotopic and photopic conditions, indicating severely affected retinal function. Four weeks after AAV injection, a-wave amplitude of the treated *rd12* eyes increased to 210.83 ± 26.70 μV (40-fold of the untreated *rd12*

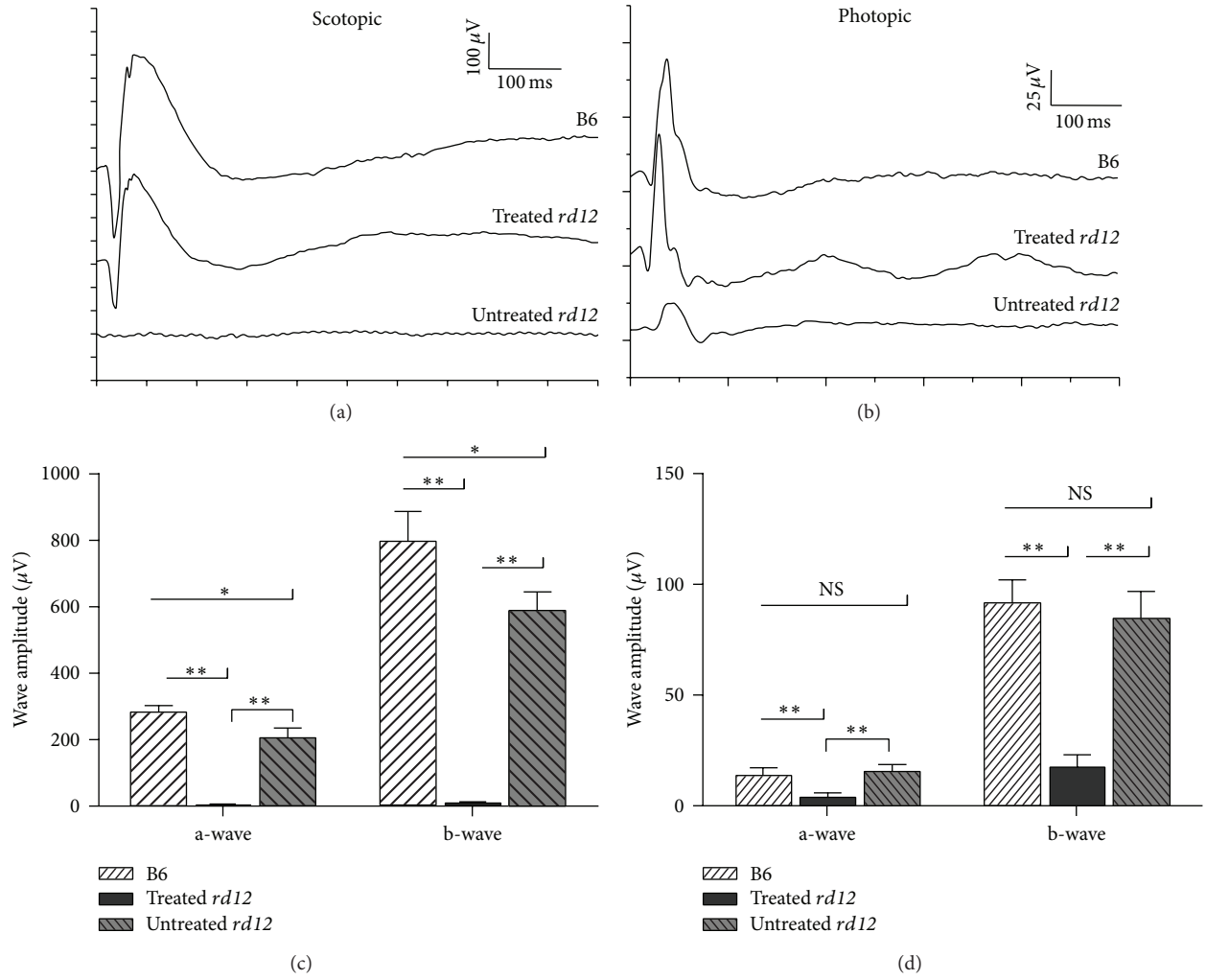

Figure 1: ERG records of untreated *rd12*, treated *rd12*, and normal control C57BL/6J eyes. (a) Scotopic ERG of the 3 groups at P42; (b) photopic ERG at P42. (c) and (d) represent statistical comparison of a-wave and b-wave amplitudes among the different groups at P42 under scotopic and photopic conditions. The untreated *rd12* eyes showed extremely low a-wave and b-wave response in both scotopic and photopic ERGs. The treated *rd12* eyes had great improvement in both a-wave and b-wave amplitudes with normal peak time, close to the wide-type control levels. NS: no significance. $^{*}P < 0.05$; $^{**}P < 0.001$.

level, $P < 0.001$), close to the $284.50 \pm 18.95\,\mu$V of the wild-type mice (74.11%, $P = 0.001$) in scotopic ERG with normal peak time; b-wave amplitude increased to $590.00 \pm 57.59\,\mu$V (48-fold of the untreated *rd12* level, $P < 0.001$), also approaching the $797.67 \pm 89.59\,\mu$V of the wild-type mice (73.97%, $P = 0.002$) with normal peak time (Figures 1(a) and 1(c)). Photopic ERG signals showed similar trend (Figure 1(b)). Photopic a-wave amplitude of the treated *rd12* eyes improved dramatically to $15.32 \pm 2.96\,\mu$V (4-fold of the untreated *rd12* level, $P < 0.001$) and was not different from the amplitude recorded from wide-type eyes ($13.38 \pm 3.43\,\mu$V, $P = 0.363$); b-wave amplitude also improved to $84.50 \pm 11.99\,\mu$V (5-fold of the untreated *rd12* level, $P < 0.001$) and was similar to the wide-type level ($91.12 \pm 10.62\,\mu$V, $P = 0.377$) (Figure 1(d)). This is in accordance with our previous findings [18] and supports the notion that gene therapy could restore retinal function in this animal model.

3.2. Identification and Quantitation of Differentially Expressed Proteins after AAV Injection. We used iTRAQ proteomics to identify and quantify proteins 4 weeks after *RPE65* gene delivery in *rd12* mice, compared with the untreated *rd12* and normal control C57BL/6J mice. A total of 14432 unique peptides were identified, corresponding to a set of 610 proteins with more than 95% confidence (ProtScore > 1.3, global false discovery rate (FDR) = 0.21%). Of these 610 proteins, 536 were identified with relative quantization, in which 7 were identified as visual cycle-associated proteins including retinaldehyde-binding protein 1 (RALBP-1), retinol-binding protein 1 (RBP-1), interphotoreceptor retinoid-binding protein (IRBP), retinal dehydrogenase 2 (RDH-2), retinal dehydrogenase 5 (RDH-5), lecithin retinol acyltransferase (LRAT), and ezrin-radixin-moesin-binding phosphoprotein 50 (EBP-50) (Table 1). Of these proteins, the expressions of RALBP-1, RBP-1, and IRBP were reduced

Table 1: The identification and quantification of the visual cycle-associated proteins.

Unused ProtScore	%Cov	Protein name	Peptides (95%)	Untreated *rd12*/B6 (119 : 118)	Treated *rd12*/B6 (121 : 118)
7.74	47	Retinaldehyde-binding protein 1	2	0.1159	0.6607
8.77	68.5	Retinol-binding protein 1	5	0.6792	1.4997
11.16	34.8	Interphotoreceptor retinoid-binding protein	5	0.6368	0.5297
2	22.4	Retinal dehydrogenase 2	1	0.9727	1.1066
41.2	22.4	Retinal dehydrogenase 5	1	1.0864	1.0186
2	63.6	Lecithin retinol acyltransferase	1	0.912	0.9285
8.09	36.9	Ezrin-radixin-moesin-binding phosphoprotein 50	4	0.9638	0.912

by at least 0.68-fold in the untreated *rd12* mice relative to the pooled sample of wild-type tissues, while the other four proteins (RDH-2, RDH-5, LRAT, and EBP-50) showed normal levels of expression. In the treated *rd12* eyes, RALBP-1 increased about 6-fold compared to the levels of the untreated *rd12* samples, although it was still lower (66.1%) than the one observed in the samples from wild-type mice. The levels of RBP-1 were also considerably increased in treated *rd12* samples, a 2-fold increase compared to the untreated *rd12* levels and 1.5-fold increase compared to the levels in wild-type mice. In contrast, the expression of IRBP did not increase on P42, and the level in the treated mice was slightly lower (83.2%) compared to the untreated mice (Figure 2). In addition, in the 536 relatively quantified proteins, 91 were downregulated and 71 were upregulated by 1.3-fold in untreated *rd12* eyes compared to the wide-type levels (see Supplementary Tables 1(a) and 1(b) in Supplementary Material available online at http://dx.doi.org/10.1155/2015/918473).

3.3. Confirmation of Differentially Expressed Proteins. Western blot analysis was performed to validate the changes observed in the differentially expressed visual cycle-related proteins before and after gene therapy. The results confirmed that the expression of RALBP-1 and RBP-1 was much weaker in the untreated *rd12* eyes and that gene therapy increased their level similar to that in the normal C57BL/6J mice (Figure 3).

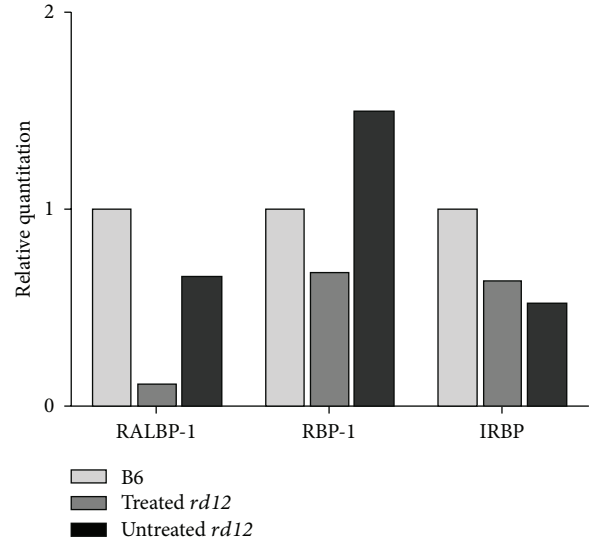

Figure 2: Identification and quantification of differentially expressed proteins by iTRAQ. The RALBP-1, RBP-1, and IRBP were identified as differentially expressed visual cycle-associated proteins among the untreated *rd12*, treated *rd12*, and normal control C57BL/6J eyes. RALBP-1, RBP-1, and IRBP were remarkably reduced in the untreated *rd12* mice (<0.7×) compared to those of C57BL/6J sample. In the treated *rd12* eyes, RALBP-1 was increased to 6-fold of the untreated *rd12* level, although it was still lower than the normal level (0.66-fold); RBP-1 was increased to 2-fold of the untreated *rd12* level and 1.50-fold of the normal level. IRBP level was still lower in the treated *rd12* eyes.

4. Discussion

Gene therapy by subretinal administration of scAAV5-smCBA-hRPE65 vector is a safe and effective treatment to rescue rod and cone photoreceptor function in *rd12* mice, as demonstrated previously [18, 21, 22]. The current investigation focuses on the changes of the visual cycle-associated proteins in *rd12* eyes before and after gene therapy, using the technique of iTRAQ-based 2D LC-MS/MS. Seven visual cycle-associated proteins in RPE layer were identified by this analysis. Three of the seven proteins, RALBP-1, RBP-1, and IRBP, were found to be downregulated in the RPE of *rd12* eyes. Subretinal delivery of *RPE65* by gene therapy demonstrated normalization of the levels of RALBP-1 and RBP-1, while no positive effect was observed on the levels of IRBP.

Visual cycle (or retinoid cycle) is the process by which 11-*cis*-retinal is regenerated from all-*trans*-retinal after photoisomerization, and it mainly takes place in the RPE layer. After conversion from all-*trans*-retinyl ester to 11-*cis*-retinol by isomerase, RALBP-1 acts as an acceptor of 11-*cis*-retinol to produce 11-*cis*-retinal and fulfill the visual cycle [23, 24]. RALBP-1 is another essential protein in the isomerization reaction of the visual cycle, and it plays a critical role to sustain normal retinal function and dark adaptation [25]. Our results demonstrated that the levels of RALBP-1 were dramatically reduced in *rd12* mice, and *RPE65* gene delivery not only regenerated the isomerase RPE65 but also increased the production of RALBP-1, leading to visual cycle restoration

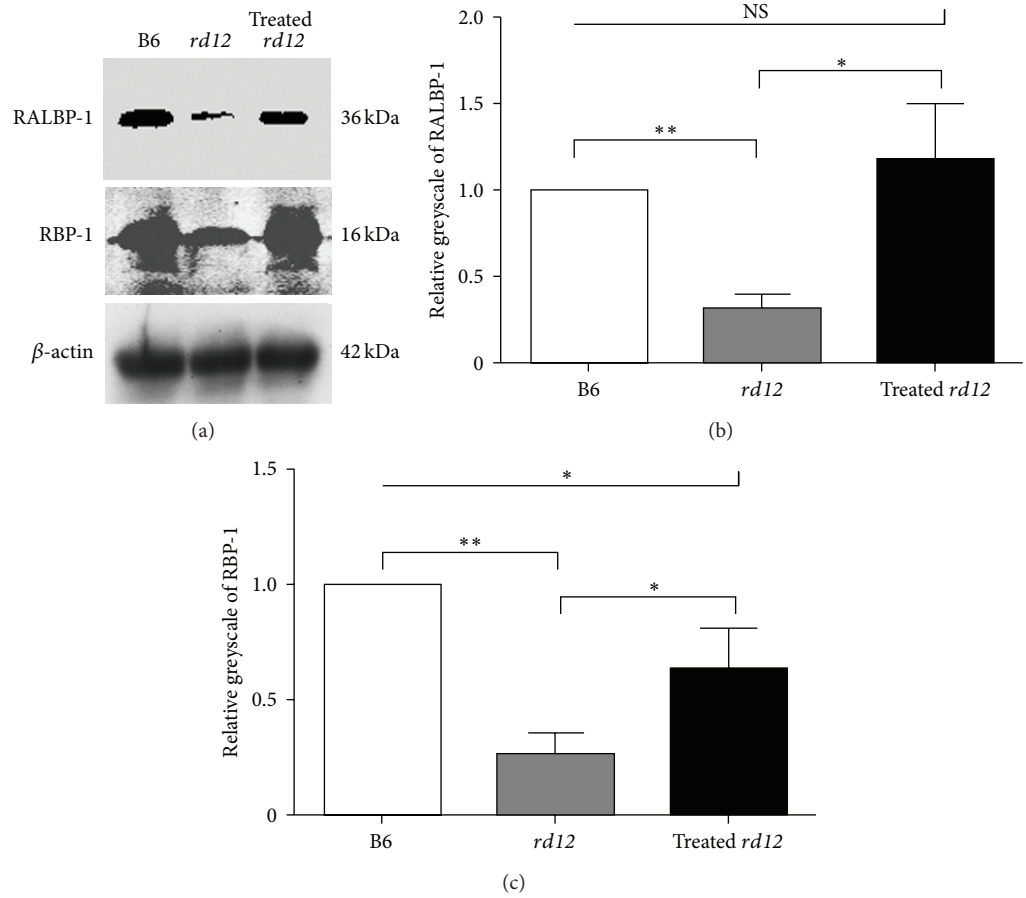

Figure 3: Western blot analysis of differentially expressed proteins. (a) The expression of RALBP-1 and RBP-1 was weak in the untreated *rd12* eyes and appeared to increase significantly following gene therapy to levels similar to those present in normal wild-type control eyes. (b) and (c) show the relative grayscale of RALBP-1 and RBP-1 compared to the wild-type values.

and normalization of the visual function. The incomplete recovery of RALBP-1 expression in treated *rd12* eyes may help to explain why the dark adaption was still delayed after similar therapy in LCA patients. Thus, a supplementation of RALBP-1 protein by certain treatment might be a strategy to solve this problem.

IRBP is a large glycoprotein synthesized in the photoreceptors and situated in the interphotoreceptor matrix [26]. It functions as a retinoid-transport vehicle to facilitate the exchange of 11-*cis*-retinal, 11-*cis*-retinol, and all-*trans*-retinol between the RPE, photoreceptors, and Müller cells [27, 28]. Despite some histological and electrophysiological changes because of cytotoxic effects of large amounts of free retinoids, the absence of IRBP in $IRBP^{-/-}$ mice did not cause gross abnormalities in the visual cycle [29]. In this study, the expression of IRBP in *rd12* mice was decreased, which might be attributed to the negatively affected function of the photoreceptors. *RPE65* gene delivery can restore rod and cone function; however, the production of IRBP was not increased and even slightly lower levels were detected compared to pretreatment. One possible explanation for this finding might be that the distribution of IRBP could be influenced by the retinal reattachment after temporary detachment caused by subretinal injection.

RBP-1 is localized in the RPE and serves as a chaperone of all-*trans*-retinol to LRAT in the visual cycle. RBP-1 has been recognized as a pigment epithelium derived factor which supports photoreceptor health and structural integrity [30]. In our results, the production of RBP-1 was reduced in *rd12* mice, suggesting that the RPE function might also be influenced by photoreceptor integrity. Gene therapy could increase the expression of RBP-1 in the RPE substantially, indicating that RBP-1 could resume its function to transport all-*trans*-retinol once the process of retinol recycling is recovered. The other four visual circle-associated proteins including LRAT, RDH-2, RDH-5, and EBP-50 were found to remain at relatively normal expression levels in the RPE of *rd12* mice, demonstrating that not all proteins implicated in vision cycle were affected by the lack of RPE65 function.

The fate of the visual cycle proteins in LCA animal models deserves further investigation since it may reveal unrecognized aspects of the disease process and provide important indications to further improve the visual function in LCA patients after gene therapy. One limitation in this

study is that only one time point (P42) after gene therapy was tested. The results could be more informative if earlier (P21) and longer time point (P98) analyses were included. Besides, the dark-adapted ERG seems normal in treated *rd12* eyes, so the ERG after photobleaching could also be tested to illustrate whether the dark adaption course was delayed only after photobleaching, as happened in LCA patients after gene therapy.

In conclusion, our study identified and quantified the RPE levels of visual cycle-associated proteins in *rd12* mice before and after gene therapy. *RPE65* gene delivery restored RPE65 expression and modified the levels of other functional proteins implicated in visual cycle. Gene therapy resulted in incomplete recovery of the levels of RALBP-1 in the RPE of *rd12* mice, indicating that this may also occur in LCA patients undergoing gene therapy and be one of the main causes of observed delayed dark adaption.

Conflict of Interests

The authors declare that there is no conflict of interests regarding the publication of this paper.

Acknowledgments

This study was funded by research grants from Zhejiang Provincial Department of Education (Y201329662 and Y200906753), the Doctoral Program of Higher Education (no. 20103321110002), and the Wenzhou Science and Technology Program (Y20120135).

References

[1] J. Buczyłko, J. C. Saari, R. K. Crouch, and K. Palczewski, "Mechanisms of opsin activation," *The Journal of Biological Chemistry*, vol. 271, no. 34, pp. 20621–20630, 1996.

[2] M. Yang and H. K. W. Fong, "Synthesis of the all-trans-retinal chromophore of retinal G protein-coupled receptor opsin in cultured pigment epithelial cells," *The Journal of Biological Chemistry*, vol. 277, no. 5, pp. 3318–3324, 2002.

[3] P. S. Bernstein, W. C. Law, and R. R. Rando, "Biochemical characterization of the retinoid isomerase system of the eye," *The Journal of Biological Chemistry*, vol. 262, no. 35, pp. 16848–16857, 1987.

[4] M. Jin, S. Li, W. N. Moghrabi, H. Sun, and G. H. Travis, "Rpe65 is the retinoid isomerase in bovine retinal pigment epithelium," *Cell*, vol. 122, no. 3, pp. 449–459, 2005.

[5] G. Moiseyev, Y. Chen, Y. Takahashi, B. X. Wu, and J.-X. Ma, "RPE65 is the isomerohydrolase in the retinoid visual cycle," *Proceedings of the National Academy of Sciences of the United States of America*, vol. 102, no. 35, pp. 12413–12418, 2005.

[6] T. M. Redmond, E. Poliakov, S. Yu, J.-Y. Tsai, Z. Lu, and S. Gentleman, "Mutation of key residues of RPE65 abolishes its enzymatic role as isomerohydrolase in the visual cycle," *Proceedings of the National Academy of Sciences of the United States of America*, vol. 102, no. 38, pp. 13658–13663, 2005.

[7] T. M. Redmond, "Focus on molecules: RPE65, the visual cycle retinol isomerase," *Experimental Eye Research*, vol. 88, no. 5, pp. 846–847, 2009.

[8] A. V. Cideciyan, "Leber congenital amaurosis due to RPE65 mutations and its treatment with gene therapy," *Progress in Retinal and Eye Research*, vol. 29, no. 5, pp. 398–427, 2010.

[9] S. M. Gu, D. A. Thompson, C. R. Srikumari et al., "Mutations in RPE65 cause autosomal recessive childhood-onset severe retinal dystrophy," *Nature Genetics*, vol. 17, no. 2, pp. 194–197, 1997.

[10] E. M. Stone, "Leber congenital amaurosis—a model for efficient genetic testing of heterogeneous disorders: LXIV Edward Jackson Memorial Lecture," *American Journal of Ophthalmology*, vol. 144, no. 6, pp. 791–811, 2007.

[11] A. I. den Hollander, R. Roepman, R. K. Koenekoop, and F. P. M. Cremers, "Leber congenital amaurosis: genes, proteins and disease mechanisms," *Progress in Retinal and Eye Research*, vol. 27, no. 4, pp. 391–419, 2008.

[12] J.-J. Pang, B. Chang, N. L. Hawes et al., "Retinal degeneration 12 (rd12): a new, spontaneously arising mouse model for human Leber congenital amaurosis (LCA)," *Molecular Vision*, vol. 11, pp. 152–162, 2005.

[13] J. J. Pang, B. Chang, A. Kumar et al., "Gene therapy restores vision-dependent behavior as well as retinal structure and function in a mouse model of RPE65 leber congenital amaurosis," *Molecular Therapy*, vol. 13, no. 3, pp. 565–572, 2006.

[14] Y. Chen, G. Moiseyev, Y. Takahashi, and J.-X. Ma, "*RPE65* gene delivery restores isomerohydrolase activity and prevents early cone loss in *Rpe65*$^{-/-}$ mice," *Investigative Ophthalmology & Visual Science*, vol. 47, no. 3, pp. 1177–1184, 2006.

[15] J. W. B. Bainbridge, A. J. Smith, S. S. Barker et al., "Effect of gene therapy on visual function in Leber's congenital amaurosis," *The New England Journal of Medicine*, vol. 358, no. 21, pp. 2231–2239, 2008.

[16] A. M. Maguire, F. Simonelli, E. A. Pierce et al., "Safety and efficacy of gene transfer for Leber's congenital amaurosis," *New England Journal of Medicine*, vol. 358, no. 21, pp. 2240–2248, 2008.

[17] A. V. Cideciyan, T. S. Aleman, S. L. Boye et al., "Human gene therapy for RPE65 isomerase deficiency activates the retinoid cycle of vision but with slow rod kinetics," *Proceedings of the National Academy of Sciences of the United States of America*, vol. 105, no. 39, pp. 15112–15117, 2008.

[18] Q. Zheng, Y. Ren, R. Tzekov et al., "Differential proteomics and functional research following gene therapy in a mouse model of Leber congenital amaurosis," *PLoS ONE*, vol. 7, no. 8, Article ID e44855, 2012.

[19] W. W. Wu, G. Wang, S. J. Baek, and R.-F. Shen, "Comparative study of three proteomic quantitative methods, DIGE, cICAT, and iTRAQ, using 2D gel- or LC-MALDI TOF/TOF," *Journal of Proteome Research*, vol. 5, no. 3, pp. 651–658, 2006.

[20] S. Wiese, K. A. Reidegeld, H. E. Meyer, and B. Warscheid, "Protein labeling by iTRAQ: a new tool for quantitative mass spectrometry in proteome research," *Proteomics*, vol. 7, no. 3, pp. 340–350, 2007.

[21] X. Li, W. Li, X. Dai et al., "Gene therapy rescues cone structure and function in the 3-month-old rd12 mouse: a model for midcourse RPE65 leber congenital amaurosis," *Investigative Ophthalmology & Visual Science*, vol. 52, no. 1, pp. 7–15, 2011.

[22] W. Li, F. Kong, X. Li et al., "Gene therapy following subretinal AAV5 vector delivery is not affected by a previous intravitreal AAV5 vector administration in the partner eye," *Molecular Vision*, vol. 15, pp. 267–275, 2009.

[23] I. Golovleva, S. Bhattacharya, Z. Wu et al., "Disease-causing mutations in the cellular retinaldehyde binding protein tighten

and abolish ligand interactions," *The Journal of Biological Chemistry*, vol. 278, no. 14, pp. 12397–12402, 2003.

[24] J. K. McBee, J. P. van Hooser, G. F. Jang, and K. Palczewski, "Isomerization of 11-cis-retinoids to all-trans-retinoids in vitro and in vivo," *The Journal of Biological Chemistry*, vol. 276, no. 51, pp. 48483–48493, 2001.

[25] J. C. Saari, M. Nawrot, B. N. Kennedy et al., "Visual cycle impairment in cellular retinaldehyde binding protein (CRALBP) knockout mice results in delayed dark adaptation," *Neuron*, vol. 29, no. 3, pp. 739–748, 2001.

[26] F. Gonzalez-Fernandez, K. L. Kittredge, M. E. Rayborn et al., "Interphotoreceptor Retinoid-Binding Protein (IRBP), a major 124 kDa glycoprotein in the interphotoreceptor matrix of *Xenopus laevis*: characterization, molecular cloning and biosynthesis," *Journal of Cell Science*, vol. 105, part 1, pp. 7–21, 1993.

[27] T. M. Redmond, B. Wiggert, F. A. Robey et al., "Isolation and characterization of monkey interphotoreceptor retinoid-binding protein, a unique extracellular matrix component of the retina," *Biochemistry*, vol. 24, no. 3, pp. 787–793, 1985.

[28] B. S. Betts-Obregon, F. Gonzalez-Fernandez, and A. T. Tsin, "Interphotoreceptor retinoid-binding protein (IRBP) promotes retinol uptake and release by rat Muller cells (rMC-1) in vitro: implications for the cone visual cycle," *Investigative Ophthalmology & Visual Science*, vol. 55, no. 10, pp. 6265–6271, 2014.

[29] H. Ripps, N. S. Peachey, X. Xu, S. E. Nozell, S. B. Smith, and G. I. Liou, "The rhodopsin cycle is preserved in IRBP 'knockout' mice despite abnormalities in retinal structure and function," *Visual Neuroscience*, vol. 17, no. 1, pp. 97–105, 2000.

[30] X. Wang, Y. Tong, F. Giorgianni, S. Beranova-Giorgianni, J. S. Penn, and M. M. Jablonski, "Cellular retinol binding protein 1 modulates photoreceptor outer segment folding in the isolated eye," *Developmental Neurobiology*, vol. 70, no. 9, pp. 623–635, 2010.

Hindawi Publishing Corporation
Journal of Ophthalmology
Volume 2015, Article ID 942740, 7 pages
http://dx.doi.org/10.1155/2015/942740

Research Article

Exome Sequencing Identified a Recessive *RDH12* Mutation in a Family with Severe Early-Onset Retinitis Pigmentosa

Bo Gong,[1,2] Bo Wei,[3] Lulin Huang,[1,2] Jilong Hao,[4] Xiulan Li,[1,2] Yin Yang,[1,2] Yu Zhou,[1,2] Fang Hao,[1,2] Zhihua Cui,[4] Dingding Zhang,[1,2] Le Wang,[4] and Houbin Zhang[1,2]

[1] *Sichuan Provincial Key Laboratory for Disease Gene Study, Hospital of University of Electronic Science and Technology of China and Sichuan Provincial People's Hospital, Chengdu, Sichuan 610072, China*
[2] *School of Medicine, University of Electronic Science and Technology of China, Chengdu, Sichuan 610072, China*
[3] *China-Japan Union Hospital of Jilin University, Neurosurgery, Changchun, Jilin 130103, China*
[4] *Department of Ophthalmology, The First Hospital of Jilin University, Changchun, Jilin 130103, China*

Correspondence should be addressed to Le Wang; wangluxin2008263@sina.com and Houbin Zhang; houbin.zhang@gmail.com

Received 26 December 2014; Revised 8 April 2015; Accepted 10 April 2015

Academic Editor: Enrico Peiretti

Retinitis pigmentosa (RP) is the most important hereditary retinal disease caused by progressive degeneration of the photoreceptor cells. This study is to identify gene mutations responsible for autosomal recessive retinitis pigmentosa (arRP) in a Chinese family using next-generation sequencing technology. A Chinese family with 7 members including two individuals affected with severe early-onset RP was studied. All patients underwent a complete ophthalmic examination. Exome sequencing was performed on a single RP patient (the proband of this family) and direct Sanger sequencing on other family members and normal controls was followed to confirm the causal mutations. A homozygous mutation c.437T<A (p.V146D) in the *retinol dehydrogenase 12 (RDH12)* gene, which encodes an NADPH-dependent retinal reductase, was identified as being related to the phenotype of this arRP family. This homozygous mutation was detected in the two affected patients, but not present in other family members and 600 normal controls. Another three normal members in the family were found to carry this heterozygous missense mutation. Our results emphasize the importance of c.437T<A (p.V146D) substitution in *RDH12* and provide further support for the causative role of this mutation in the pathogenesis and clinical diagnosis of RP.

1. Introduction

Retinitis pigmentosa (RP) is a phenotypically and genetically heterogeneous group of inherited retinal degenerations characterized by night blindness, progressive loss of peripheral vision in early stage, and complete loss of vision at late stages [1]. RP is the most common cause of hereditary blindness and affects approximately 1 in 3,500 to 1 in 5,000 people worldwide [2]. While the majority of RP patients have ocular symptoms only, about 20~30% of patients with RP are complicated with nonocular disorders such as hearing loss, obesity, and cognitive impairment [3].

RP is a prototypic, genetically heterogeneous disorder transmitted as autosomal dominant, autosomal recessive, X-linked, or mitochondrial modes of inheritance [1]. Presently, 54 genes involved in human nonsyndromic RP have been recognized. Among genes identified, a total of at least 35 genes and loci have been found to cause arRP (RetNet, https://sph.uth.edu/retnet/sum-dis.htm). However, the identified genes still explain no more than half of the RP clinical cases and there has been limited success with approaches of screening known candidate genes for RP by conventional Sanger sequencing. Recently, exome sequencing has been successfully used for the disease gene identification of Mendelian disorders [4, 5]. Coupled with DNA capture technology, this next-generation sequencing (NGS) analysis enables rapid and cost-effective parallel sequencing of a large panel of disease genes. In several recent studies, NGS has provided a promising alternative for the molecular diagnosis and gene identification of RP [6–10].

Here, we used exome sequencing to identify *retinol dehydrogenase 12* (*RDH12*) as responsible for RP in a Chinese

Table 1: Family member phenotypes and genotypes.

Family member	Age (year)/sex	Onset age (year)	Visual acuity (OD/OS)	Fundus appearance	Mutation	Mutation type
I1	74/M		0.6/0.6[#]	Normal	—	—
I2	72/F		0.6+/0.8+	Normal	c.437T<A (p.V146D)	Het
I4	83/F		0.5/0.5	Normal	c.437T<A (p.V146D)	Het
II2	52/F		1.0/1.0	Normal	c.437T<A (p.V146D)	Het
II3	62/F		0.8/0.8	Normal	—	—
III1	28/M	3	Light perception	PP and RVA	c.437T<A (p.V146D)	Hom
III2	19/F	3	Counting fingers	PP and RVA	c.437T<A (p.V146D)	Hom

PP: peripheral pigmentation; RVA: retinal vascular attenuation; RCA: retinal and choroidal atrophy; Hom: homozygous mutation; Het: heterozygous mutation.
[#]Visual acuity of I: 1 was reduced due to the presence of age-related cataract.

family, of which 2 patients showed typical clinical symptoms of RP.

2. Materials and Methods

2.1. Subjects. This study was approved by Institutional Review Boards of the Hospital of University of Electronic Science and Technology of China and Sichuan Provincial People's Hospital and the First Hospital of Jilin University. Written informed consents were obtained from all subjects prior to the studies. Control subjects were recruited from the Hospital of University of Electronic Science and Technology of China and Sichuan Provincial People's Hospital.

2.2. Clinical Diagnosis. Clinical information about the family is listed in Table 1. Complete ophthalmic examination of each family member was performed, including best corrected visual acuity (BCVA), slit-lamp biomicroscopy, fundus photography if possible, visual field tests (Octopus; Interzeag, Schlieren, Switzerland), and electroretinography (ERG). ERGs were performed using a multifocal ERG recorder (GT-2008V-IV, Chongqing, China) and corneal contact lens electrodes. The ERG protocol complied with the standards of the International Society for Clinical Electrophysiology of Vision. Diagnosis of arRP was based on the presence of night blindness, fundus observations (retinal pigmentation, vessel attenuation, and various degrees of retinal atrophy), severe loss of peripheral visual field, abnormal ERG measurements (dramatic diminution in amplitudes or complete absence of response), and family history.

2.3. DNA Extraction. All genomic DNA was extracted from peripheral blood using a blood DNA extraction kit (QIAamp DNA Blood Midi Kit; Qiagen, Hilden, Germany) according to the manufacturer's protocol. DNA samples were stored at −20°C until use. DNA integrity was evaluated by 1% agarose gel electrophoresis.

2.4. Exome Sequencing and Variant Detection. The proband of this family (III: 1) was initially analyzed by exome sequencing provided by Axeq Technology Inc., Seoul, Republic of Korea. The sequenced sample was prepared according to the Illumina protocols of Sure Select Target Enrichment System Capture Process and exome sequencing analysis was performed as described previously [11]. Briefly, the reads were mapped against UCSC hg19 (http://genome.ucsc.edu/) by BWA (http://bio-bwa.sourceforge.net/). The SNPs and Indels are detected by SAMTOOLS (http://samtools.sourceforge.net/). The detected variants were annotated and filtered based on public and in-house databases: (i) variants within intergenic, intronic, and UTR regions and synonymous mutations were excluded from downstream analysis; (ii) variants in dbSNP138 (http://www.ncbi.nlm.nih.gov/projects/SNP/), 1000 Genomes Project (ftp://ftp.1000genomes.ebi.ac.uk/vol1/ftp), YH Database (http://yh.genomics.org.cn/), HapMap Project (ftp://ftp.ncbi.nlm.nih.gov/hapmap), and our in-house database generated from 1927 samples of whole exome sequencing were excluded; (iii) possible damaging effect of each variant on protein structure/function was as predicted by SIFT (http://sift.jcvi.org/www/SIFT_chr_coords_submit.html).

2.5. Mutation Validation. The homozygous *RDH12* mutation identified by whole exome sequencing was further confirmed with all the members of the family and 600 normal controls by direct sequencing. Primers flanking the mutation were designed based on genomic sequences of Human Genome database and synthesized by Invitrogen Life Technologies (Shanghai, China): *RDH12*-F: TAAAAGGAAGGGGCAGAGCA; *RDH12*-R: GGTACAGTGAACAACAAGCCA. Direct sequencing was performed according to ABI BigDye sequencing protocols and processed samples were sequenced via an ABI3130XL genetic analyzer.

3. Results

3.1. Clinical Data of the Family. A three-generation family from Jilin Province of China was recruited (Figure 1). Since the parents and grandparents of two affected subjects had no apparent RP symptoms, the disease exhibited a pattern of recessive inheritance in this family. Ophthalmic examinations identified two affected individuals (III: 1 and III: 2) among the 7 examined family members. Affected members with RP in this family exhibited similar clinical features.

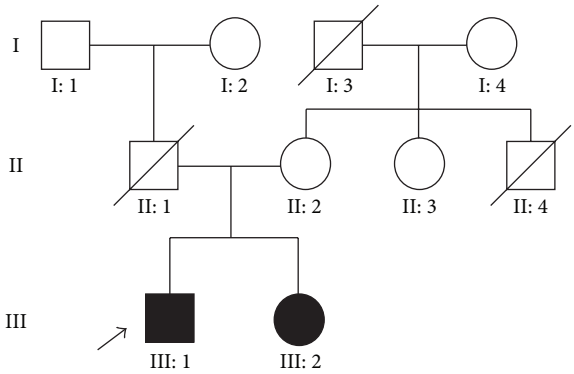

Figure 1: Pedigree of the family with RP. Solid symbols indicate affected individuals. Open symbols indicate unaffected individuals and arrow indicates the proband and slash indicates deceased person.

Fundus examination for the proband showed peripheral pigmentation and retinal vascular attenuation (Figure 2(a), left panel). ERG showed no recordable response under either scotopic or photopic condition, indicating significant loss of the function of both rods and cones (Figure 2(b)). Affected members presented with an early-onset and markedly decreased visual acuity (OD: 20/400, OS: 20/400) in both eyes (Table 1, Figure 2(c)).

3.2. Whole Exome Sequencing and Data Analysis. By exome sequencing of patient III: 1, the proband, with the mean read depth of target regions (52.3x), we identified 20817 SNPs in coding regions (9531 nonsynonymous SNPs, 10732 synonymous SNPs, and 554 other types of SNPs) and 424 coding Indels that may affect amino acid sequence.

To identify the disease-causing mutation, we focused on the functional SNP/Indel in homozygous or compound heterozygous status, including nonsynonymous variants (NS), splice acceptor and donor site mutations (SS), and frameshift coding-region insertions or deletions (Indels), which were more likely to be pathogenic. These proband variants were then compared with the dbSNP138, 1000 Genomes Project, HapMap Project, YH Database, and our in-house generated database using 1927 whole exome sequencing pieces of data. The in-house whole exome variant data were collected from people without any eye disease. Therefore, we could filter out the variants with high frequency in normal controls. Under the autosomal recessive model, the filtered data was narrowed down to 4 compound heterozygous and 13 homozygous variants.

3.3. Mutation Detection and Validation. These filtered variants were then compared with reported retina genes (https://sph.uth.edu/Retnet/) and further confirmed by Sanger sequencing on other family members and normal controls. Finally, we found a homozygous mutation c.437T<A (p.V146D) in the *RDH12* gene (NM_152443) satisfying an autosomal recessive inheritance model (Figure 3). Direct Sanger sequencing confirmed the homozygous mutation in the proband as well as in the proband's affected siblings and found that their mother (II: 2) and grandmothers (I: 2 and I: 4) were unaffected heterozygous carriers of c.437T<A (p.V146D), showing complete cosegregation of the mutation with disease (Table 1). The homozygous mutation described above was absent in 600 ethnicity-matched control samples and the heterozygous mutation was found in only 4 of 600 controls screened by direct sequencing. Together with the clinical presentation of the two affected siblings, these data demonstrate that the homozygous mutation, c.437T<A (p.V146D), in the *RDH12* gene is responsible for RP.

Comparative amino acid sequence alignment of other RDH12 proteins across different species revealed that the mutation occurred at highly conserved positions of exon 4 (Figure 3). This mutation was predicted to be damaging by the SIFT homology tool, usually applied to determine the potential of a substituted amino acid to be deleterious in a protein sequence. The substituted amino acid is predicted to alter the hydrophobicity of RDH12 protein, that is, changing a hydrophobic Valine to a hydrophilic Aspartic acid at position 146.

4. Discussion

Autosomal recessive RP is the most frequent inheritance pattern of RP inheritance, accounting for approximately 50%~60% of all RP patients [1], and the genetic mutations close to 30% of all arRP cases still remain unknown [12]. Next-generation sequencing has proven to be a powerful and cost-effective method for detecting causative mutations in familial RP. Using the techniques of this study, we identified a homozygous mutation, c.437T<A (p.V146D), in *RDH12* as a cause of arRP in a Chinese family.

RDH12, located at chromosome 14q23 with 7 exons and encoding an NADPH-dependent retinal reductase, belongs to the subfamily of retinol dehydrogenases involved in the conversion of all-*trans*-retinal and 11-*cis* retinal to the corresponding retinols [13]. RDH12 protein is expressed predominantly in the inner segments of rod and cone photoreceptors where it plays a critical role in the visual cycle of regenerating 11-cis retinal, the light-absorbing chromophore of rhodopsin, and cone opsins [14]. Defects in this gene have been demonstrated to be a cause of LCA3 (Leber's congenital amaurosis 3) or early-onset retinal dystrophy [15, 16]. Patients with *RDH12* mutations showed severe loss of visual acuity (VA) at an early age and severe reductions in full-field ERG amplitudes [16–18]. Deletion of this gene in mice has been shown to slow the kinetics of all-*trans*-retinal reduction, delaying dark adaptation [18]. Retinas of $Rdh12^{-/-}$ mice had less retinoids compared with $Rdh12^{+/+}$ mice, suggesting that broad photoreceptor outer segment loss occurred in $Rdh12^{-/-}$ mice after intense light. Previous studies also showed that p.Thr49Met mutation in the *RDH12* gene severely decreased RDH activity [15, 18].

It is estimated that *RDH12* mutations account for approximately 3–7% of autosomal recessive retinal dystrophy cases [19–23]. Mutations in *RDH12* as a cause of retinal dystrophy were first reported by Janecke et al. [15] in patients with

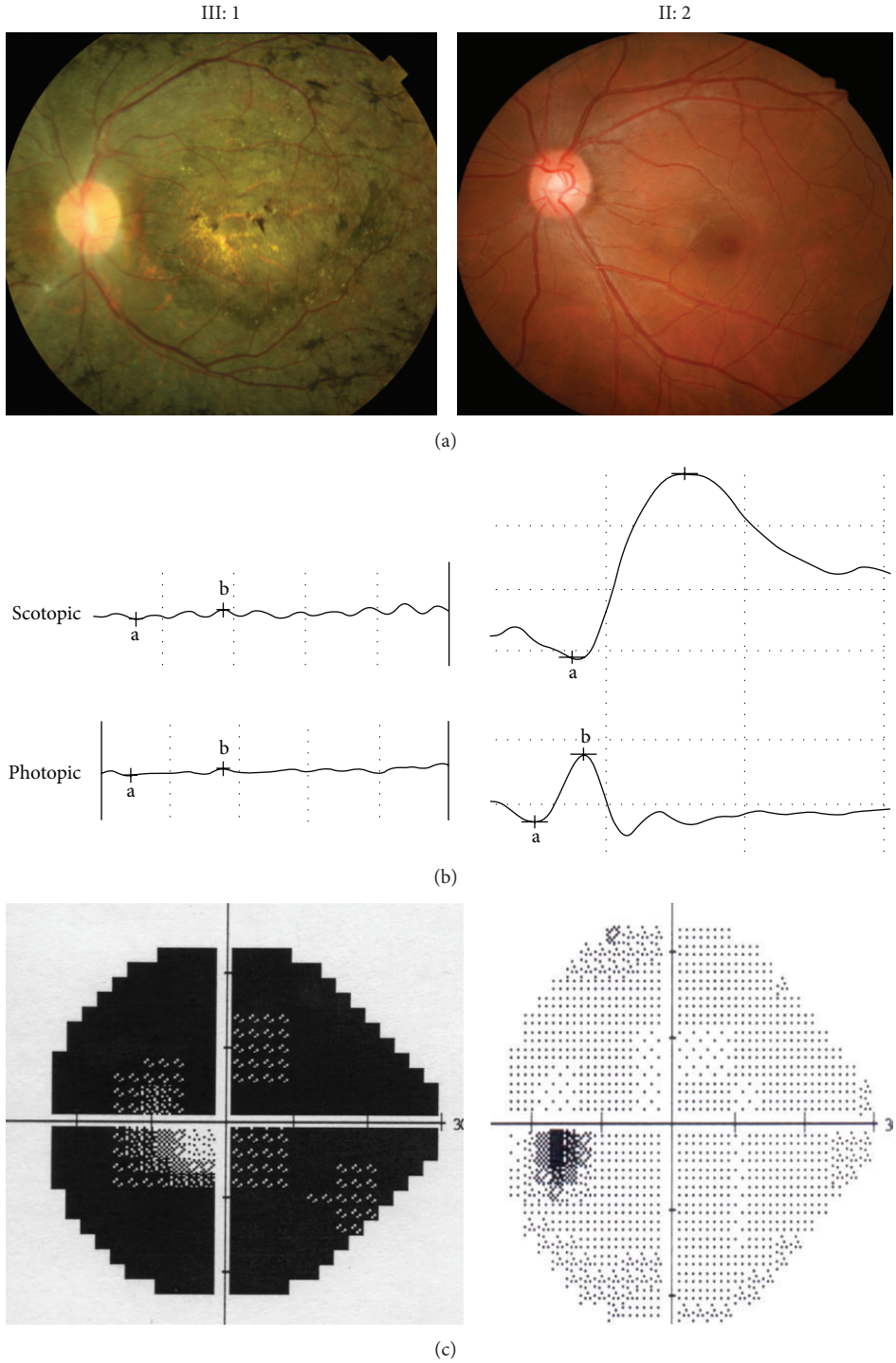

Figure 2: Representative photographs of the proband (III: 1) and one of normal individuals (II: 2) in the Chinese arRP family. (a) Compared to II: 2, the proband's fundus photographs showed peripheral pigmentation and retinal vascular attenuation. (b) ERG records showed no detectable rod and cone responses in the proband (left), compared to the normal rod and cone responses in the normal individual (right). (c) Visual field results showed low vision in the proband, compared to the normal vision in the unaffected individual (right).

early-onset retinal dystrophy. The study identified three homozygous mutations, c.677A<C (p.Y226C), 806delCC-CTG (p.A269fsX270), and c.565C<T (p.Q189X), and two missense mutations in compound heterozygosity, c.146C<T (p.T49M) and c.184C<T (p.R62X). Another study closely followed and reported 11 distinct *RDH12* mutations in homozygosity or compound heterozygosity in 8/44 patients with LCA who were affected with the congenital severe yet progressive rod-cone dystrophy form of the disease [16]. To date, over 60 different *RDH12* mutations have been reported

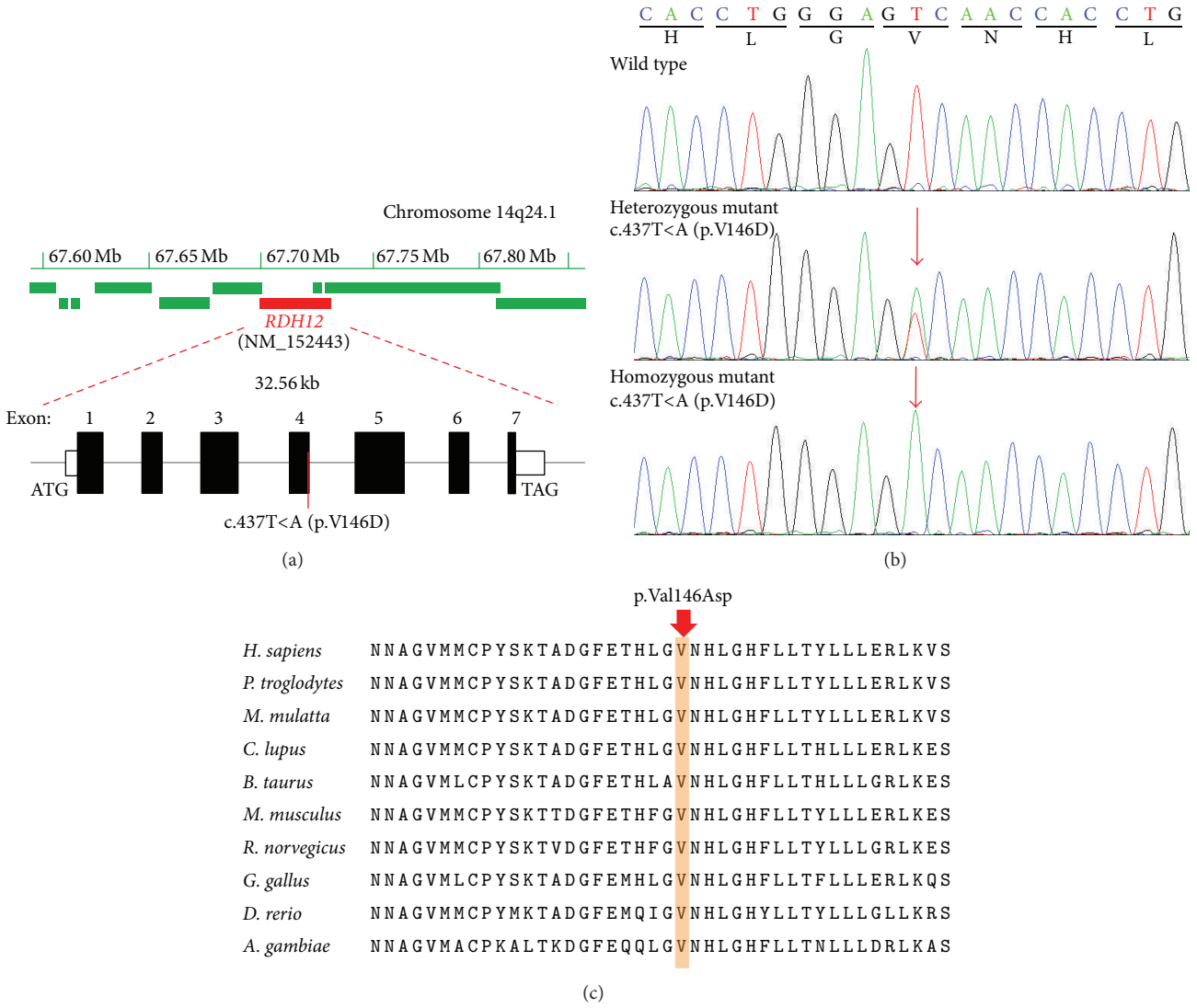

Figure 3: Representative chromatogram of *RDH12* sequence. (a) The *RDH12* gene (red filled box) spanning 32.56 kb on chromosome 14q24.1 (upper panel) contains 7 exons. The identified homozygous variant, c.437T<A (p.V146D), was located in exon 4 of this gene; (b) normal sequence from an unaffected member (I: 1), a heterozygous T to A substitution at codon 146 from unaffected member (I: 2, I: 4, II: 2), and a homozygous change from (III: 1 and III: 2). (c) Orthologous protein sequence alignment of *RDH12* from different species; the mutated residue showing conservation of Valine (V) at codon 146 was shaded in brown.

predominantly in LCA patients [15–17, 21, 23–27] but also in early-onset retinal dystrophy [8, 15, 20, 21, 24, 25], in families with arRP [26, 27], and in a family with autosomal dominant RP [19]. These findings above have shown that mutations in the human *RDH12* gene are responsible for severe forms of blindness.

In our study, a homozygous mutation c.437T<A (p.V146D) of the *RDH12* gene in exon 4 was identified, close to the previously reported missense mutation p.L149P [27]. Initial exome sequencing showed that the mutation was found in a homozygous state in the proband of this family. Further sequence verification showed that the proband's affected sibling (III: 3) also had the same mutation, and the mother (II: 2) of the two affected subjects as well as II: 2's mother (I: 4) in this study was found to carry the mutation c.437T<A (p.V146D) in heterozygosity. The father (II: 1) of the affected subjects was a presumed carrier of the heterozygous mutation in the autosomal recessive model. However, his DNA sample was not collected due to his accidental death several years ago. DNA samples of the grandfather (I: 1) and grandmother (I: 2) of the affected subjects were collected and the heterozygous mutation was found to be present in the grandmother (I: 2). Therefore, it was presumed that this heterozygous variation was inherited from the grandmother (I: 2), and carrying this heterozygous variation was nonpathogenic in the autosomal recessive model. This mutation was absent from 600 normal controls and public databases such as 1000 genomes or Exome Variant Server, excluding them as common polymorphisms. This mutation has been detected in a small arRP family and

considered as a putative pathogenic mutation [28]. Therefore, our results further support the causative role of this *RDH12* mutation in the pathogenesis of RP.

For the p.V146D mutation identified in this pedigree, the p.V146D mutation is predicted probably to be damaging to protein function (PolyPhen2 scores close to 1.0). Through the analysis of membrane topology by TMHMM2.0, we found that the substitution of this mutation is located at the NAD(P)-binding domain of RDH12 protein, which is involved in nucleotide binding. How the mutation exactly affects enzymatic activity of RDH12 is yet to be studied. In order to better understand RP pathogenesis, a functional study is needed to confirm the role of *RDH12* and the underlying mechanisms in the disease.

In conclusion, a homozygous mutation p.V146D in the *RDH12* gene was identified in a Han Chinese family with RP by exome sequencing. Our study not only demonstrates that exome sequencing can be a powerful method for the identification of causative mutations in arRP pedigrees and the diagnosis of genetic diseases, but also provides helpful clues to further investigate genetic factors for arRP.

Conflict of Interests

The authors report no conflict of interests. The authors alone are responsible for the content and writing of the paper.

Authors' Contribution

Bo Gong and Bo Wei contributed equally to this study.

Acknowledgments

This study was supported by grants from the Natural Science Foundation of China (81371048 (Bo Gong), 81400437 (Yu Zhou), 8140030069 (Le Wang), and 81371030 (Houbin Zhang)); the Department of Sichuan Provincial Health (130167 (Bo Gong)); the Science and Technology Department of Sichuan Province of China (2014HH0009 (Houbin Zhang) and 2015HH0031 (Bo Gong)). The authors thank all the participants in this study.

References

[1] D. T. Hartong, E. L. Berson, and T. P. Dryja, "Retinitis pigmentosa," *The Lancet*, vol. 368, no. 9549, pp. 1795–1809, 2006.

[2] C. Rivolta, D. Sharon, M. M. DeAngelis, and T. P. Dryja, "Retinitis pigmentosa and allied diseases: numerous diseases, genes, and inheritance patterns," *Human molecular genetics*, vol. 11, no. 10, pp. 1219–1227, 2002.

[3] C. Hamel, "Retinitis pigmentosa," *Orphanet Journal of Rare Diseases*, vol. 1, no. 1, article 40, 2006.

[4] S. B. Ng, E. H. Turner, P. D. Robertson et al., "Targeted capture and massively parallel sequencing of 12 human exomes," *Nature*, vol. 461, no. 7261, pp. 272–276, 2009.

[5] S. B. Ng, K. J. Buckingham, C. Lee et al., "Exome sequencing identifies the cause of a mendelian disorder," *Nature Genetics*, vol. 42, no. 1, pp. 30–35, 2010.

[6] K. Neveling, R. W. J. Collin, C. Gilissen et al., "Next-generation genetic testing for retinitis pigmentosa," *Human Mutation*, vol. 33, no. 6, pp. 963–972, 2012.

[7] J. O'Sullivan, B. G. Mullaney, S. S. Bhaskar et al., "A paradigm shift in the delivery of services for diagnosis of inherited retinal disease," *Journal of Medical Genetics*, vol. 49, no. 5, pp. 322–326, 2012.

[8] S. Katagiri, M. Akahori, Y. Sergeev et al., "Whole exome analysis identifies frequent CNGA1 mutations in Japanese population with autosomal recessive retinitis pigmentosa," *PLoS ONE*, vol. 9, no. 9, Article ID e108721, 2014.

[9] J. Wu, L. Chen, O. S. Tam, X. F. Huang, C. P. Pang, and Z. B. Jin, "Whole exome sequencing reveals genetic predisposition in a large family with retinitis pigmentosa," *BioMed Research International*, vol. 2014, Article ID 302487, 6 pages, 2014.

[10] A. Villanueva, J. R. Willer, J. Bryois, E. T. Dermitzakis, N. Katsanis, and E. E. Davis, "Whole exome sequencing of a dominant retinitis pigmentosa family identifies a novel deletion in *PRPF31*," *Investigative Ophthalmology & Visual Science*, vol. 55, no. 4, pp. 2121–2129, 2014.

[11] Y. Zhou, S. Tao, H. Chen et al., "Exome sequencing analysis identifies compound heterozygous mutation in ABCA4 in a Chinese family with Stargardt disease," *PLoS ONE*, vol. 9, no. 3, Article ID e91962, 2014.

[12] S. P. Daiger, L. S. Sullivan, and S. J. Bowne, "Genes and mutations causing retinitis pigmentosa," *Clinical Genetics*, vol. 84, no. 2, pp. 132–141, 2013.

[13] O. V. Belyaeva, O. V. Korkina, A. V. Stetsenko, T. Kim, P. S. Nelson, and N. Y. Kedishvili, "Biochemical properties of purified human retinol dehydrogenase 12 (RDH12): catalytic efficiency toward retinoids and C9 aldehydes and effects of cellular retinol-binding protein type I (CRBPI) and cellular retinaldehyde-binding protein (CRALBP) on the oxidation and reduction of retinoids," *Biochemistry*, vol. 44, no. 18, pp. 7035–7047, 2005.

[14] F. Haeseleer, G.-F. Jang, Y. Imanishi et al., "Dual-substrate specificity short chain retinol dehydrogenases from the vertebrate retina," *Journal of Biological Chemistry*, vol. 277, no. 47, pp. 45537–45546, 2002.

[15] A. R. Janecke, D. A. Thompson, G. Utermann et al., "Mutations in RDH12 encoding a photoreceptor cell retinol dehydrogenase cause childhood-onset severe retinal dystrophy," *Nature Genetics*, vol. 36, no. 8, pp. 850–854, 2004.

[16] I. Perrault, S. Hanein, S. Gerber et al., "Retinal dehydrogenase 12 (RDH12) mutations in leber congenital amaurosis," *American Journal of Human Genetics*, vol. 75, no. 4, pp. 639–646, 2004.

[17] A. Schuster, A. R. Janecke, R. Wilke et al., "The phenotype of early-onset retinal degeneration in persons with RDH12 mutations," *Investigative Ophthalmology & Visual Science*, vol. 48, no. 4, pp. 1824–1831, 2007.

[18] W. Sun, C. Gerth, A. Maeda et al., "Novel RDH12 mutations associated with Leber congenital amaurosis and cone-rod dystrophy: biochemical and clinical evaluations," *Vision Research*, vol. 47, no. 15, pp. 2055–2066, 2007.

[19] J. H. Fingert, K. Oh, M. Chung et al., "Association of a novel mutation in the retinol dehydrogenase 12 (RDH12) gene with autosomal dominant retinitis pigmentosa," *Archives of Ophthalmology*, vol. 126, no. 9, pp. 1301–1307, 2008.

[20] D. S. Mackay, A. D. Borman, P. Moradi et al., "RDH12 retinopathy: novel mutations and phenotypic description," *Molecular Vision*, vol. 17, pp. 2706–2716, 2011.

[21] D. Valverde, I. Pereiro, E. Vallespín, C. Ayuso, S. Borrego, and M. Baiget, "Complexity of phenotype-genotype correlations in Spanish patients with RDH12 mutations," *Investigative Ophthalmology & Visual Science*, vol. 50, no. 3, pp. 1065–1068, 2009.

[22] D. A. Thompson, A. R. Janecke, J. Lange et al., "Retinal degeneration associated with RDH12 mutations results from decreased 11-cis retinal synthesis due to disruption of the visual cycle," *Human Molecular Genetics*, vol. 14, no. 24, pp. 3865–3875, 2005.

[23] Y.-Y. Didem, T. Berçin, K. Hayyam, and O. R. Köksal, "Genome-wide homozygosity mapping in families with leber congenital amaurosis identifies mutations in *AIPL1* and *RDH12* genes ," *DNA and Cell Biology*, vol. 33, no. 12, pp. 876–883, 2014.

[24] S. Walia, G. A. Fishman, S. G. Jacobson et al., "Visual acuity in patients with Leber's congenital amaurosis and early childhood-onset retinitis pigmentosa," *Ophthalmology*, vol. 117, no. 6, pp. 1190–1198, 2010.

[25] A. Beryozkin, L. Zelinger, D. Bandah-Rozenfeld et al., "Identification of mutations causing inherited retinal degenerations in the Israeli and Palestinian populations using homozygosity mapping," *Investigative Ophthalmology & Visual Science*, vol. 55, no. 2, pp. 1149–1160, 2014.

[26] A. Ávila-Fernández, D. Cantalapiedra, E. Aller et al., "Mutation analysis of 272 Spanish families affected by autosomal recessive retinitis pigmentosa using a genotyping microarray," *Molecular Vision*, vol. 16, pp. 2550–2558, 2010.

[27] O. F. Chacon-Camacho, S. Jitskii, B. Buentello-Volante, J. Quevedo-Martinez, and J. C. Zenteno, "Exome sequencing identifies RDH12 compound heterozygous mutations in a family with severe retinitis pigmentosa," *Gene*, vol. 528, no. 2, pp. 178–182, 2013.

[28] Q. Fu, F. Wang, H. Wang et al., "Next-Generation sequencing-based molecular diagnosis of a Chinese patient cohort with autosomal recessive retinitis pigmentosa," *Investigative Ophthalmology and Visual Science*, vol. 54, no. 6, pp. 4158–4166, 2013.

Hindawi Publishing Corporation
Journal of Ophthalmology
Volume 2015, Article ID 309510, 8 pages
http://dx.doi.org/10.1155/2015/309510

Research Article

Histological Characterization of the Dicer1 Mutant Zebrafish Retina

Saeed Akhtar,[1] Sarita Rani Patnaik,[2] Rakesh Kotapati Raghupathy,[2] Turki M. Al-Mubrad,[1] John A. Craft,[2] and Xinhua Shu[2]

[1]*Cornea Research Chair, Department of Optometry, King Saud University, P.O. Box 10219, Riyadh 11433, Saudi Arabia*
[2]*Department of Life Sciences, Glasgow Caledonian University, Glasgow G4 0BA, UK*

Correspondence should be addressed to Xinhua Shu; xinhua.shu@gcu.ac.uk

Received 29 August 2014; Accepted 29 October 2014

Academic Editor: Houbin Zhang

DICER1, a multidomain RNase III endoribonuclease, plays a critical role in microRNA (miRNA) and RNA-interference (RNAi) functional pathways. Loss of *Dicer1* affects different developmental processes. Dicer1 is essential for retinal development and maintenance. DICER1 was recently shown to have another function of silencing the toxicity of *Alu* RNAs in retinal pigment epithelium (RPE) cells, which are involved in the pathogenesis of age related macular degeneration. In this study, we characterized a *Dicer1* mutant fish line, which carries a nonsense mutation (W1457Ter) induced by N-ethyl-N-nitrosourea mutagenesis. Zebrafish DICER1 protein is highly conserved in the evolution. Zebrafish Dicer1 is expressed at the earliest stages of zebrafish development and persists into late developmental stages; it is widely expressed in adult tissues. Homozygous *Dicer1* mutant fish (DICER1$^{W1457Ter/W1457Ter}$) have an arrest in early growth with significantly smaller eyes and are dead at 14–18 dpf. Heterozygous *Dicer1* mutant fish have similar retinal structure to that of control fish; the retinal pigment epithelium (RPE) cells are normal with no sign of degeneration at the age of 20 months.

1. Introduction

DICER1, the RNase III enzyme, plays a central role in processing the long double stranded RNA (dsRNA) into small RNA molecules, including microRNAs (miRNAs) and small interfering RNAs (siRNAs) [1]. Both miRNAs and siRNAs regulate gene expression through assembling an RNA-induced silencing complex and consequently reducing the levels of functional protein within cells [1, 2]. DICER1 contains different functional domains including N-terminal helicase, DUF283, PAZ, two RNase III, and one dsRNA-binding domain [2]. The helicase domain is necessary for siRNA processing, producing endogenous siRNAs, the PAZ and RNase III domains function in RNA binding and cleavage to produce 2-nt 3′ overhangs and the dsRNA-binding domain has a role for dsRNA and cleavage [3, 4]. The role of DUF283 is unknown. The physiological role of DICER1 is indicated by several studies. Mutation in the *Dicer* gene of zebrafish or of *Caenorhabditis elegans* resulted in developmental arrest [5, 6]. Depletion of *Dicer1* in mouse caused early embryonic lethality [7], while tissue-specific conditional knock-outs of dicer 1 suggested the essential role of Dicer1 in development of various organs [8].

DICER1 plays an important role in regulating retinal development. Damiani et al. conditionally knocked out (CKO) *Dicer1* in mouse retinal progenitors using the Chx10Cre mouse and found abnormal retinal phenotypes after the second postnatal week [9]. Both homozygous and heterozygous *Dicer1* CKO mice exhibited decreased electroretinaogram (ERG) responses, with the lowest ERG response in the homozygous mouse eyes. The homozygous mice presented photoreceptor rosettes at age P16 which increased further by P45, along with displaced photoreceptor clusters. When mice reached the age of 3 months, the rosettes became small and disappeared, following the degeneration of photoreceptors. Georgi and Reh [10] conditionally knocked out Dicer1 using the αPax6cre transgenic line and found that DICER1 depleted retinal progenitor cells did not progress to the late progenitor state, resulting in the lack of horizontal cells and amacrine cells and reduced photoreceptors at P5.

Dicer1 CKO mouse retinas are thinner compared to those of heterozygous littermates, because most of *Dicer1*-depleted cells die through apoptosis. Depletion of *Dicer1* in mature postmitotic rods resulted in fast degeneration with 90% of the outer nuclear layer disappearing at 14 weeks old [11]. The above data suggest *Dicer1* is required for the differentiation and survival of retinal cells.

Recently studies suggest DICER1 plays an important role in the pathogenesis of dry age-related macular degeneration (AMD). Dry AMD patients have a lower DICER1 level in retinal pigment epithelium (RPE) cells compared to that of healthy individuals. Deficiency of DICER1 in mouse RPE cells results in RPE degeneration induced by *Alu* RNA toxicity [12]. Further study discovered that *Alu* RNA accumulation could activate the NLRP3 inflammasome and trigger MyD88-mediated signaling, which lead to RPE cell degeneration [13]. Zebrafish has been widely used as a model to study retinal development and to understand the molecular mechanisms of retinal degeneration [14, 15]. To use zebrafish as a model to study the functional role of DICER1 in zebrafish retina, we examined the expression of *Dicer1* during development and in adult tissues. We also morphologically characterized the retina of aged *Dicer1* mutant zebrafish.

2. Materials and Methods

2.1. Ethics Statement. All the experiments using zebrafish were approved by the Animal Ethics and Welfare Committee, Department of Life Sciences, Glasgow Caledonian University. The project was approved by Home Office under a Project License PPL 60/4169.

2.2. Zebrafish Maintenance. AB strain zebrafish were obtained from the MRC Human Genetics Unit, Edinburgh, and maintained as an inbred stock in Glasgow Caledonian University Zebrafish Facility. Larvae and adult fish were kept in the ZEBTEC zebrafish housing system (Tecniplast) on a 14 : 10 h light/dark photoperiod at 28°C and were fed with brine shrimp twice a day.

2.3. Zebrafish Dicer1 Mutant Line. The *Dicer1* mutant zebrafish line (Hu0894) was obtained from Wellcome Trust Sanger Institute and bred in our zebrafish facility. The Hu0894 mutant strain was induced by ENU (N-ethyl-N-nitrosourea) mutagenesis [16] and carried a premature stop mutation: G4371A (W1457Ter) referencing zebrafish *Dicer1* in the Ensembl website (ENSDART00000045881.5). Wienholds et al. [5] reported an ENU-induced mutant zebrafish strain (hu894) carrying a G4338A mutation (W1446X) and we compared the originally reported sequence (GenBank accession number AY386319) with the current referencing zebrafish *Dicer1* gene (GenBank accession number NM_001161453.2) and found that both mutant strains carried the same mutation.

2.4. Genotyping. Zebrafish tail clips were placed in 96-well plate. 25 μL of 100% ethanol was added to each well and incubated at 80°C. 25 μL of TE Tween-20 (with 5 mg/mL of Proteinase K) was added to each well and then incubated overnight at 56°C. The samples were then heated to 95°C for 15 min to inactivate Proteinase K. 75 μL of dH_2O was added to each sample.

Polymerase chain reaction (PCR) was performed using *Taq* DNA polymerase (NEB, M0273X) using the manufacturer's instructions. PCR reactions were set up in a 96-well PCR plate using the following protocol: 95°C for 2 min and then 35 cycles of 94°C for 30 sec, 58°C for 30 sec and 72°C for 60 sec, cooling to 4°C, and storage at 4°C. Aliquots of PCR were loaded onto 1% agarose gel and visualized with ethidium bromide staining. The primers specific for Dicer1 were 5′ TGCCATGTATGTGGCCATCCA 3′ and reverse: 5′ AACACAGTGCTGTCTGGAGGT 3′. Products of PCR reactions were sent for sequence determination.

2.5. Bioinformatic Analysis. Peptide sequences of Human (*Homo sapiens*: NP_803187.1), Cow (*Bos taurus*: NP_976235.1), Mouse (*Mus musculus*: NP_683750.2), Chicken (*Gallus gallus*: NP_001035555.1), Platanna (*Xenopus laevis*: NP_001163918.1), Zebrafish (*Danio rerio*: NP_001154925.1), Fruit fly (*Drosophila melanogaster*: NP_524453.1), Nematode (*Caenorhabditis elegans*: NP_498761.2), and Yeast (*Schizosaccharomyces pombe*: NP_588215.2) were obtained from NCBI and aligned using CLUSTALW program (http://www.ebi.ac.uk/Tools/msa/clustalw2/) and conserved regions were boxshaded using BoxShade 3.21 (http://www.ch.embnet.org/software/BOX_form.html). The primers were designed using NCBI primer design tool (http://www.ncbi.nlm.nih.gov/tools/primer-blast/) based on the coding sequences of Zebrafish *Dicer1* (NM_001161453.2) and *Beta-actin* (NM_131031.1).

2.6. Expression Analysis. Total RNA was extracted from different adult tissues and development stages of Zebrafish using Absolutely RNA Miniprep kit (Agilent) and reverse transcribed using Trancriptor high fidelity cDNA synthesis kit (Roche). Temporal and spatial gene expression patterns were examined by reverse transcript PCR (RT-PCR) using the NEB standard Taq polymerase system with the obtained cDNA of different tissues and development stages as a template. A 570 bp *Dicer1* fragment was amplified using forward: 5′ CAGAATAAAGATTTAGCGAATGG 3′ and reverse 5′ CTGCTTCTCCGGTGGTAG 3′ primers. Beta actin has been used as a house keeping gene and the primers forward: 5′ TGCCATGTATGTGGCCATCCA 3′ and reverse: 5′ AACACAGTGCTGTCTGGAGGT 3′ were used to amplify a 517 bp fragment. Gel electrophoresis was carried out on a 1% agarose gel.

2.7. Histology and Ultrastructure of Zebrafish Retina. Zebrafish were sacrificed using Schedule 1 method. Eyes from wild type and heterozygous Dicer mutant zebra fish at age of 20 months were fixed in 2.5% glutaraldehyde in 0.1 M phosphate buffer (PBS). The eyes were washed in 0.1 M PBS (15 minutes ×3) then fixed in 1% osmium tetroxide in 0.1 M PBS. The eyes were washed with distilled water and dehydrated (15 minutes ×3) in the graded series of ethanol (50% to 100%) and acetone (100%). The eyes were then infiltrated with a mixture

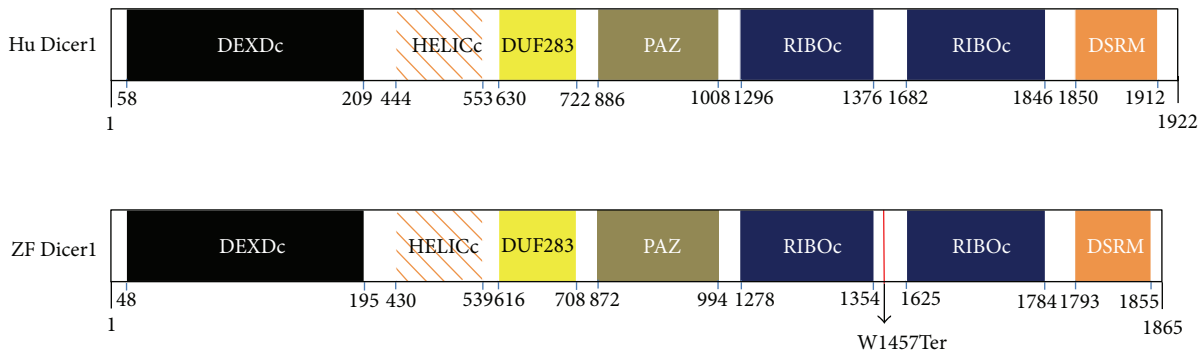

FIGURE 1: Schematic structure of human (Hu) and zebrafish (ZF) DICER1 proteins. Both human and zebrafish DICER1 have similar functional domains: N-terminal helicase domains (DEXDc and HELICc), Dicer dimerization domain (DUF283), PAZ domain, two ribonuclease III C terminal domains, and the double-stranded RNA binding motif (DSRM). The W1457Ter mutation was shown.

of acetone + spur resin (50 : 50) for one hour and then into 100% resin (for 8 hours ×3). The eyes were polymerized into spur resin ant 70°C for 8 hours. Ultrathin sections were stained with uranyl acetate and lead citrate and observed under transmission electron microscope JEOL 1400. Digital micrographs were taken by side mounted *Valita* and bottom mounted *Quamisa* camera.

3. Results

3.1. Expression of Zebrafish Dicer1. Zebrafish *Dicer1* encodes an open reading frame of 1865 amino acids and consists of at least 27 exons, spanning ~43 kb of genomic sequence on chromosome 17. Zebrafish DICER1 has similar functional domains to that of human DICER1 (Figure 1). Alignment of DICER1 protein sequences from zebrafish and other species exhibited that zebrafish DICER1 is highly homologous to other vertebrate species and less homologous to invertebrate and yeast. The functional domains of zebrafish DICER1 are also strongly conserved across vertebrate species. The helicase superfamily c-terminal domain (HELICc) and the second ribonuclease III C terminal domain (RIBOc) are conserved across vertebrate, invertebrate, and yeast species. The PAZ domain and the double-strand RNA binding motif (DSRM) are conserved across vertebrate and invertebrate species but not in yeast (data not shown).

The temporal and spatial expression pattern of zebrafish *Dicer1* gene during embryogenesis, RT-PCR was carried out; zebrafish *Dicer1* mRNA was readily detected at the time of fertilization and persisted during gastrulation and through the tailbud and larval stages (Figure 2(a)). Zebrafish *Dicer1* expression in adult tissues was examined in total RNAs from zebrafish testis, brain, heart, eye, skin, intestine, liver, ovary, muscle, and kidney by RT-PCR. Zebrafish Dicer1 expression was readily detected in the eye and was detected in other tissues (Figure 2(b)).

3.2. Structure of Dicer Mutant Zebrafish Retina. All the homozygous zebrafish DICER1$^{W1457Ter/W1457Ter}$ fish died on 14–18 dpf because of the general arrest of growth caused by the depletion of DICER1. The eyes of those homozygous mutant fish are significantly smaller than those of age-matched wild type fish at age of 7 dpf. Here we focused on characterising the aged heterozygous DICER1$^{WT/W1457Ter/+}$ fish (Figure 3). Light microscopy observation showed that similar to wild type zebrafish, DICER1$^{WT/W1457Ter/+}$ retina contained an outer nuclear layer, outer plexiform layer, inner nuclear layer, inner plexiform layer, and ganglion cell layer (Figure 4). No abnormality was observed in each layer.

Ultrastructural studies showed that the structure of the retinal pigmented epithelial cells (RPE) of heterozygous *Dicer1* zebrafish was similar to the structure of the RPE cells of age-control zebrafish described by Tarboush et al. [17]. Upper parts of the RPE cells were interdigitated with the outer segment of the photoreceptor and the lower parts of the RPE cells were extended between the outer segments of the photoreceptors (Figure 5(a)). The spindle shape or rounded shape melanin pigmented granules (melanosome) were dispersed in the apical and extended-part of the RPE cells (Figure 5(a)). Above the RPE, Bruch's membrane and blood vessels were observed (Figures 5(a) and 5(b)). The Bruch's membrane had a normal fibrillar structure and did not contain any drusen, a key feature of AMD (Figures 5(a) and 5(b)). The RPE cells contained a large nucleus, mitochondria, melanosomes, and lysosomes (Figure 5(c)). In most of the cones the lamellae were regularly stacked (Figure 5(d)).

The ultrastructure of rods and cones of retina of heterozygous *Dicer1* zebra fish was similar to the structure of rods and cones of retina of normal zebrafish described by Tarboush et al. [17]. The rods consisted of outer segment and inner segment (Figure 6(a)). The outer segment contained parallel disc lamellae (Figure 6(b)) while the inner segment contained large nucleus, electron dense and electron lucent mega mitochondria (Figures 6(a) and 6(c)). The electron dense mega mitochondria consisted of electron dense cisternae which enclosed very narrow electron lucent spaces (Figures 6(d) and 6(e)). The electron lucent mega mitochondria contained cisternae which are surrounded by large electron lucent spaces (Figure 6(f)). The inner nuclear layer, inner plexiform, layer and ganglion cell layers were also similar to those of the

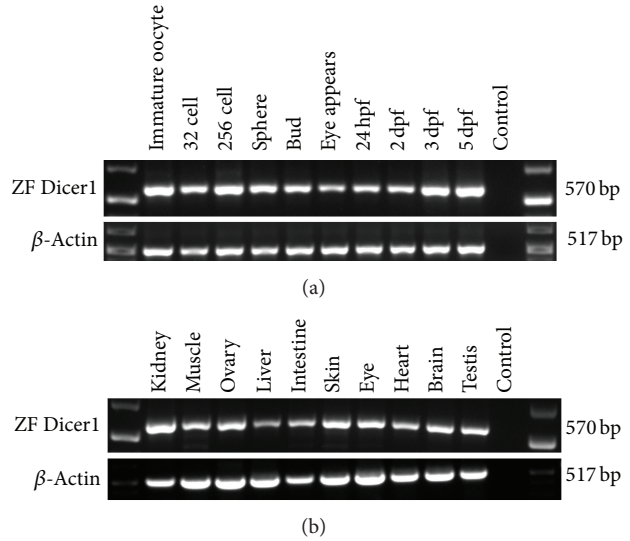

FIGURE 2: Expression of zebrafish *Dicer1*. (a) Temporal expression of zebrafish *Dicer1* transcripts detected by RT-PCR from total RNA extracted from oocytes and at different developmental stages. (b) Zebrafish *Dicer1* expression in different adult tissues detected by RT-PCR.

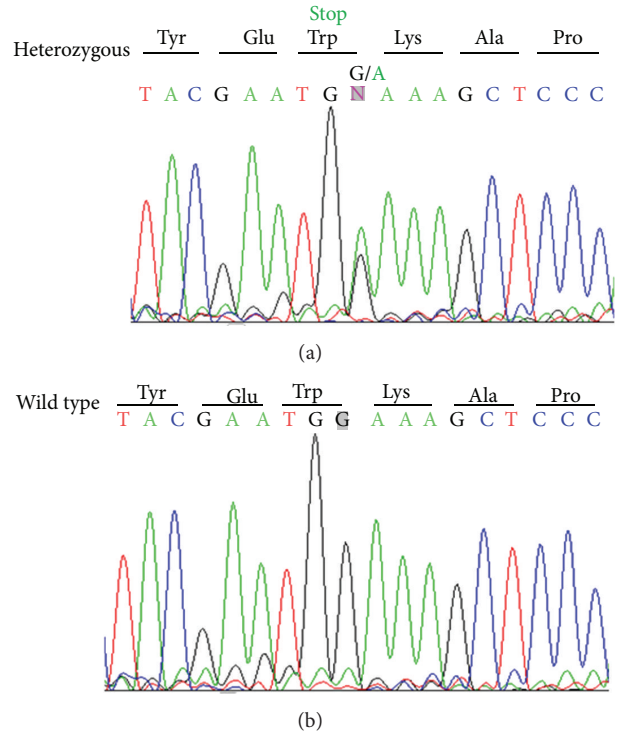

FIGURE 3: Sequence analysis of *Dicer1* genomic DNA in wild type zebrafish (b) and heterozygous zebrafish (a), with predicted changes to the sequence.

normal zebra fish layers (Figures 7(a) and 7(b)). Large nuclei were present in the ganglion cells (Figure 7(b)).

4. Discussion

DICER proteins have been identified in most eukaryotes, for example, animals, plants, and fungi. All DICER proteins reported to date have two RNase III domains. Dicers of higher species generally contain multiple functional domains, but lower eukaryotes frequently have few functional domains, for example, Trypanosoma Dicer has two RNase III domains only [18]. Zebrafish Dicer1 has a complex domain organization, similar to that of other vertebrate species (Figure 1 and data not shown). The zebrafish *Dicer1* gene encodes a protein of 1865 amino acids, which is highly homologous to the Dicer1 proteins identified in other vertebrate species (76%–81% amino acid identity) but shows lower homology to Dicer1 transcripts identified in invertebrate species (31%–49% identity). Analyses of zebrafish *Dicer1* during zebrafish development showed that *Dicer1* is highly expressed in oocytes, early cleavage stage embryos, and at late stage of development. The results are consistent with the recent findings of porcine *Dicer1* that was expressed during embryogenesis [19]. In the adult zebrafish, *Dicer1* expression was observed in all the tissues examined. The expression patterns of *Dicer1* in development and tissues suggest that *Dicer1* has a widespread role in tissue development and maintenance.

DICER1 is required for the production of small RNA molecules (siRNAs and miRNAs) that regulate gene expression [18]. Mouse embryonic stem cells with Dicer1 depletion were defective in differentiation *in vitro* and *in vivo* [20], *Dicer1* complete knock-out mice die before axis formation [21], suggesting that miRNAs play a critical role in mammalian early development. Conditional knock-out of *Dicer1* in mouse retina resulted in abnormal retinal cell differentiation [9, 10, 22]. Inhibition of three miRNAs, let-7, miR-125, and miR-9, caused similar defects in retinal development shown in *Dicer1* conditional knock-out mice, further confirming that miRNAs are essential for early retinal development [23]. Zebrafish *Dicer1* mutant fish, DICER1$^{W1457ter/W1457Ter}$, are not embryonic lethal and go through early developmental stages, presumably due to the function of maternal Dicer1. This is supported by the observation that morpholino knock-down of *Dicer1* caused an earlier developmental arrest [5]. Depletion of both maternal and zygotic zebrafish DICER1 resulted in severe early embryonic morphogenesis, affecting gastrulation, somitogenesis, heart, and neural development [24]. Early eye development was highly delayed in DICER1$^{W1457ter/W1457Ter}$ mutant fish, which presented with very small eyes, compared to those of wild type fish. The heterozygous mutant fish, DICER1$^{WT/W1457Ter}$, did not show any abnormal eye development or any retinal degeneration (Figure 4).

Kaneko et al. showed DICER1 had the ability to degrade toxic RNA molecules [12], which might be involved in the pathogenesis of AMD. AMD is the most common cause of blind registration in the aged population, characterized by a late-onset degeneration of macula. AMD is likely to be a complex disease with the involvement of environmental and genetic factors. Late AMD occurs in two types: dry AMD with geographic atrophy and wet AMD with

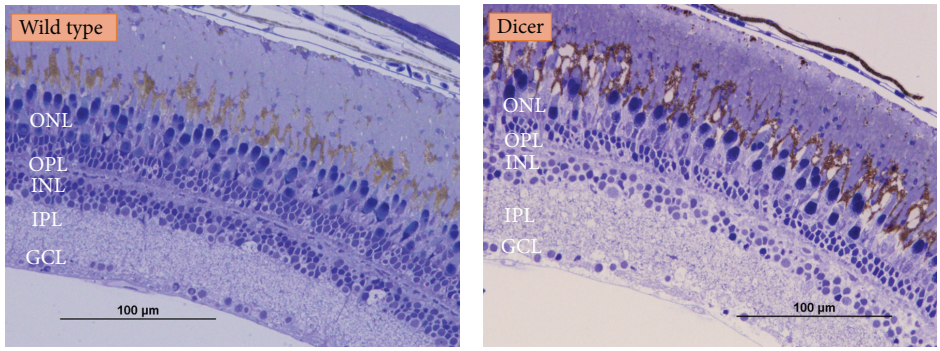

(a) (b)

Figure 4: Light micrograph of histology of retina of normal and *Dicer1* mutant zebrafish. Light micrograph of part of retina showing retinal layers of wild type zebra fish (a); Light micrograph of part of retina showing retinal layers of *Dicer1* heterozygous mutant zebrafish (b). ONL: outer nuclear layer; OPL: outer plexiform layer; INL: inner nuclear layer; IPL: inner plexiform layer; GCL: ganglion cell layer.

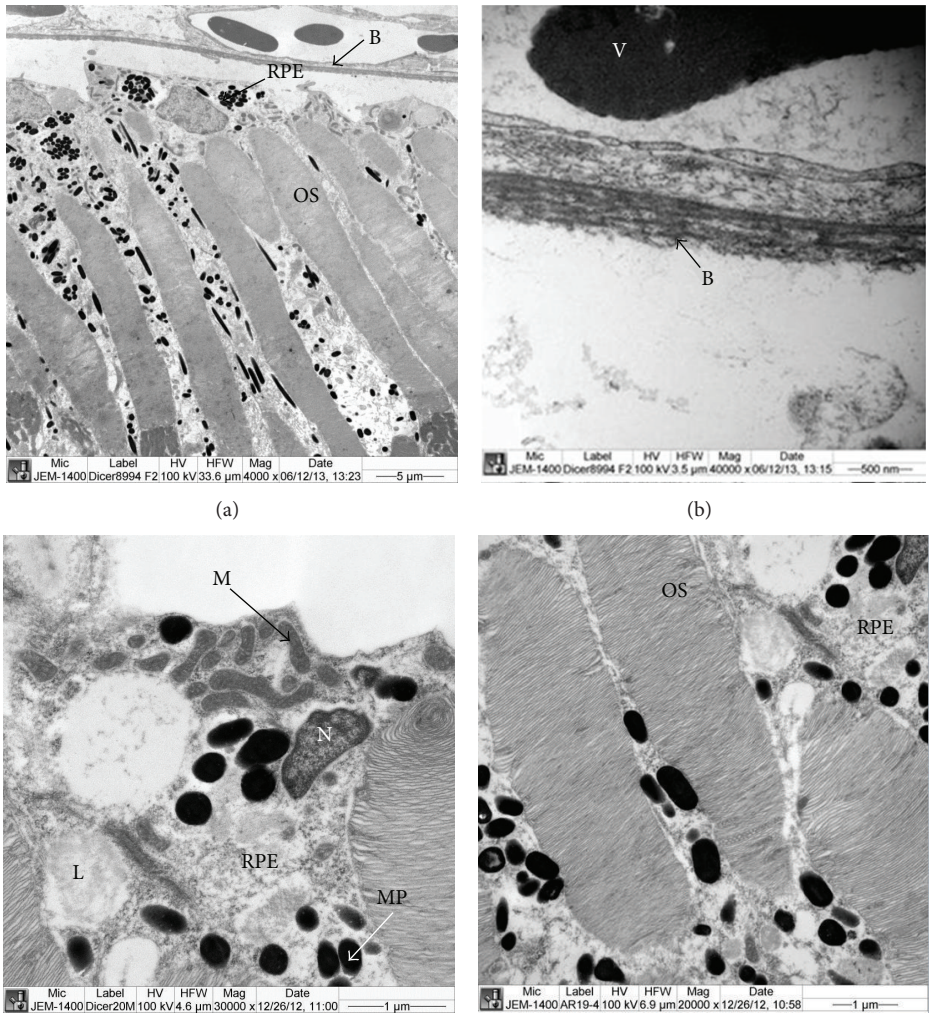

(a) (b)

(c) (d)

Figure 5: Ultrastructure of RPE cells and outer segment of photoreceptor of *Dicer1* mutant zebrafish. (a) Part of Bruch's membrane and RPE cells interdigitate with outer segments (OS) of photoreceptor. The RPE cells contained a large nucleus and melanin pigmented granules. Drusen were not present above the Bruch's membrane. (b) Part of the Bruch's membrane showing the normal fibrillar structure. Drusens were not present above the Bruch's membrane. (c) Part of the outer segment (OS) and RPE containing large nucleus, lysosome, mitochondria, and melanosomes (melanin pigmented granules). (d) Part of the outer segment showing regular disc lamellae. B: Bruch's membrane, GCL: ganglion cell layer, INL: inner nuclear layer, IPL: inner plexiform layer, L: lysosome, M: mitochondria, MP: melanosome (melanin pigmented granules), N: nucleus, ONL: outer nuclear layer, OS: outer segment, PL: photoreceptor layer, RPE: retinal pigmented epithelial cells.

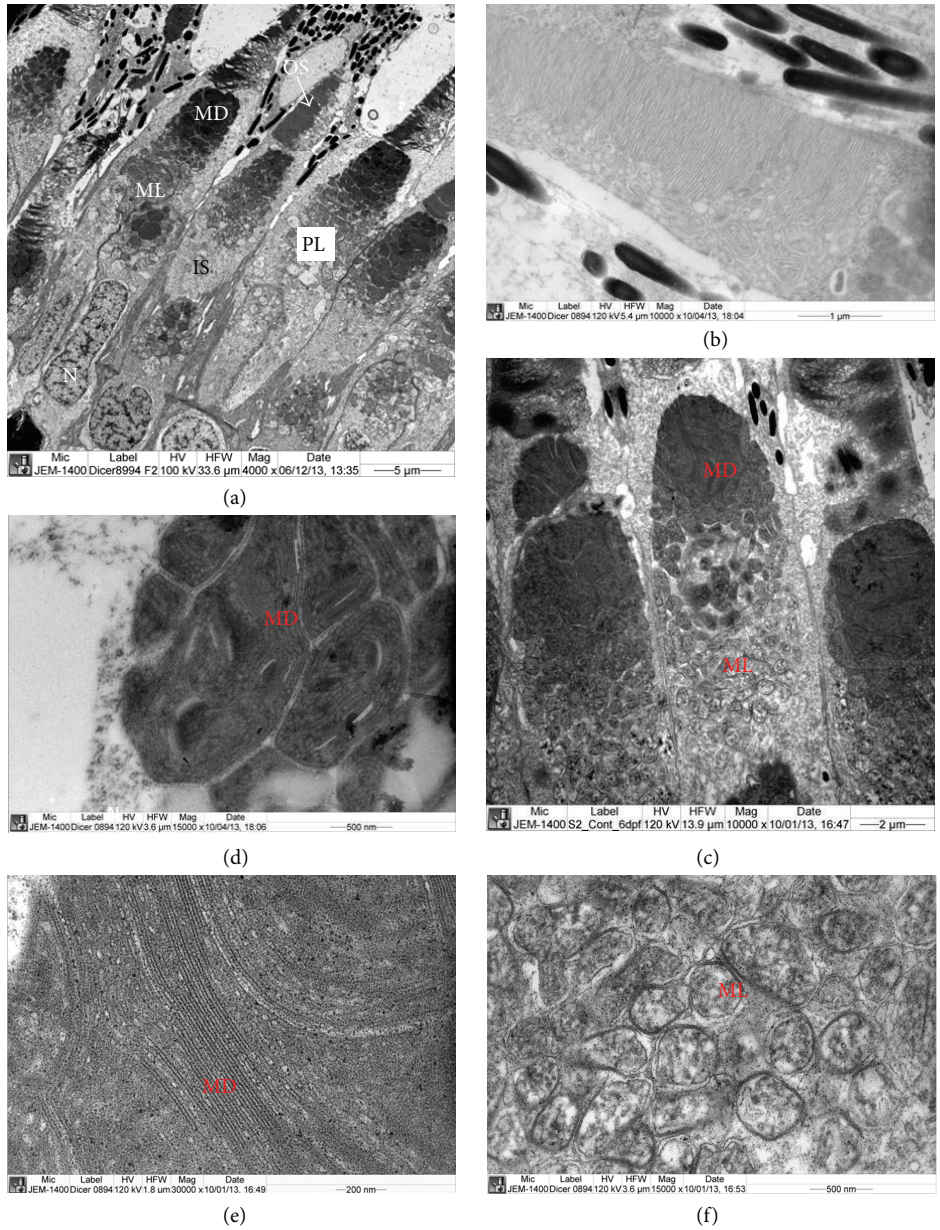

Figure 6: Ultrastructure of the photoreceptor layer of retina of *Dicer1* mutant zebrafish. (a) Part of the photoreceptor layer showing inner and outer segments of cones and rods. The inner segment contains electron dense mega-mitochondria (MD), electron lucent mega-mitochondria (ML), and nucleus. (b) Part of the outer segment containing disc lamellae. (c) Magnified image inner segment containing electron lucent and electron dense mega-mitochondria and large nucleus. (d) Magnified image of MD containing electron dense cisternae. (e) Magnified image of cisternae of MD containing electron lucent spaces between cisternae. (f) Magnified image of ML containing electron lucent cisternae. IS: inner segment, MD: electron dens mega mitochondria, ML: electron lucent mega mitochondria, N: nucleus, OS: outer segment, PL: photoreceptor layer.

choroidal neovasculation [25]. In the RPE cells from dry AMD patients, DICER1 protein level was less than that of RPE cells from controls, but the abundance of *Alu* RNA was significantly increased compared to control RPE cells. DICER1 can degrade *Alu* RNA *in vitro* and *in vivo*, suggesting that reduced DICER1 level leads to the accumulation of Alu RNA and subsequent degeneration of RPE cells in dry AMD patients. Depletion of Dicer1 in mouse RPE cells caused RPE degeneration, which is similar to that in dry AMD patients. Knockdown of *Dicer1* in human RPE cells induced accumulation of *Alu* RNA which caused cytotoxicity [12]. Kaneko et al. did not examine whether there is any RPE degeneration in Dicer1 heterozygous knock-out mice. The *Dicer1* heterozygous mutant fish (DICER1$^{WT/W1457Ter}$) are supposed to have 50% DICER1 protein in RPE cells. Since the function of DICER1 is conserved in evolution, decreased DICER1 protein level might also cause RPE degeneration in aged zebrafish. However, ultrastructural examination of the

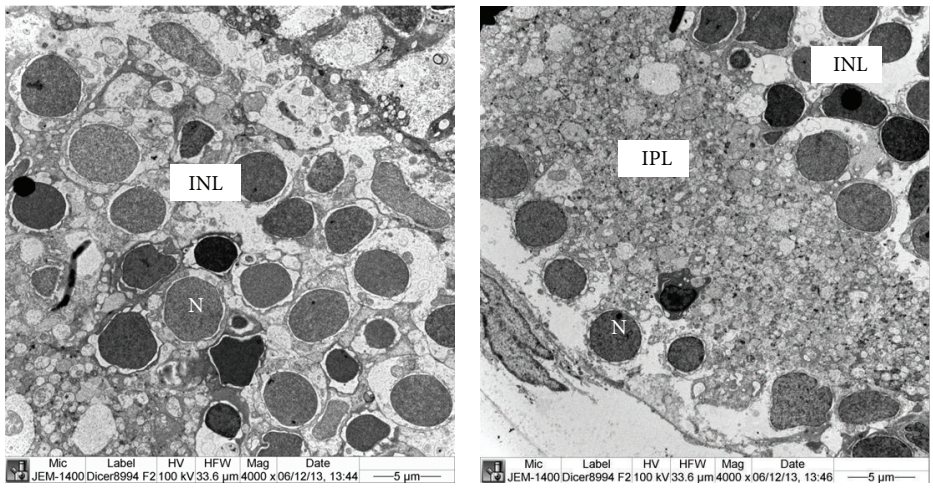

(a) (b)

Figure 7: Ultrastructure of inner nuclear layer and ganglion cell layer of retina of *Dicer1* mutant zebrafish. (a) Part of the inner nuclear layer showing large nuclei. (b) Part of inner plexiform layer and ganglion cell layer containing large nuclei. GCL: ganglion cell layer, INL: inner nuclear layer, IPL: inner plexiform layer, N: nucleus.

heterozygous mutant zebrafish RPE cells did not show any degeneration. Since AMD is a complex disease, both genetic and environmental factors contribute to the progression of the disorder [25]. The complement factor H (CFH) is a major AMD susceptibility gene for AMD, the Y402H substitution is associated with AMD risk [26–28]. Alignment of both human and zebrafish CFH proteins revealed that the human CFH Y402H variant is not conserved in zebrafish CFH (data not shown). So it is possible that the genetic difference results into no RPE degeneration in the heterozygous *Dicer1* mutant fish. It is also possible that zebrafish RPE cells have different microenvironment from mammalian RPE cells. Answers for the above questions require further investigation.

Conflict of Interests

The authors declare that there is no conflict of interests regarding the publication of this paper.

Acknowledgments

The authors would like to thank the Royal Society of London, TENOVUS Scotland, National Eye Research Centre, Visual Research Trust, the W. H. Ross Foundation, the Rosetrees Trust, Fight for Sight, and the Carnegie Trust for the Universities of Scotland for supporting this work. The authors also would like to extend their sincere appreciation to the Deanship of Scientific Research at King Saud University for its funding of this research through the Research Project (RGP-VPP-219). The maintenance of GCU Zebrafish Facility was funded by the EU INTERREG NEW noPILLS programme.

References

[1] V. N. Kim, J. Han, and M. C. Siomi, "Biogenesis of small RNAs in animals," *Nature Reviews Molecular Cell Biology*, vol. 10, no. 2, pp. 126–139, 2009.

[2] M. Jinek and J. A. Doudna, "A three-dimensional view of the molecular machinery of RNA interference," *Nature*, vol. 457, no. 7228, pp. 405–412, 2009.

[3] H. Zhang, F. A. Kolb, L. Jaskiewicz, E. Westhof, and W. Filipowicz, "Single processing center models for human Dicer and bacterial RNase III," *Cell*, vol. 118, no. 1, pp. 57–68, 2004.

[4] I. J. MacRae, K. Zhou, F. Li et al., "Structural basis for double-stranded RNA processing by Dicer," *Science*, vol. 311, no. 5758, pp. 195–198, 2006.

[5] E. Wienholds, M. J. Koudijs, F. J. M. Van Eeden, E. Cuppen, and R. H. A. Plasterk, "The microRNA-producing enzyme Dicer1 is essential for zebrafish development," *Nature Genetics*, vol. 35, no. 3, pp. 217–218, 2003.

[6] A. Grishok, A. E. Pasquinelli, D. Conte et al., "Genes and mechanisms related to RNA interference regulate expression of the small temporal RNAs that control *C. elegans* developmental timing," *Cell*, vol. 106, no. 1, pp. 23–34, 2001.

[7] E. Bernstein, S. Y. Kim, M. A. Carmell et al., "Dicer is essential for mouse development," *Nature Genetics*, vol. 35, no. 3, pp. 215–217, 2003.

[8] J. J. D. Ho and P. A. Marsden, "Dicer cuts the kidney," *Journal of the American Society of Nephrology*, vol. 19, no. 11, pp. 2043–2046, 2008.

[9] D. Damiani, J. J. Alexander, J. R. O'Rourke et al., "Dicer inactivation leads to progressive functional and structural degeneration of the mouse retina," *Journal of Neuroscience*, vol. 28, no. 19, pp. 4878–4887, 2008.

[10] S. A. Georgi and T. A. Reh, "Dicer is required for the transition from early to late progenitor state in the developing mouse retina," *The Journal of Neuroscience*, vol. 30, no. 11, pp. 4048–4061, 2010.

[11] T. R. Sundermeier, N. Zhang, F. Vinberg et al., "DICER1 is essential for survival of postmitotic rod photoreceptor cells in mice," *The Journal of the Federation of American Societies of Experimental Biology*, vol. 28, no. 8, pp. 3780–3791, 2004.

[12] H. Kaneko, S. Dridi, V. Tarallo et al., "DICER1 deficit induces Alu RNA toxicity in age-related macular degeneration," *Nature*, vol. 471, no. 7338, pp. 325–332, 2011.

[13] V. Tarallo, Y. Hirano, B. D. Gelfand et al., "DICER1 loss and Alu RNA induce age-related macular degeneration via the NLRP3 inflammasome and MyD88," *Cell*, vol. 149, no. 4, pp. 847–859, 2012.

[14] X. Shu, Z. Zeng, P. Gautier et al., "Zebrafish Rpgr is required for normal retinal development and plays a role in dynein-based retrograde transport processes," *Human Molecular Genetics*, vol. 19, no. 4, pp. 657–670, 2010.

[15] R. K. Raghupathy, D. L. McCulloch, S. Akhtar, T. M. Al-Mubrad, and X. Shu, "Zebrafish model for the genetic basis of X-linked retinitis pigmentosa," *Zebrafish*, vol. 10, no. 1, pp. 62–69, 2013.

[16] E. de Bruijn, E. Cuppen, and H. Feitsma, "Highly efficient ENU mutagenesis in zebrafish," *Methods in Molecular Biology*, vol. 546, pp. 3–12, 2009.

[17] R. Tarboush, G. B. Chapman, and V. P. Connaughton, "Ultrastructure of the distal retina of the adult zebrafish, *Danio rerio*," *Tissue and Cell*, vol. 44, no. 4, pp. 264–279, 2012.

[18] L. Jaskiewicz and W. Filipowicz, "Role of Dicer in posttranscriptional RNA silencing," *Current Topics in Microbiology and Immunology*, vol. 320, pp. 77–97, 2008.

[19] H. M. Stowe, E. Curry, S. M. Calcatera, R. L. Krisher, M. Paczkowski, and S. L. Pratt, "Cloning and expression of porcine Dicer and the impact of developmental stage and culture conditions on MicroRNA expression in porcine embryos," *Gene*, vol. 501, no. 2, pp. 198–205, 2012.

[20] C. Kanellopoulou, S. A. Muljo, A. L. Kung et al., "Dicer-deficient mouse embryonic stem cells are defective in differentiation and centromeric silencing," *Genes & Development*, vol. 19, no. 4, pp. 489–501, 2005.

[21] E. Bernstein, S. Y. Kim, M. A. Carmell et al., "Dicer is essential for mouse development," *Nature Genetics*, vol. 35, no. 3, pp. 215–217, 2003.

[22] A. Iida, T. Shinoe, Y. Baba, H. Mano, and S. Watanabe, "Dicer plays essential roles for retinal development by regulation of survival and differentiation," *Investigative Ophthalmology and Visual Science*, vol. 52, no. 6, pp. 3008–3017, 2011.

[23] A. La Torre, S. Georgi, and T. A. Reh, "Conserved microRNA pathway regulates developmental timing of retinal neurogenesis," *Proceedings of the National Academy of Sciences of the United States of America*, vol. 110, no. 26, pp. E2362–E2370, 2013.

[24] A. J. Giraldez, R. M. Cinalli, M. E. Glasner et al., "MicroRNAs regulate brain morphogenesis in zebrafish," *Science*, vol. 308, no. 5723, pp. 833–838, 2005.

[25] L. G. Fritsche, R. N. Fariss, D. Stambolian, G. R. Abecasis, C. A. Curcio, and A. Swaroop, "Age-related macular degeneration: genetics and biology coming together," *Annual Review of Genomics and Human Genetics*, vol. 15, pp. 151–171, 2014.

[26] J. L. Haines, M. A. Hauser, S. Schmidt et al., "Complement factor H variant increases the risk of age-related macular degeneration," *Science*, vol. 308, no. 5720, pp. 419–421, 2005.

[27] R. J. Klein, C. Zeiss, E. Y. Chew et al., "Complement factor H polymorphism in age-related macular degeneration," *Science*, vol. 308, no. 5720, pp. 385–389, 2005.

[28] A. O. Edwards, R. Ritter III, K. J. Abel, A. Manning, C. Panhuysen, and L. A. Farrer, "Complement factor H polymorphism and age-related macular degeneration," *Science*, vol. 308, no. 5720, pp. 421–424, 2005.

Hindawi Publishing Corporation
Journal of Ophthalmology
Volume 2015, Article ID 421269, 6 pages
http://dx.doi.org/10.1155/2015/421269

Review Article

Retinitis Pigmentosa Treatment with Western Medicine and Traditional Chinese Medicine Therapies

Jian Xu[1] and Qinghua Peng[2]

[1]*Post-Graduate School, Hunan University of Traditional Chinese Medicine, Changsha, Hunan 410208, China*
[2]*Department of Ophthalmology, the First Affiliated Hospital of Hunan University of Traditional Chinese Medicine, Changsha, Hunan 410007, China*

Correspondence should be addressed to Qinghua Peng; pqh410007@126.com

Received 31 October 2014; Revised 15 February 2015; Accepted 27 February 2015

Academic Editor: David Mansfield

Current management of retinitis pigmentosa (RP) includes an attempt at slowing down the degenerative process through therapies that use either Western or traditional Chinese medicine (TCM). Novel therapies in Western medicine (WM) include use of tailor-made gene therapy, transplantation of stem cells, or neuroprotection treatment. TCM treatment includes two major approaches. These are orally applied herbal decoctions and acupuncture. In fact, all TCM treatments are based on the differentiation of a symptom-complex, which is the characteristic essence of TCM. Thus, diagnosed RP may be treated via the liver, the kidney, and the spleen. The principle behind these treatments is to invigorate the blood and brighten the eyes by toning up the liver and the kidney. Also treatments to cope with deficiencies in the two concepts that are unique and fundamental to TCM are considered: Qi or "vital energy" and Yin and Yang or the harmony of all the opposite elements and forces that make up existence. In particular, the Qi deficiency that results from blood stasis is addressed in these treatments. This paper also puts forward the existing problems and the prospect of the future development on integrating TCM with WM.

1. Introduction

Retinitis pigmentosa (RP) is a group of inherited degenerative retinal diseases, involving progressive degeneration of the retina, typically starting in the midperiphery and advancing toward the macula and fovea [1]. It is associated with night blindness, progressive peripheral visual field loss followed by reduction in central vision, and abnormalities in the electroretinogram (ERG). The prevalence of RP is reported to be 1 in 3000–7000 individuals worldwide [2], with more than 1.5 million patients who suffer from progressive visual deterioration with this disorder [3]. Most RP patients suffering from low-vision or blindness are often severely disabled or legally blind by the end of the second, third, or fourth decade of life. For that reason, it is important that our work focuses on therapy. Over the last few decades, several therapies have been devised for the treatment of RP with gene therapy, stem cell therapy [4], neuroprotection therapy, and TCM treatment, included amongst them.

2. Western Medicine Therapies

2.1. Stem Cell Therapy. Various types of stem cells have been isolated from a variety of tissues including preimplantation embryos, fetuses, birth-associated tissues, and adult organs. Based on the source, these cells can be broadly classified into embryo-derived stem cells (ESCs) and adult tissue-derived stem cells. And based on biochemical and genomic markers, these stem cells can be broadly classified into embryonic stem cells (ESCs), mesenchymal stem cells (MSCs), hematopoietic stem cells (HPSCs), and induced pluripotent stem cells (IPSCs). Stem cell therapy is a novel approach for vision restitution in retinitis pigmentosa [5]. Transplantation of stem cells that can be stimulated to become replacement photoreceptors and be supportive of outer retina cells can theoretically lead to treatments that restore visual function [6].

In recent years, stem cell transplantation therapy in RP has made progress. The mechanisms of stem cells therapy for this disease include the following.

(1) Cell replacement: transplanted stem cells can differentiate into retinal cells and integrate into the retina of patients, and the differentiated stem cells replace the apoptotic or injured retinal cells [7].

(2) Nutritional support: the function of transplanted cells is to release diffusible factors and nutritional substances which act as a local cell delivery system for trophic factors and can promote photoreceptor cell survival [8–10].

(3) Protection of the retinal blood vessels and cones: bone marrow derived stem cells contain endothelial precursors. Through significant upregulation of many antiapoptotic genes, these stem cells can rescue retinal blood vessels that would ordinarily degenerate completely [11, 12]. Researchers have observed that in humans, either the patient's or a normal person's bone marrow cells may provide potential cone neuroprotection to preserve central vision [13].

(4) Promotion synaptic connections: many studies have shown donor cells taken from developing mouse retina at a time coincident with the peak of rod genesis can blend in with cells in a normal adult or a degenerating mouse retina and subsequently build synaptic connections with the remaining retinal cells and, thus, effectively improve visual function [14]. Despite the recent progress made by stem cell transplantation therapy as a treatment for retinal degeneration, many challenges remain. Firstly, the problem of low rate of stem cell survival and migration needs to be resolved. Secondly, despite the retina being physically isolated from the immune system, the immune response that is triggered when stem cells are transplanted into the subretinal space during therapy and hampers their survival cannot be ignored. Thirdly, there are some biosafety issues. For example, the formation of tumors by transplants cannot be ruled out and, therefore, the therapeutic suitability of the stem cells transplanted which include factors such as the age of the patient cannot be ruled out.

2.2. Gene Therapy. The mechanism in gene therapy is the transfer of a therapeutic gene by use of viral or nonviral vectors and requires genetic modification of the ocular cells to produce its therapeutic effect. There are two methods to replace or correct abnormal genes: (1) gene augmentation therapies, where a normal gene is inserted into the genome to replace nonviable or diseased genes using a carrier vector; (2) gene silencing therapies, in which the expression of the mutated gene is inhibited by use of ribozyme or RNA interference [15].

Successful augmentation therapies are dependent on efficient transduction of the target cell by Adeno-associated virus (AAV) and sustained expression of the recombinant virus at a sufficient level. To date, more than 30 patients have so far received the gene therapy, ranging in follow-up from 90 days to 1.5 years and no major side effects have been reported [16, 17]. Two approaches have been proposed to silence the abnormal gene: ribozymes and RNAinterference (RNAi). RNAinterference (RNAi) knockdown is an efficacious therapeutic strategy for silencing genes causative for dominant retinal dystrophies [18]. Some studies showed that allele-specific or non-allele-specific knockdown of a dominant GCAP1 mutant can ameliorate photoreceptor dystrophy in dominant RP and cone-rod dystrophy mouse models caused by GCAP1 mutations [18]. However, it may be difficult to judge which model is most relevant to a specific condition in humans. Some of the mutations between humans and animals are not similar. The mutation and the phenotype in the animal model must be viewed with some degree of caution. It cannot therefore be assumed that these are truly representative of the disease that is occurring in the patient until the phenotypes are critically examined using the same criteria. Translational clinical research initiatives are finally offering hope to relatives and patients with RP, but the safety of these techniques has yet to be established in large animal and human experiments.

2.3. Neuroprotection Therapy. Neuroprotection provides a sympathetic environment to prolong the viability of the photoreceptors by their effect on the secondary biochemical pathways. It is a therapeutic strategy which can be achieved either by delivering neurotrophic growth factors, on the one hand, or inhibiting proapoptotic pathways on the other. It can also be delivered by the implementation of viability factors such as the rod-derived cone viability factor for the treatment of retinal neurodegenerative disease that is independent of the etiology of the degeneration. A number of neurotrophic growth factors that slow photoreceptor death in animal models have been identified: basic fibroblast-derived growth factor (bFGF), brain-derived neurotrophic factor (BDNF), cardiotrophin-1, nerve growth factor (NGF), fibroblast growth factor (FGF), and CNTF.

The final common pathway of all types of RP is photoreceptor cell death. Leonard et al. [19] reported that the X-linked inhibitor of apoptosis protein (XIAP) was thought to be the most potent member to promote cell preservation. They used Adeno-associated virus (AAV) mediated delivery of XIAP to study its neuroprotective effect. Their results showed that XIAP treated eyes of homozygous albino transgenic rats had significantly preserved outer nuclear layers than their contralateral untreated counterparts. Recent evidence [20, 21] has highlighted the importance of calpain activation for both photoreceptor cell death and survival. The authors of these studies have proposed the use of highly specific calpain inhibitors to prevent or delay RP. Recent evidence derived from studies on rod-derived cone viability factor (RdCVF) protein injections in a type of rhodopsin mutation, in the P23H rat, showed that this induced an increase in cone cell number. This suggests that RdCVF is a promising therapeutic option for saving rods [22]. Another new study [3] has shown that decreased cellular ATP levels may result in the pathology of this eye disease and perhaps also in RP and other similar neurodegenerative diseases. Therefore, neuroprotection may prevent or forestall the progression of such incurable eye diseases that ultimately lead to blindness. Ikeda et al. [3] described small compounds (Kyoto University Substances, KUSs) that were developed

to inhibit the ATPase activity of valosin-containing protein (VCP), which is the most abundant soluble ATPase in the cell. The authors showed that KUSs, as well as exogenous ATP or ATP-producing compounds, suppressed endoplasmic reticulum stress and demonstrably protected various types of cultured cells including retinal ones from death. KUSs prevented photoreceptor cell death and preserved visual function in rd10, a mouse model of RP.

3. Traditional Chinese Medicine (TCM) Therapies

3.1. TCM Pathogenesis of RP. TCM therapy is based mainly on the practice of Chinese medicine and is constantly enriched and developed by practical experience. In ancient times, Chinese people discovered that certain foods reduced or eliminated certain diseases. This became the basis of Chinese herbal medicine. It is thought that ancient peoples discovered that fomenting a painful area of the body with the warmth of a fire or the use of warm leather or bark bags or hot stones or sand eliminated the discomfort caused by pain. While using stone as a production tool, people discovered that after a certain part of the body being stabbed, the pain in another part could be relieved, thereby creating treatment methods of using stone and bone needles, which was developed into acupuncture and therefore the formation of meridian.

Retinitis pigmentosa (RP) belongs to the high-altitude wind sparrow's vision category in TCM. High-altitude wind sparrow's vision was described in the book *Taiping-sengxian Prescriptions* in 992 AD for the first time. This classical work recorded more than 16,800 prescriptions and was descended to later generations popularly. Treatment determination based on syndrome differentiation is an essential principle in TCM in understanding and treating disease. It is a specific research and treatment method of disease in TCM and also one of the essential characteristics of TCM. TCM believes that the congenital deficiency with debilitation of the life gate fire is the main reason that causes RP. Other pathogenic factors of RP in TCM include liver and kidney deficiency with essence and blood insufficiency, or spleen and stomach deficiency with Qi and blood insufficiency. Finally, these elements can result in blood stagnation and vessel insufficiency, leading to a loss of nourishment to the eyes, and these will whittle down the spirit light of the pupil, narrow of the visual field, and nocturnal blindness. In TCM, this condition is referred to as high-altitude wind internal obstruction or high-altitude wind sparrow's vision. In recent years, many TCM ophthalmologists conducted further study of the pathogenesis of this disease. For example, Peng [23] proposed and demonstrated blood stasis in deficient pattern type of pathogenesis in patients with retinitis pigmentosa. They put forward that in the treatment of this disease, some additional Chinese medicines which can remove the blood stasis and promote the blood circulation need to be used on the basis of ameliorating deficient pattern and, by doing so, may achieve more satisfactory results [24]. This study gives some new insights on Chinese medicine treatment for RP. However, the main hurdle remaining in the traditional Chinese medicine (TCM) theory is that the success of these treatments depends on proper symptom-complex differentiation, which may also include the stage of the disease, the patient's age, systemic and environmental factors, and so on.

Orally applied herbal decoctions and acupuncture treatment have a role in relieving symptoms and improving visual function in patients.

3.2. Oral Herbal Decoctions for RP Treatment. All TCM treatments are differentiated on the symptom-complex seen. This is the essence of TCM therapy. High-altitude wind sparrow's vision can be treated from the liver, the kidney, or the spleen. TCM differentiates the pathogenesis of this disease into four different syndromes, including deficiency of the liver-Yin and kidney-Yin, deficiency of the spleen and Qi, insufficiency of the kidney-Yang, and deficiency of the Qi and blood stasis. Among these multifaceted symptom complexes, deficiency of the liver-Yin and kidney-Yin is the most common clinical pattern observed. Different syndromes are prescribed very different treatments. For example, deficiency of the liver-Yin and kidney-Yin is treated by modified Ming Mu Di Huang decoction, which nourishes and tones the liver and the kidney and leads to invigorating the blood and brightening the eyes. In this formula of modified Ming Mu Di Huang decoction, the Chinese herbal drugs, Shudihuang, Danggui, Wuweizi, and Gouqizi, work on supplementing liver and kidney. The Chinese herbal drugs, Danpi, Danshen, Yemingsha, and Chongweizi, can also clear heat and invigorate blood. Chinese herbal drugs Shan Zhu Yu and Shen Di Huang reinforce the kidney, which may improve eyesight by replenishing vital essence. The formula achieves the purpose of seeking Yang within Yin, bringing true Yang back to its origin and unblocking the vessels and collaterals. So the actions of this formula are nourishing and tonifying liver and kidney. And they can invigorate blood and brighten the eyes. A recent study [25] in China reported that using TCM treatment on RP resulted in a satisfactory clinical curative affect, and it was worth publicizing. In this study, researchers observed 83 eyes of 42 patients whose TCM diagnoses were high-altitude wind sparrow's vision (deficiency of the liver-Yin and kidney-Yin). After treatment by modified Ming Mu Di Huang decoction, the visual acuity and visual fields in these cases had obvious improvement. Many studies demonstrate that the modified Ming Mu Di Huang decoction may protect apoptosis of photoreceptor cells in retinal degeneration. So it stabilizes the symptoms and delays the progression of RP. The blood moving medicinals include Dang Gui and Dan San that enhance the effect of nourishing and invigorating blood. And thus, they make an impact on the preserving the vision and prevent optic atrophy or blindness.

3.3. Acupuncture for RP Treatment. Acupuncture has been applied as a therapeutic medical technique in China since at least 2,000 years ago, when stone knives and other sharp instruments were used. The term itself is derived from Latin "acus" meaning needles and "punctura" meaning puncture. In this form of treatment, some diseases of the body can be treated by puncturing the points on the body surface to

Table 1: Common clinical patterns and clinical treatments in TCM.

	Kidney-Yang deficiency	Liver- and Kidney-Yin deficiency	Spleen Qi deficiency
Tongue body	Pale with a white coating	Pink with a thin coating	Pale with teeth marks and a thin white coating
Pulse	Deep and weak	Thready	Thready and weak
Principles	Warm and tonify kidney-yang, invigorate blood, and brighten the eyes	Nourish and tonify liver and kidney, invigorate blood, and brighten the eyes	Supplement the spleen and benefit Qi, invigorate blood, and brighten the eyes
Formula	Modified You Gui Wan Zhi Fu Zi 6 g Rou Gui 6 g Shu Di Huang 15 g Shan Zhu Yu 10 g Sang Shen Zi 12 g Gou Qi Zi 15 g Huai Shan Yao 10 g Dang Gui 10 g Tu Si Zi 15 g Rou Cong Rong 10 g Chuan Xiong 10 g Niu Xi 15 g	Modified Liu Wei Di Huang Wan Shudihuang 15 g Shan Zhu Yu 15 g Huai Shan Yao 15 g Mu Dan Pi 10 g Fu Ling 10 g Ze Xie 10 g Dan Shen 10 g Niu Xi 10 g Chuan Xiong 10 g Gan Cao 6 g	Modified Bu Zhong Yi Qi Tang Chai Hu 10 g Huang Qi 15 g Dang Shen 10 g Bai Zhu 10 g Dang Gui 10 g Ge Gen 20 g Hong Hua 3 g Man Jing Zi 10 g Bai Ji Li 10 g Dan Shen 12 g Ye Ming Sha 12 g Cang Zhu 10 g Gan Cao 5 g
Acupuncture (main points)	BL1 (Jing Ming) ST1 (Cheng Qi) EX-HN7 (Qiu Hou) GB20 (Feng Chi) BL18 (Gan Shu) BL23 (Shen Shu) ST36 (Zu San Li) GB37 (Guang Ming) SP6 (San Yin Jiao)	GB20 (Feng Chi) EX-HN13 (Yi Ming) EX-HN7 (Qiu Hou) BL2 (Cuan Zhu) ST2 (Si Bai) SI6 (Yang Lao) LI4 (He Gu) SP6 (San Yin Jiao) LR3 (Tai Chong) BL18 (Gan Shu) BL23 (Shen Shu) KI3 (Tai Xi)	BL17 (Ge Shu) BL20 (Pi Shu) GB20 (Feng Chi) EX-HN13 (Yi Ming) EX-HN7 (Qiu Hou) BL2 (Cuan Zhu) ST2 (Si Bai) SI6 (Yang Lao) LI4 (He Gu) SP6 (San Yin Jiao) LR3 (Tai Chong)

regulate the meridians, Zang-Fu organs, and the circulation of Qi and blood. Acupuncture treatment in RP cases often takes the acupoints such as BL1 (Jing Ming), EX-HN7 (Qiu Hou), GB20 (Feng Chi), LB18 (Gan Shu), LB20 (Pi Shu), ST36 (Zu San Li), and SP6 (San Yin Jiao). The therapist selects 1-2 local points along with two distal acupoints each time. The points should be made with the reinforcing method of needle, which is thought to invigorate the body's healthy Qi and to strengthen weakened physiological function. The filiform needle should be kept for 20–30 minutes in place insertion. For patients who are chronically Yang deficient, one should apply the moxibustion on the distal points or use both needling with moxa. Moxibustion is a therapy in which burning moxa is used to produce a heat stimulation to the human body. It affects the function of the meridians and points to treat or prevent diseases.

Acupuncture may improve the activities and speed of the rod and cone cells of retina, enhance the neural networks and biological activity of the retina cells, and improve the inner circulation, the metabolic activities of retinal epithelium-photoreceptors complexes, and the damages to visual function. Ma et al. [26] used acupuncture dialectical therapy in 15 cases of RP and observed visual acuity, visual field, ERG, and other indicators. The clinical study showed that after treatment, the vision acuity, the visual field distribution, and the ERG-b wave had been improved. The total effective rate was 86.7% and the differences were statistically significant.

However, one problem of acupuncture therapy is that there is no uniform standard and parameters on acupuncture point selection, needling techniques, depth and angle of piercing, gas-getting status, needle retention time, and stimulation methods.

3.4. Common Clinical Patterns and Clinical Treatments in TCM. Some common clinical patterns and clinical treatments in traditional Chinese medicine is summarized in Table 1.

4. Challenges and Outlook

There are many topics in clinical studies on RP. The current approaches against RP include the Chinese herbal medicine, acupuncture, moxibustion, gene therapy, neuroprotection therapy, neurotrophic growth factors, antiapoptotic agents, ribozyme therapy, RNAi, retinal transplantation, dietary supplementation, retinal prostheses, stem cell therapy, and

so on. However, due to the complexity of RP pathogenesis, multiple risk factors, long cycle of RP prevention and control, and the overall prognosis of severe RP remains dismal. There are some obstacles: the success of these treatments depends on proper patient selection; how to successfully translate new therapies in the animal models of the disease; how to effective delivery of the therapy, both genetic material and other neurotrophic factors, and stem cell to the target tissue have been a formidable task. Worldwide researches with numerous samples are expected.

From the long-term perspective, delaying the occurrence and progression of RP and establishing an efficient and practical prevention and control system is the focus of the future RP research in the world. TCM may be able to play an important role in this. Possible future research direction of integrating TCM with western medicine may include (a) TCM treatment of RP by regulating stem cells and (b) TCM treatment of RP by regulating microglia.

In addition, for complicated life phenomenon, both metabonomics and pharmacometabonomics take an organic conception of the human body, which conforms to the way of thinking of traditional Chinese medicine (TCM). The application of metabonomics and pharmacometabonomics in the TCM treatment in RP can deepen the evaluation of the therapeutic effects of TCM in RP through the study of intrinsic quality of TCM syndrome and the treatment by differentiation of syndrome. The research about integration of TCM with modern biological science and technology in RP may provide a new space for the development of therapy against RP, and these treatments would fill an enormous therapeutic gap that we have right now.

Conflict of Interests

The authors declare that there is no conflict of interests regarding the publication of this paper.

Acknowledgment

This study is supported by High-level Health Personnel Training Program Foundation (225 Project) of Hunan Province, China.

References

[1] D. T. Hartong, E. L. Berson, and T. P. Dryja, "Retinitis pigmentosa," *The Lancet*, vol. 368, no. 9549, pp. 1795–1809, 2006.

[2] S. Ferrari, E. Di Iorio, V. Barbaro, D. Ponzin, F. S. Sorrentino, and F. Parmeggiani, "Retinitis pigmentosa: genes and disease mechanisms," *Current Genomics*, vol. 12, no. 4, pp. 238–249, 2011.

[3] H. O. Ikeda, N. Sasaoka, M. Koike et al., "Novel VCP modulators mitigate major pathologies of rd10, a mouse model of retinitis pigmentosa," *Scientific Reports*, vol. 4, article 5970, 2014.

[4] M. A. Musarella and I. M. Macdonald, "Current concepts in the treatment of retinitis pigmentosa," *Journal of Ophthalmology*, vol. 2011, Article ID 753547, 8 pages, 2011.

[5] H. S. Uy, P. S. Chan, and F. M. Cruz, "Stem cell therapy: a novel approach for vision restoration in retinitis pigmentosa," *Medical Hypothesis, Discovery and Innovation in Ophthalmology*, vol. 2, no. 2, pp. 52–55, 2013.

[6] G. Colozza, M. Locker, and M. Perron, "Shaping the eye from embryonic stem cells: biological and medical implications," *World Journal of Stem Cells*, vol. 4, no. 8, pp. 80–86, 2012.

[7] M. S. Singh and R. E. MacLaren, "Stem cells as a therapeutic tool for the blind: biology and future prospects," *Proceedings of the Royal Society B: Biological Sciences*, vol. 278, no. 1721, pp. 3009–3016, 2011.

[8] Y. Inoue, A. Iriyama, S. Ueno et al., "Subretinal transplantation of bone marrow mesenchymal stem cells delays retinal degeneration in the RCS rat model of retinal degeneration," *Experimental Eye Research*, vol. 85, no. 2, pp. 234–241, 2007.

[9] S. Wang, B. Lu, S. Girman et al., "Non-invasive stem cell therapy in a rat model for retinal degeneration and vascular pathology," *PLoS ONE*, vol. 5, no. 2, Article ID e9200, 2010.

[10] M. Mauri, D. Lentini, M. Gravati et al., "Mesenchymal stem cells enhance GABAergic transmission in co-cultured hippocampal neurons," *Molecular and Cellular Neuroscience*, vol. 49, no. 4, pp. 395–405, 2012.

[11] A. Otani, K. Kinder, K. Ewalt, F. J. Otero, P. Schimmel, and M. Friedlander, "Bone marrow-derived stem cells target retinal astrocytes and can promote or inhibit retinal angiogenesis," *Nature Medicine*, vol. 8, no. 9, pp. 1004–1010, 2002.

[12] A. Otani, M. I. Dorrell, K. Kinder et al., "Rescue of retinal degeneration by intravitreally injected adult bone marrow-derived lineage-negative hematopoietic stem cells," *The Journal of Clinical Investigation*, vol. 114, no. 6, pp. 765–774, 2004.

[13] L. E. H. Smith, "Bone marrow-derived stem cells preserve cone vision in retinitis pigmentosa," *Journal of Clinical Investigation*, vol. 114, no. 6, pp. 755–757, 2004.

[14] U. Bartsch, W. Oriyakhel, P. F. Kenna et al., "Retinal cells integrate into the outer nuclear layer and differentiate into mature photoreceptors after subretinal transplantation into adult mice," *Experimental Eye Research*, vol. 86, no. 4, pp. 691–700, 2008.

[15] J. N. Sahni, M. Angi, C. Irigoyen, F. Semeraro, M. R. Romano, and F. Parmeggiani, "Therapeutic challenges to retinitis pigmentosa: from neuroprotection to gene therapy," *Current Genomics*, vol. 12, no. 4, pp. 276–284, 2011.

[16] A. V. Cideciyan, W. W. Hauswirth, T. S. Aleman et al., "Human RPE65 gene therapy for leber congenital amaurosis: persistence of early visual improvements and safety at 1 year," *Human Gene Therapy*, vol. 20, no. 9, pp. 999–1004, 2009.

[17] F. Simonelli, A. M. Maguire, F. Testa et al., "Gene therapy for leber's congenital amaurosis is safe and effective through 1.5 years after vector administration," *Molecular Therapy*, vol. 18, no. 3, pp. 643–650, 2010.

[18] L. Jiang, J. M. Frederick, and W. Baehr, "RNA interference gene therapy in dominant retinitis pigmentosa and cone-rod dystrophy mouse models caused by GCAP1 mutations," *Frontiers in Molecular Neuroscience*, vol. 7, article 25, 2014.

[19] K. C. Leonard, D. Petrin, S. G. Coupland et al., "XIAP protection of photoreceptors in animal models of retinitis pigmentosa," *PLoS ONE*, vol. 2, no. 3, article e314, 2007.

[20] J. Sancho-Pelluz, B. Arango-Gonzalez, S. Kustermann et al., "Photoreceptor cell death mechanisms in inherited retinal degeneration," *Molecular Neurobiology*, vol. 38, no. 3, pp. 253–269, 2008.

[21] F. Paquet-Durand, D. Sanges, J. McCall et al., "Photoreceptor rescue and toxicity induced by different calpain inhibitors," *Journal of Neurochemistry*, vol. 115, no. 4, pp. 930–940, 2010.

[22] Y. Yang, S. Mohand-Said, A. Danan et al., "Functional cone rescue by RdCVF protein in a dominant model of retinitis pigmentosa," *Molecular Therapy*, vol. 17, no. 5, pp. 787–795, 2009.

[23] Q. Peng, *The Integrated Traditional Chinese and Western Medicine: Ocular Fundus Diseases*, vol. 1, People's Military Medical Press, 2011.

[24] P. E. N. G. Qinghua and L. I. Chuanke, "Blood stasis in deficient pattern type of pathogenesis in retinitis pigmentosa," *China Journal of Traditional Chinese Medicine and Pharmacy*, vol. 8, no. 6, pp. 7–10, 1993.

[25] D. Luo, "Bright eye to add and subtract the hope for retinal pigment kidney Yin deficiency degeneration of clinical research," *Chinese and Foreign Medical Research*, vol. 10, no. 5, pp. 4–6, 2012.

[26] S. Ma, J. Ma, H. Peng, D. Yu, L. Yan, and W. Peng, "Acupuncture dialectical retinitis pigmentosa 15 cases," *Guiding Journal of Traditional Chinese Medicine and Pharmacy*, vol. 18, no. 6, pp. 54–55, 2012.

Hindawi Publishing Corporation
Journal of Ophthalmology
Volume 2015, Article ID 145468, 6 pages
http://dx.doi.org/10.1155/2015/145468

Research Article

Eye Motility Alterations in Retinitis Pigmentosa

Raffaele Migliorini, Anna Maria Comberiati, Giovanni Galeoto, Manuela Fratipietro, and Loredana Arrico

Department of Sense Organs, University of Rome "La Sapienza," Via del Policlinico 155, 00161 Rome, Italy

Correspondence should be addressed to Loredana Arrico; loredana.arrico@uniroma1.it

Received 14 July 2014; Revised 25 September 2014; Accepted 14 October 2014

Academic Editor: Xinhua Shu

Purpose. We evaluated a sample of individuals with retinitis pigmentosa (RP) with the aim of assessing the presence or absence of ocular motility (OM) disorders. *Materials and Methods*. We included 23 out of the 25 individuals from the sample (9 females and 14 males) with an average visual acuity of 6/10. *Results*. The cover test about the vertical deviation in near distance showed an r/l in 3.45% and an l/r in 6.9%. The assessment of OM showed that 39.1% of the sample had a severe hyperfunction of the IO of the right eye and a severe hyperfunction (34.5%) of the SO of the left eye; 21.8% had a moderate hypofunction of right SO with a moderate percentage of hypofunction of 17.5% for the SO of the left eye; 30.5%, however, showed a serious hypofunction of the SR of both eyes; 21.7% of the sample showed a hyperfunction in both eyes of the IR. *Conclusion*. This alteration, however, is not attributable to either a high refractive defect (medium-low myopia: −1 diopter ±3 SD) or to a severely impaired binocular vision (visual acuity, motor fusion, and stereopsis are normal or within a range of values commonly accepted). Therefore, the disorders of OM lead to a genetic origin.

1. Introduction

Retinitis pigmentosa (RP) is an inherited retinal disease characterized by the degeneration of photoreceptor rods and cones [1, 2]. In the majority of RP cases, there is a primary degeneration of rod photoreceptors with a secondary degeneration of cones. Thus, the typical RP is also described as a "rod-cone dystrophy" where photoreceptor rods are more affected than cones. This explains why patients show only a night blindness at first and a visual impairment later in daylight [3, 4].

In some cases, the clinical presentation is "cone-rod dystrophy" type with a predominant involvement of the cones or the central retinal photoreceptors. The decrease of visual acuity consequently predominates over visual field loss [1, 5].

The worldwide prevalence of retinitis pigmentosa is about 1 in 4,000 healthy people for a total of over 1 million people affected. In the USA it is about 1 : 3500–1 : 4000 with significant differences between the various states; in Switzerland 1 : 7000; China 1 : 4016; Norway 1 : 4440; in Israel 1 : 4500 [6].

The disease can be inherited as autosomal-dominant (about 30–40% of cases), autosomal-recessive (50–60%), or X-linked (5 to 15%) [6]. On the basis of this data, an observational study was performed on a sample of individuals suffering from retinitis pigmentosa. In the literature, we did not find any other studies concerning the alterations of ocular motility in retinitis pigmentosa.

The purpose of the study was to highlight the presence or absence of eye movement disorders in a genetically determined disease like RP while excluding all those influential factors used in recruiting binocular vision and the development of abnormal ocular motility such as high refractive errors [7], visual acuity < 6/10, pituitary adenomas, and related eye diseases in order to show the type of muscle alteration, if present, and then reconnect it to a genetic cause like RP.

2. Materials and Methods

Our sample consisted of 50 eyes (25 individuals) with retinitis pigmentosa from the Center for Pediatric Ophthalmology at the Eye Clinic of the Policlinico Umberto I, University of Rome La Sapienza. Patients were evaluated by the same examiner, and after a careful history and a thorough eye

examination of both the anterior segment and posterior segment with indirect ophthalmoscopy (Schepens), they were put through the following orthotic tests:

(i) visual acuity or visual acuity;

(ii) corneal reflex (CR);

(iii) stereopsis test;

(iv) cover test (CT);

(v) ocular motility (OM);

(vi) convergence objective.

The inclusion criteria of our study were as follows.

(i) Age between 6 and 80.

(ii) Patients with the typical form of nonsyndromic RP and patients with syndromes that are associated with various types of pigmentary retinopathy (e.g., Usher syndrome, Cockayne syndrome, Best's disease, etc.).

(iii) Patients with suspected RP: by careful history the presence of RP was discovered in other family members (i.e., brother, cousin, and grandparent).

(iv) Visual acuity between 6/10 and a maximum of 10/10 (via the Snellen optotype).

The exclusion criteria were as follows.

(i) Preschool age (from 1 to 5 years).

(ii) Patients who had undergone ocular surgery.

(iii) Patients with systemic, vascular, and neurodegenerative disease (e.g., the "multiple sclerosis") that can affect the orthoptic assessment.

(iv) Patients with visual field (CV) electronic Humphrey $< 10^{\circ}$.

(v) Visual acuity below 6/10.

(vi) Presence of pituitary adenomas.

In the evaluation of ocular motility, we considered the 12 extraocular muscles of both eyes in different positions of gaze. We have assigned a gradient equal to 0 in the case of normal ocular motility, +1 in the case of mild hyperfunction, +2 in the presence of moderate, and +3 in the case of severe hyperfunction. The same score was given in the case of hypofunction of the contralateral synergist muscle but with a negative value. A statistical analysis of this pilot study was performed by a Pearson correlation between the contralateral synergist muscles: ri SR-le SO, ri IR-le GO, le SR-riSO, and le IR-ri GO.

3. Results

The sample consisted of 25 individuals but was reduced to 23 individuals, because two patients reporting a severe mental retardation (IQ < 40) were unable to cooperate with most important orthotic tests such as an accurate assessment of ocular motility.

Thus, out of the 25 individuals, 23 have been included with 9 females and 14 males. The average age for women was 45 years ±25.18 SD while the average age found in men was 43 age ±21.42 SD (Figure 1).

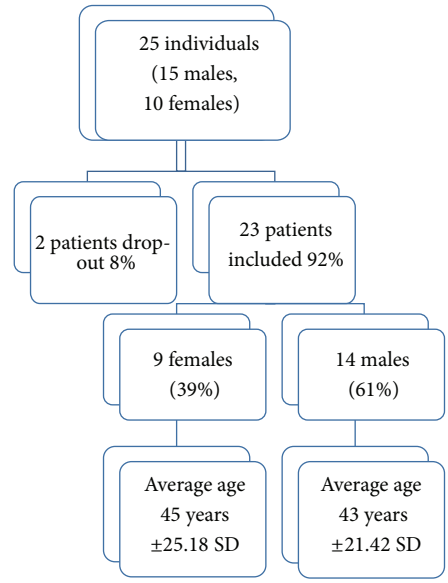

Figure 1: Stratification of the sample by age and sex.

Of the 23 patients included, 69.5% were suffering from typical retinitis pigmentosa (rod cone dystrophy) and 4.3% by RP atypical (cone-rod dystrophy). Patients with syndromes associated with RP (such as S. Cockayne and S. Uscher) showed the same percentage of disease incidence of 4.3%. Among macular dystrophy, Best's disease was found in 13.3%: 4 patients belonging to the same family (father with sons and grandson). We also found a case report with Cones dystrophy (incidence 4.3%).

Among refractive defects found in our sample, we found the presence of myopia with an average of 1 diopter ±3.15 SD for the right eye and 1.5 diopter ±3.53 SD for the left eye. Astigmatism, compared to myopia, was not statistically significant in both eyes. In fact, there has only been an average of −0.25 for the right eye with SD equal to 1.13. This data showed refractive errors (myopia of middle-grade and low, irrelevant, astigmatism) that are not able to affect binocular vision and therefore the ocular motility of the tested patients (Figure 2).

In the evaluation of visual acuity in tenths by the Snellen optotype, it is appropriate to mention the presence of an average of 6/10 ± SD of 2.9 for the right eye and 3.2 for the left eye. This data does not show a significant reduction in visual acuity that can hinder the development of binocular vision. The latter has also been evaluated through some stereoscopic tests (Lang I and II) that show full results in 22 of the 23 patients. In only one patient (a child with exotropia) and when detecting only the star image, the three-dimensional sense was absent. We can say that the development of binocular vision is not compromised due to alack in the whole sample of diplopia guarantor of an optimal sensorial fusion. Thereafter in the study of fusional amplitude, except for the young exotropic girl, the rest of the sample showed normal motor fusion values.

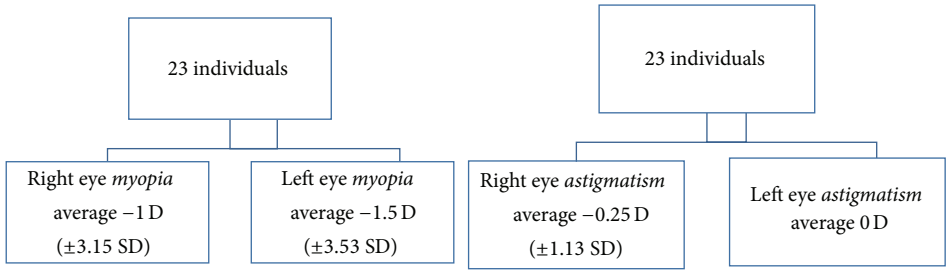

Figure 2: Evaluation of refractive errors. The data showed refractive errors (mild myopia and low astigmatism) not able to alter binocular vision and therefore the ocular motility of the examined patients.

In the evaluation of ocular motility, we took into account the different positions of gaze: primary position, left, right, up, up right and left, down, down left, and right. It was found that no patient had an alteration of the medial rectus muscle, and the lateral rectus was present in the right and left side sight. It is necessary, however, to highlight the presence of the alteration in 50% of the sample in various degrees of ocular motility regarding the small oblique muscles, large oblique, rectus superior, and inferior rectus. In the upper left gaze, there has been a severe grade (score = +3) hyperfunction of the small oblique muscle (SO) of the right eye in 39.1% of cases compared with a normal ocular motility (score = 0) in 34.7% of our sample. We also verified a moderate hyperfunction (score = +2) in 17.4% of cases and an equal incidence of 4.4% of the cases in both the mild hyperfunction (score = +1) and the severe hypofunction (score = −3) of the muscle. Besides finding a severe hyperfunction of the right SO in the look upward and left, we found in 30.5% of the cases studied the presence of a severe hypofunction of the contralateral synergist, namely, the superior rectus of the left eye. In addition, out of the 23 individuals, we also found a normal motility in 34.8% of cases, a moderate hypofunction in 21.8% of cases, a severe hyperfunction in 8.6%, and a mild hypofunction in 4.3% for the superior rectus muscle of the left eye. In the ocular motility evaluation, we also took into consideration the position of gaze at the bottom left. In that position, we found the presence of a hypofunction of the great oblique muscle of the right eye of a moderate degree (score = −2). In 21.8% of the 23 individuals considered and, on the other hand, in 61% of cases, the ocular motility was normal. With the same percentage of the total 4.3%, the large oblique muscle of the right eye showed a moderate hyperfunction, a mild hyperfunction, and a severe hypofunction. In versions, considering the gaze of eyes to the bottom left, the grand oblique muscle of the right eye enters to play together with the contralateral synergist, that is, the inferior rectus muscle of the left eye. Next to a moderate hypofunction of the right GO, we noted the presence of an alteration of the OM of different degrees in left IR. In fact, the lower rectus left eye showed, in 21.7% of cases, a severe hyperfunction this time (score = +3). In addition, our sample showed an optimum operation of the inferior rectus muscle of the left eye in 60.9% and a moderate hypofunction in 8.7% with the same percentage of 4.4% of cases, and the IR of the left eye presented a mild and moderate hyperfunction.

Another gaze direction where we found an alteration of ocular motility is the one in the top right. We noticed the presence of a severe hypofunction of the right superior rectus muscle (score = −3) observed in 30.5% of cases compared to 39.1% of cases who reported a normal function of this muscle. Furthermore, in 17.5% of cases, the SR of the right eye showed a Moderate hypofunction, 8.6% a severe hyperfunction, and a mild hypofunction of only 4.3%.

For the diagnostic position of gaze in the top right, as well as, having experienced a severe hypofunction of the SR of the right eye, we also detected a hyperfunction of the same grade (score = +3) of the contralateral synergist muscle, that is, the small oblique of left eye with an incidence in 34.8% of cases. In 39.1% of the 23 individuals, however, the operation of the SO of the left eye was optimal while 13% had a moderate hyperfunction, 8.7% a severe hypofunction, and 4.4% a mild hyperfunction.

Finally, we found the presence of an alteration of ocular motility in the gaze to the lower right. This alteration was found in the inferior rectus muscle of the right eye that showed a severe hyperfunction in 21.7% of cases and the same percentage of incidence equal to 4.4% of the cases for a mild hyperfunction and moderate hypofunction. Instead in 69.5% of cases, the inferior rectus muscle of the right eye showed a normal operation. In the diagnostic position in the lower right corner, as well as in the gaze to the lower left, we noted the presence of an alteration in ocular motility of different degrees for contralateral synergist muscles. In fact, a severe hyperfunction (score = +3) of the IR of the right eye is associated with a moderate hypofunction (score = −2) of large oblique muscle of the left eye in 17.5% of cases. Taking into consideration the position of gaze, the GO muscle of the left eye worked normally in 69.6% of cases, while it showed a severe hypofunction and moderate hyperfunction with the same percentage of 4.3% (Table 1). Through a Pearson correlation, we can say that the contralateral synergist muscles being compared from the evaluation of ocular motility are inversely correlated, and this allows us to state that there is a direct relationship between the retinitis pigmentosa and ocular motility disorders (Table 2).

Prime Position Muscle Hypofunction Mild Hypofunction Moderate Hypofunction Severe Normal Hyperfunction Mild Hyperfunction Moderate Hyperfunction Severe.

Table 1: Evaluation of ocular motility.

Primary position	Muscle	Ipofunction slight	Ipofunction moderate	Ipofunction severe	Normal motility	Iperfunction slight	Iperfunction moderate	Iperfunction serious
In the left upward	Inferior oblique of the right eye	0	0	4.4%	34.7%	4.4%	17.4%	39.1%
	Superior rectus of the left eye	4.3%	21.8%	30.5%	34.8%	0	0	8.6%
In the right upward	Superior rectus of the right eye	4.3%	17.5%	30.5%	39.1%	0	0	8.6%
	Inferior oblique of the left eye	0	8.7%	0	39.1%	4.4%	13%	34.8%
In the left downward	Superior oblique of the right eye	4.3%	21.8%	4.3%	61%	0	4.3%	4.3%
	Inferior rectus of the left eye	0	8.7%	0	60.9%	4.4%	4.4%	21.7%
In the right downward	Superior oblique of the left eye	4.3%	17.5%	4.3%	69.6%	0	4.33%	0
	Inferior rectus of the right eye	0	4.4%	0	69.5%	4.4%	0	21.7%

Table 2: Pearson correlation in ocular motility.

Right SR—Left IO	−0.99
Right IR—Left SO	−0.97
Left SR—Right IO	−0.74
Left IR—Right SO	−0.96

In the upper left: right Inferior Oblique 0 0 4.4% 34.7% 4.4% 17.4% 39.1%—left Superior Rectus 4.3% 21.8% 30.5% 34.8% 0 0 8.6%.

In the upper right: right Superior Rectus 4.3% 17.5% 30.5% 39.1% 0 0 8.6%—left Inferior Oblique 0 8.7% 0 39.1% 4.4% 13% 34.8%.

In the bottom left: right Superior Oblique 4.3% 21.8% 4.3% 61% 0 4.3% 4.3%—left Inferior Rectus 0 8.7% 60.9% 0 4.4% 4.4% 21.7%.

In the bottom right: left Superior Oblique 4.3% 17.5% 4.3% 69.6% 0 4.33% 0—right Inferior Rectus 0 4.4% 0 69.5% 4.4% 0 21.7%.

Using the test cover, the evaluation of 25 patients examined with and without corrective lenses for near and evaluated for near (by observing a target light) and for far (indicating a letter of the optotype in relation to the patient's visual acuity) showed interesting data. Indeed, in our sample we have found the presence of a vertical deviation in 4 patients; among these, 2 (a patient with RP and one with S. of Uscher) reported a deviation L/R with and without the lens, and the other 2 (a typical patient with RP and the other with atypical RP) that reported a deviation R/L. Considering the vertical deviation of the cover test examination, we found a L/R with an incidence of 8.69% and a R/L in 4.35% of cases tested for near with and without corrective lenses (Figure 3). In the evaluation, however, for far (with and without lens), the cover test has highlighted the presence of a R/L in 4.35% of the 23 individuals observed; while in almost all of our sample (95.65% of cases) ortoforia was present.

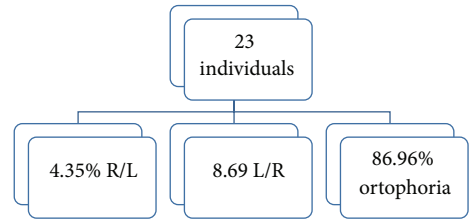

Figure 3: Cover test: evaluation of vertical deviation for near (with or without corrective lenses).

This vertical deviation could justify the alteration of ocular motility observed in our RP sample, but the percentage is statistically insignificant.

The data concerning the horizontal deviation highlighted with alternate cover test in the 25 patients evaluated with and without corrective lenses for near and far were 3 individuals during the dissociation cover test for near with lens showed no changes in refixation (orthoforic subjects), while 5 patients had a recovery movement of the eye just discovered from the outside inwards (exoforia). In cases of deviation greater than 2 PD, the angle of deviation has been measured with a prism with a base opposite to the direction of the deviation and assigning the + sign in the case of ESO and the − sign in the case of EXO. The cover-uncover was essential to establish the quality of the deviation: if it is phoria or tropiaor if there is a recovery of deviation (phoria-tropia) and what is the fixing eye. We noted only one case of exotropia of the left eye of 16 PD and two cases of tropia-phoria of −14 PD. Only in these 3 cases has there been an alteration of ocular motility directly proportional to the amount of deviation in the primary position. Moreover, the presence of a case of esoforia of 8 PD and two cases of phoria-tropia, one of −10 PD and the other one of −6 PD, were found. In 6 patients, there was exoforia ranging from 4 PD to 8 PD. Finally, 3 patients showed a phoria-tropia of −8 PD. (Figure 4). In the same patients, CT

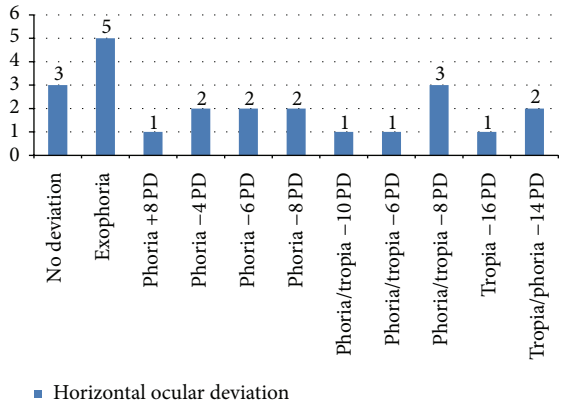

Figure 4: Cover test: evaluation of horizontal deviation for near with the lens.

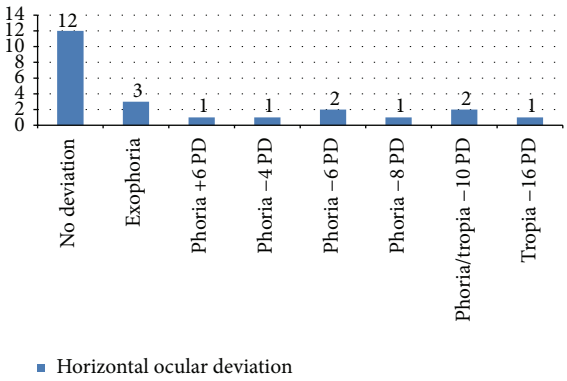

Figure 5: Cover test: evaluation of the horizontal deviation for near without lens.

was performed always for near but without corrective lenses. We found that 12 patients had no movements of refixation, 3 patients were exoforical, and 2 patients showed a phoria-tropia of –10 PD. There was only one case of a 15-year-old girl who, even without corrective lenses, had a tropia (–16 PD). Additionally, 3 patients had, respectively, anesoforia of 6 PD and anexoforia of 4 PD and 8 PD (Figure 5). Finally, in the CT evaluation with or without a lens for far, almost all of our sample did not show any significant horizontal deviation. In fact, the CT for distance with lens showed that 22 individuals did not show any deviation, and a tropia-phoria of –12 PD was found in a 15-year-old deaf and dumb girl who presented an exotropia to corneal reflexes. While always considering the CT for distance but without corrective lenses, we found in the same 15-year-old child a tropia-phoria of –14 PD and 3 cases of exoforia. Most of our sample, however, showed no deviation (19 individuals out of 23).

4. Conclusions

The sample recruited showed a significant proportion of patients with pure retinitis pigmentosa (69.5%), and the remaining part was suffering from associated syndromes. From the assessment of ocular motility, it was evident that in no patient had an alteration of the medial rectus and lateral rectus muscles in left and right side gaze.

It is instead essential to mention the presence of an ocular motility alteration for the small oblique, large oblique, superior rectus, and inferior rectus muscles in 50% of the sample.

39.1% of the sample has a severe hyperfunction of the small oblique muscle of the right eye and a severe hyperfunction (34.5%) of the small oblique of the left eye; 21.8% have a moderate hypofunction of the large oblique muscle of the right eye with a moderate percentage of hypofunction of 17.5% for the great oblique of the left eye; 30.5% of the sample has, however, a percentage of 30.5% of severe hypofunction of both eyes' superior rectus muscles; 21.7% of the sample showed a hyperfunction of the inferior rectus muscle in both eyes.

The results show that there is an impaired motility in 50% of patients in this inherited disorder. This alteration of the ocular motility is not, however, due either to a high refractive defect (size medium-low myopia: –1 diopter ±3 SD) or to a binocular vision severely impaired (visual acuity, motor fusion, and stereopsis are normal or within commonly accepted limit values). These ocular motility disorders are ascribed to a genetic origin factor. In fact, since RP is a genetically determined disease, the absence of eye movement disorders in the other 50% of the sample could be linked to the different penetrance of the disease that determines the existence of healthy carriers. Therefore, the results of this study indicate that, in patients with RP, there is an alteration of ocular motility and this indicates that a careful orthotic screening may allow a further contribution to an early diagnosis especially in those cases of RP with family history and in healthy carriers.

Conflict of Interests

The authors declare that there is no conflict of interests regarding the publication of this paper.

References

[1] C. H. Bunker, E. L. Berson, W. C. Bromley, R. P. Hayes, and T. H. Roderick, "Prevalence of retinitis pigmentosa in maine," *The American Journal of Ophthalmology*, vol. 97, no. 3, pp. 357–365, 1984.

[2] K. Novak-Lauš, S. Kukulj, M. Zorić-Geber, and O. Bastaić, "Primary tapetoretinal dystrophies as the cause of blindness and impaired vision in the republic of Croatia," *Acta Clinica Croatica*, vol. 41, no. 1, pp. 23–27, 2002.

[3] F. Ammann, D. Klein, and A. Franceschetti, "Genetic and epidemiological investigations on pigmentary degeneration of the retina and allied disorders in Switzerland," *Journal of the Neurological Sciences*, vol. 2, no. 2, pp. 183–196, 1965.

[4] E. L. Berson, B. Rosner, M. A. Sandberg et al., "A randomized trial of vitamin A and vitamin E supplementation for retinitis pigmentosa," *Archives of Ophthalmology*, vol. 111, no. 6, pp. 761–772, 1993.

[5] J. A. Boughman, P. M. Conneally, and W. E. Nance, "Population genetic studies of retinitis pigmentosa," *The American Journal of Human Genetics*, vol. 32, no. 2, pp. 223–235, 1980.

[6] M. Jay, "On the heredity of retinitis pigmentosa," *British Journal of Ophthalmology*, vol. 66, no. 7, pp. 405–416, 1982.

[7] R. Forte, A. Jannaccone, L. Pannarale, L. Arrico, and M. R. Pannarale, "Myopic shift of refractive error in retinitis pigmentosa," *Investigative Ophthalmology and Visual Science*, vol. 37, no. 3, p. S501, 1996.

Hindawi Publishing Corporation
Journal of Ophthalmology
Volume 2015, Article ID 414781, 10 pages
http://dx.doi.org/10.1155/2015/414781

Review Article

The Role of RPGR and Its Interacting Proteins in Ciliopathies

Sarita Rani Patnaik,[1] Rakesh Kotapati Raghupathy,[1] Xun Zhang,[1] David Mansfield,[2] and Xinhua Shu[1]

[1]*Department of Life Sciences, Glasgow Caledonian University, Glasgow G4 0BA, UK*
[2]*Inverclyde Royal Hospital, Greenock PA16 0XN, UK*

Correspondence should be addressed to Xinhua Shu; xinhua.shu@gcu.ac.uk

Received 26 December 2014; Revised 13 April 2015; Accepted 19 April 2015

Academic Editor: Hyeong Gon Yu

Ciliopathies encompass a group of genetic disorders characterized by defects in the formation, maintenance, or function of cilia. Retinitis pigmentosa (RP) is frequently one of the clinical features presented in diverse ciliopathies. RP is a heterogeneous group of inherited retinal disorders, characterized by the death of photoreceptors and affecting more than one million individuals worldwide. The *retinitis pigmentosa GTPase regulator* (*RPGR*) gene is mutated in up to 20% of all RP patients. RPGR protein has different interacting partners to function in ciliary protein trafficking. In this review, we specifically focus on RPGR and its two interacting proteins: RPGRIP1 and RPGRIP1L. We summarize the function of the three proteins and highlight recent studies that provide insight into the cellular function of those proteins.

1. Introduction: Cilia and Photoreceptor

1.1. Cilia Architecture. Cilia are tiny, hair-like structures protruding from the cell surface. They are highly conserved organelles and serve a variety of sensory functions in both unicellular and multicellular organisms. Historically, cilia have been classified into two categories: motile and nonmotile cilia (primary cilia), depending on the arrangement of the microtubule triplets, termed the axoneme. The axoneme of motile cilia is built in the classical 9+2 arrangement, where nine outer microtubule doublets surround a central pair of singlet microtubules. The axoneme of primary cilia lacks the central pairs of microtubules and is arrayed in a 9+0 configuration [1]. Primary cilia are immotile and can sense extracellular physical and biochemical signals, acting as a coordination centre of multiple signal transduction pathways [2]. Some epithelial cell surfaces contain a large number of motile cilia, which beat cooperatively to generate fluid movement. For instance, cells lining in the epididymis, the oviducts, the respiratory tract, and ependymal surfaces of the brain have large clusters of motile cilia, which beat in coordinated waves and perform a broad range of functions. The central microtubules within the motile cilia help in the bending motion. Flagella are found on single-celled eukaryotes and sperm cells and are primarily involved in cell locomotion. Prokaryotic flagella are structurally similar to eukaryotic flagella, although there are distinctions made according to the function and the length. Flagella also have a 9+2 axoneme arrangement which is similar to that of motile cilia.

1.2. Protein Transport in Cilia. All protein synthesizing machineries are restricted to the cytoplasm, so continued elongation of the cilium requires the selective import and transport of ciliary proteins by intraflagellar transport (IFT), which mediates bidirectional movement of multiprotein loaded particles along the axoneme. IFT was initially discovered in flagella of *Chlamydomonas reinhardtii*, in which anterograde and retrograde movements of particles were observed through differential interference contrast microscopy [3]. IFT polypeptides are found in all ciliated organisms and are highly conserved in the evolution, ranging from *C. elegans* to primates [4, 5]. The transport of IFT particles is powered by motors that include the heterotrimeric kinesin for anterograde movement [4, 6] and the cytoplasmic dynein for retrograde movement [7, 8]. Based on directionality of IFT's movement along the axoneme, IFT particles

are organized into two complexes: IFT complex A and IFT complex B. In vertebrate at least six proteins (IFT43, IFTA-1, IFT122, IFT139, IFT140, and IFT144) and ten different proteins (IFT20, 27, 46, 52, 57, 74, 80, 81, 88, and 172) are in complex A and complex B, respectively [9]. IFT complex A is responsible for retrograde transport and complex B organizes anterograde transport towards the microtubule plus-ends of the ciliary tip. The bidirectional movement of IFT particles is continuous without reversing. Although the anterograde movement is slower than the retrograde movement, there is no accumulation of IFT particle in the distal tip of the cilium, suggesting cargo loading and release, IFT particle turn-around, and motor exchange are well regulated at the base and tip of cilia [10]. Most of these cargoes are derived from the Golgi body vesicles, which could explain why cilia usually form apically to the trans-Golgi network. IFT is essential for assembling all eukaryotic cilia and flagella, and defects in IFT can cause a variety of diseases and abnormal developments.

1.3. Photoreceptors. Photoreceptors are the photosensitive cells of the retina responsible for converting incident light into electric signals that are transmitted to the brain via the optic nerves and are interpreted by the nervous system. Rods and cones are the two types of photoreceptors, classified according to their shape and function. The human retina contains over 120 million rods and 6 million cones. Rods and cones are unevenly distributed across the retina. Some organisms, such as mouse, also have a rod dominant retina; others, such as zebrafish and squirrel, have a cone dominant retina. In humans, the central region of the retina is the macula. The central part of the macula is referred to as the "fovea," which only contains cones and is the region showing highest visual acuity [11]. Rods are responsible for vision at low light levels (scotopic or night vision) and are very sensitive even under dim conditions. Cones are responsible for colour or day vision (photopic vision). They are much less sensitive than rods and generate signals at higher levels of light.

Photoreceptors consist of four distinct components: a synaptic terminal, an outer segment (OS), an inner segment (IS), and a connecting cilium (CC) that connects the IS and OS (Figure 1). The OS is a highly modified primary cilium that contains numerous light sensitive stacks. These stacked lamellae are actual sites of photo transduction. The CC is a structural homologue to the transition zone of cilia [12]. Structurally rods and cones share a similar architecture. However, there is a difference in the way their outer segments are built. In rods, there are large numbers of membrane discs stacked on top of each other unconnected to the ciliary membrane, while the discs in cones are invaginations of the plasma membrane. The inner segment contains cellular organelle such as mitochondria, endoplasmic reticulum, and Golgi body so that they do not interfere with the outer segment biochemical reactions. The visual pigment in both rods and cones consists of opsin proteins. Rods are able to operate in dim light using only one type of opsin, rhodopsin, whereas cones contain several types of opsins thereby detecting different colours. The human eye contains three different types of cones for perception of different colours: blue cones (short wavelength or S cones), green cones (middle wavelength or M cones), and red cones (long wavelength or L cones) which allow us to respond to different wavelengths of light [13]. Many animals including birds, reptiles, and fish have four different types of cones. Cones have a longer lifespan than rods and do not undergo circadian phagocytosis by RPE cells [14]. The molecular processes like IFT or vesicle trafficking observed in primary cilia are also conserved in photoreceptor outer segments (Figure 1).

2. Ciliopathies

The cilium proteome contains hundreds of different proteins involved in cilia protein trafficking, structure, and signal transductions [15, 16]. Deficiency of one of these proteins may be enough to produce cilia defects, giving rise to a broad spectrum of genetic disorders termed ciliopathies. Wide ranges of extracellular signals are sensed by the cilia and then transduced into decisions required for proliferation, differentiation, polarity, development, and tissue maintenance. A broad range of signals like photosensation, thermosensation, mechanosensation, hormone sensation, and olfactory sensation are received and propagated by specific ciliary receptors [17]. So, ciliary dysfunction can manifest as a variety of clinically overlapping features including primarily retinal degeneration, kidney diseases, and brain anomalies [18].

Phenotypic manifestations of ciliopathies can range from isolated blindness or renal disease to multiorgan system disorders such as retinitis pigmentosa, Meckel-Gruber syndrome (MKS), Joubert syndrome, or Bardet-Biedl syndrome (BBS). Defects of ciliary proteins can give rise to broad range of defects, including retinitis pigmentosa, hepatic, pancreatic, and kidney cyst formation, polydactyly, situs inversus, brain malformations, encephalocele, hydrocephalus, sensory defects, and skeletal abnormalities. However, mutations in the same ciliary gene can give rise to heterogeneous clinical phenotypes with different levels of severity [19]. Conversely, mutations in distinct genes can lead to the same phenotype, for example, mutations in at least eleven genes causing nephronophthisis (NPHP) [20]. In the wide phenotypic spectrum, NPHP is considered to be the mildest, BBS is intermediate in severity, and MKS is lethal. Retinal degeneration is often observed in diverse ciliopathies.

3. Retinitis Pigmentosa

Retinitis pigmentosa (RP) encompasses a group of inherited retinal degenerations that show progressive loss of photoreceptors with highly variable clinical and genetic heterogeneity. It is one of the most heterogeneous genetic disorders known in man [21], resulting from a mutation in one or more genes. It affects 1 in 4000 individuals worldwide. RP is caused by mutations in more than 50 genes, including 23 genes for autosomal dominant RP, 36 for autosomal recessive RP, and 3 for X-linked RP (XLRP) (http://www.sph.uth.tmc.edu/Retnet/). Symptoms of RP include accumulation of intraretinal pigment-like deposits, retinal vessel attenuation, and characteristic changes in electroretinogram (ERG) patterns

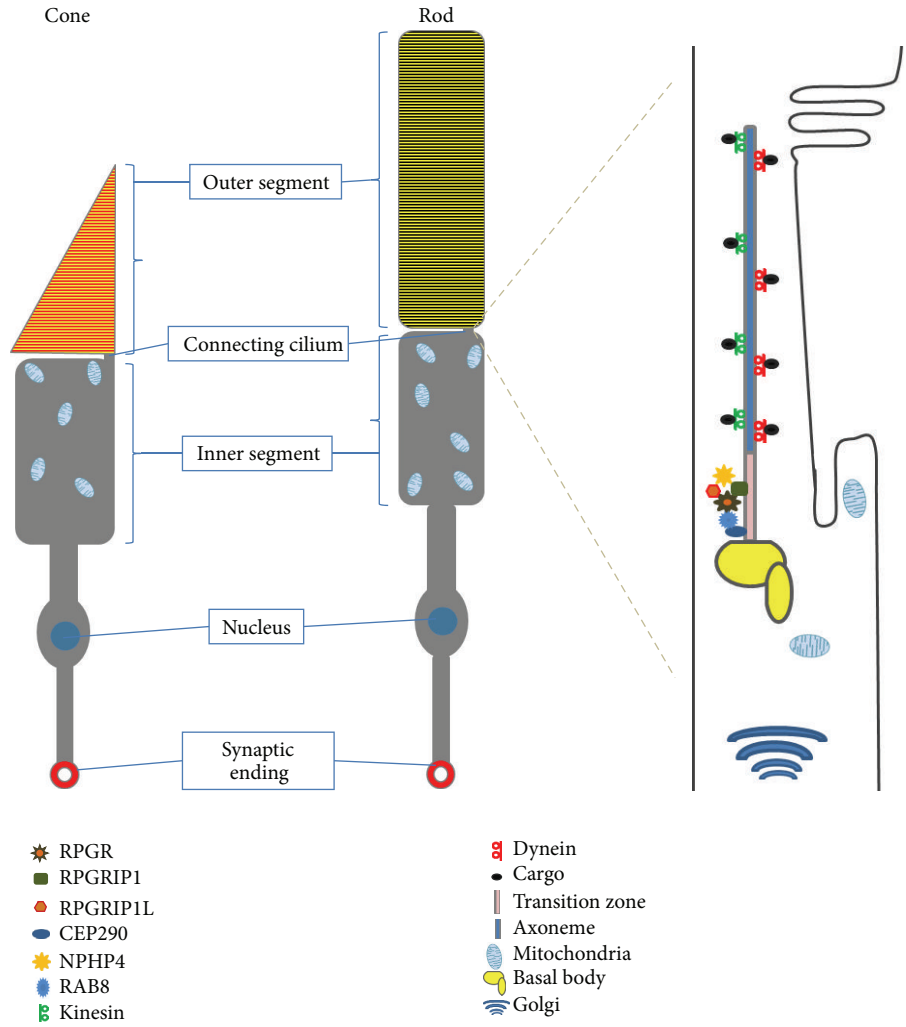

Figure 1: The photoreceptor primary cilia. The distinct compartments of both rod and cone cells (left side). Protein trafficking in photoreceptor connecting cilium through intraflagellar transport (IFT) is carried out by motor proteins, kinesin and dynein (right side). CEP290, centrosomal protein 290 kDa; NPHP4, nephronophthisis 4; RPGR, retinitis pigmentosa GTPase regulator; RPGRIP1, RPGR interacting protein 1; RPGRIP1L, RPGR interacting protein 1-like (right side).

[22]. The typical signs of early disease are night blindness and tunnel vision with progressive constriction of the visual field. The progression of typical RP can be divided into 3 stages. The early stage of the disease is within the first decade or second decade of life. The typical signs of early disease are night blindness, although at this stage visual acuity and fundus examinations appear normal; at the midstage, rod photoreceptors degeneration starts at the periphery of the retina and then progresses towards the central region during the third or fourth decade, eventually causing tunnel vision with progressive constriction of the visual field; at this stage the presence of bone spicule-shaped pigment deposits is observed in the midperiphery of the retina. At the end-stage, complete loss of peripheral vision (classical tunnel vision) is sufficiently disabling to make independent movement difficult. There is a clear deposition of pigment at different retinal regions and a clear reduction of retinal vessel thickness. At this stage cone degeneration also takes place, leading to central vision impairment (Figure 2) [23].

4. The Retinitis Pigmentosa GTPase Regulator (RPGR)

Mutations in the *RPGR* gene are the major cause of RP, accounting for more than 70% of XLRP and over 20% of nonsyndromic RP in North American families [24, 25]. *RPGR* mutations are responsible for 8.8% of Japanese RP patients [26] and 4.26% of Chinese patients with cone-rod dystrophy [27]. The *RPGR* gene is located in chromosomal region Xp21.1, spanning 172 kilobases. It was first cloned in 1996 and was initially reported to consist of 19 exons [28, 29]. Later, Vervoort and colleagues identified an additional alternatively spliced C-terminal exon, called open reading frame (ORF) 15, which is highly expressed in photoreceptors [30]. The $RPGR^{ex1–19}$ transcript contains 19 exons, coding a protein with 815 amino acids with an isoprenylation motif at the C-terminus; the $RPGR^{ORF15}$ has 15 exons, encoding a protein with 1152 amino acids. It shares exons 1–14 with $RPGR^{ex1–19}$ plus the exon ORF15, encoding 567 amino acids

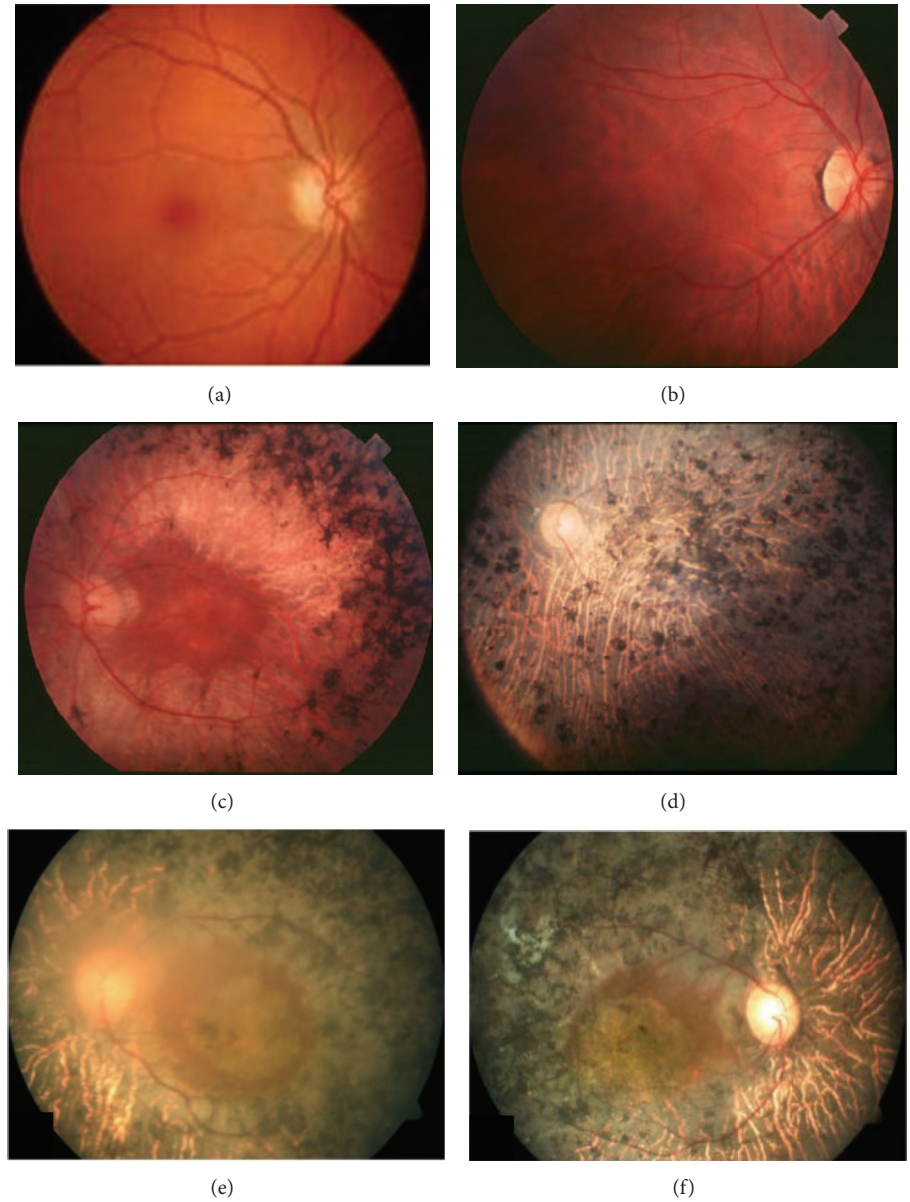

Figure 2: Fundus of an RP patient at different stages. (a) Image of a normal healthy eye. (b) Fundus of an RP patient at early stage. (c) Midstage of the disease showing midperipheral pigment deposits. (d) End-stage fundus showing pigment deposit present all over retina with thin retinal vessels and pale optic disc, modified from Hamel [23]. (e-f) End-stage fundus of an RP patient with an *RPGR* mutation c.852c>G (p.S284X), modified from Yang et al., 2014 [73].

with a repetitive glycine and glutamic acid-rich domain and a conserved basic C-terminal domain (Figure 3). In addition to these two major transcripts of the gene, RPGR encodes complex alternative spliced transcripts and many novel tissue-specific exons have been reported [31, 32]. All of the transcripts encode an amino (N)-terminal RCC1-like domain that is structurally similar to the RCC1 protein, a guanine nucleotide exchange factor for the small GTP-binding protein, Ran. Mutations have been reported in exon 2 to exon ORF15, where most mutations are taking place in the latter, which is regarded as a mutation hot spot [30, 33]. More than 300 mutations have been identified to cause X-linked forms of RP (Figures 2(e) and 2(f)), cone-rod, cone, and macular dystrophies, or syndromal forms of XLRP with hearing loss and primary ciliary dyskinesia [25].

Localization of RPGR in the retina is species dependent. RPGR is localized predominantly in the connecting cilia of mouse photoreceptors, but, in human and bovine photoreceptors, localization has been reported in the outer segments of both rod and cone cells [34, 35]. Outside of the retina, RPGR is also detected in motile cilia of airway epithelia and the centrosomes/basal bodies of cultured cells [34, 36, 37]. RPGR has been reported to interact with different proteins. The first RPGR interacting protein, the delta subunit

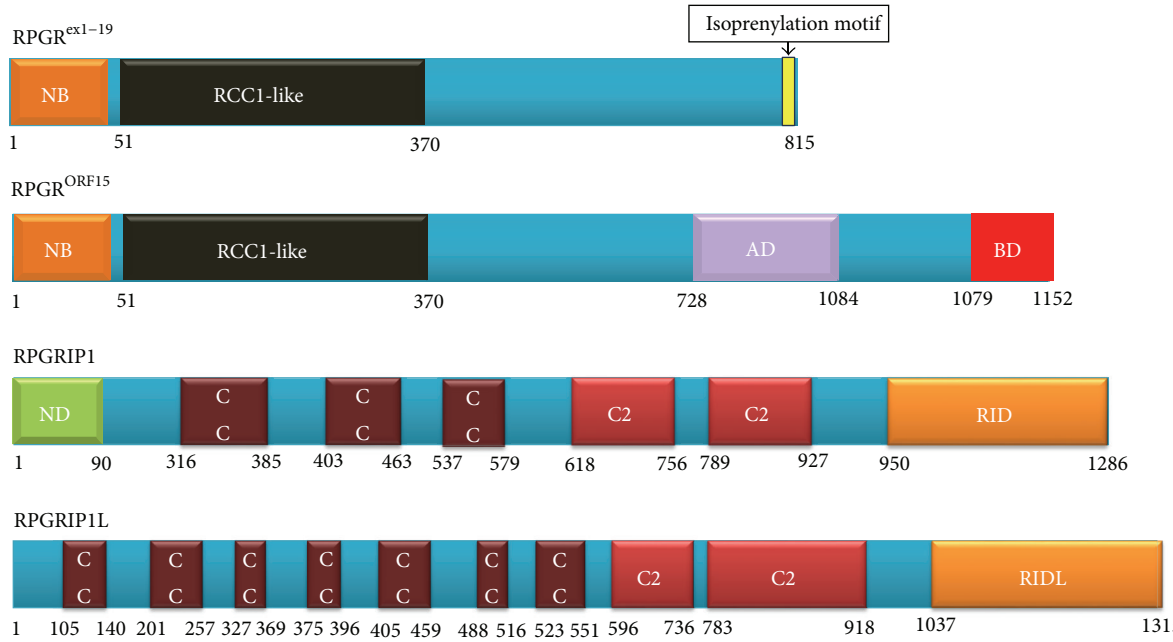

FIGURE 3: Structures of RPGR and its interacting proteins: RPGRIP1 and RPGRIP1L. The protein sequences of RPGR^{ex1-19} (NP_000319.1), RPGR^{ORF15} (NP_001030025.1), RPGRIP1 (NP_065099.3), and RPGRIP1L (NP_056087.2) were obtained from Ensembl database (http://www.ensembl.org) and domains were identified using InterPro, protein sequence analysis, classification tool (http://www.ebi.ac.uk/interpro/search/sequence-search), and details are from the literature. The isoprenylation motif (CAAX), four peptides at the N-terminal of the RPGR^{ex1-19}, is marked in yellow vertical rectangle. AD, acidic domain; BD, basic domain; C2, protein kinase C conserved domain 2; CC, coiled-coil domain; NB, GTP-binding motif; ND, nuclear domain; RID, RPGR interacting domain; RIDL, RPGR interacting domain-like.

of the rod cyclic phosphodiesterase (PDEδ), was identified by yeast two-hybrid screening mouse embryonic cDNA library using the RCC1-like domain [38]. Using a similar strategy, three groups independently found the RPGR interacting partner: RPGR interacting protein 1 (RPGRIP1) [39–41]. Coimmunoprecipitation and mass spectrometry analysis showed that SMC1 and SMC3 proteins interact with the RCC1-like domain [42]. The C-terminal of RPGR^{ORF15} interacts with whirlin, whose mutations cause Usher syndrome, and with nucleophosmin, which functions in cell division [36, 43]. Coimmunoprecipitation also found RPGR formed protein complexes with other ciliary proteins: IFT88, 14-3-3ε, γ tubulin, kinesin II subunit KIF3A and KAP3, dynein subunit intermediate chain, dynactin subunits: P150^{Glued} and P50-dynamitin, IQCB1 (NPHP5), and CEP290 (NPHP6) (Figure 4) [42, 44, 45]. Mutations in the *IQCB1* gene cause Senior-Loken syndrome (SLS), an inherited disorder characterized by RP and renal diseases [44]. Genetic deficiency in CEP290 is responsible for 15% of Leber congenital amaurosis (LCA) cases and has been implicated in other ciliopathies including SLS, nephronophthisis, Joubert syndrome, Bardet-Biedl syndrome (BBS), and Meckel syndrome (MKSS) [46–48]. IQCB1 physically interacts with CEP290 and both proteins involved in ciliogenesis [49].

5. RPGRIP1 and RPGRIP1L

Mutations in *RPGRIP1* lead to LCA, a severe retinal dystrophy causing blindness or severe visual defects at birth or in early childhood [50]. Defects in *RPGRIP1L* cause either the lethal Meckel syndrome (MKSS) or Joubert syndrome type B (JBTS), which show much broader cilia defects [51, 52]. Human *RPGRIP1* gene is located on chromosome 14q11 and encodes a protein with 1286 residues. *RPGRIP1L* gene is located on chromosome 16q12.2 and encodes a protein of 1315 residues [51]. RPGRIP1 protein has 29% amino acid identity to RPGRIP1L, which possesses similar functional domains. The N-terminals of both proteins contain coiled-coil domain with two leucine zipper motifs; the central regions contain two protein kinase C conserved region 2 (C2) domains; the C-terminal regions have an RPGR-interacting domain (Figure 3). Though the RPGR-interacting domain of RPGRIP1L is less homologous to that of RPGRIP1, the interaction with RPGR was confirmed by yeast two-hybrid and pull-down assays [53, 54]. The expression of RPGRIP1 is restricted to the retina, but RPGRIP1L is detected in retina and other tissues [35, 41, 51, 52]. Both RPGRIP1 and RPGRIP1L have similar localization to that of RPGR in retina and cultured cells [36, 51, 52]. Previous reports predicted there is a putative $Ca2^{+}$-binding site in RPGRIP1 C-terminal C2 (C2-C) domain, but the recent crystal structure of RPGR-interacting domain of RPGRIP1 did not support the prediction [54, 55]. Both RPGRIP1 and RPGRIP1L interact with NPHP4, whose mutations result in nephronophthisis [51, 55]. Mutations in RPGRIP1, RPGRIP1L, or NPHP4 disrupted the interaction. Coene et al. used tandem affinity purification and mass spectrometry to identify that nek4 serine/threonine kinase also interacts with both RPGRIP1

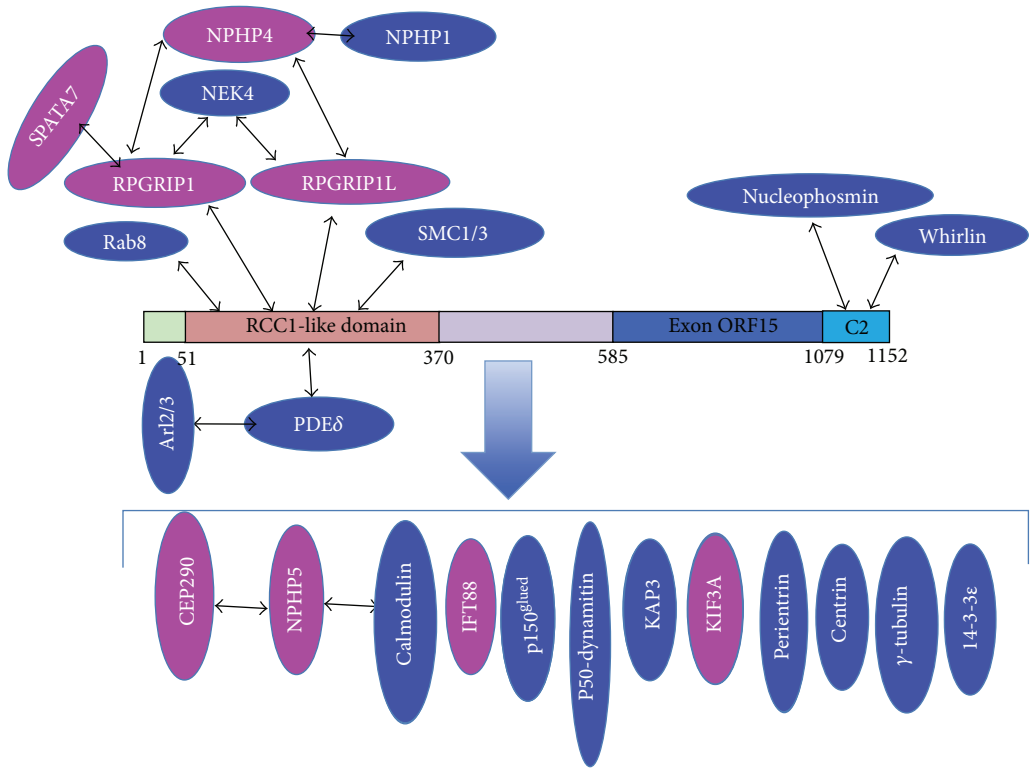

Figure 4: RPGR interacting protein network. Black arrows show direct interaction; the big blue arrow shows proteins in RPGR complex detected by coimmunoprecipitation. Proteins labelled in pink are implicated in retinal degeneration. The RCC1-like domain directly interacts with RPGRIP1, RPGRIP1L, SMC1/3, PDEδ, and Rab8. The end section of the C-terminal directly interacts with nucleophosmin and whirlin. Mutations in RPGRIP1, RPGRIP1L, CEP290, NPHP4, NPHP5, IFT88, KIF3A, and SPATA7 also cause ciliopathies.

and RPGRIP1L proteins [56]. More recently, SPATA7, which is responsible for LCA3 and juvenile RP, was identified as an RPGRIP1 interacting partner (Figure 4) [57]. Mislocalization of RPGRIP1 was detected in SPATA7 knockout mouse photoreceptor connecting cilium, suggesting SPATA7 is required for RPGRIP1 targeting to cilia.

6. The Role of RPGR and Its Interacting Proteins in Cilia Defects

Large amounts of data from studies in cell lines and animal models suggest RPGR and interacting proteins play a critical role in cilia genesis, maintenance, and function. Knockdown of RPGR in hTERT-RPE1 cells resulted in defects in ciliogenesis with a reduced number of cilia or shortened cilia [58, 59]. Morpholino knockdown of RPGR in zebrafish embryos led to defects in retinal development, such as defective lamination of retinal cell layers and abnormal photoreceptors. Other ciliary defects in *RPGR* morphants include shorter Kupffer's vesicle cilia, a shortened body axis, kinked tail, and hydrocephaly [60, 61]. *RPGR* knockout (KO) mice showed a slow retinal degeneration with photoreceptor death noted by 6 months of age [62]. Although mislocalization of cone opsins was detected as early as postnatal day 20, degenerative changes were found at age of two months. The connecting cilia of KO mice initially appeared normal and the discs of outer segments were well packed, suggesting RPGR is not necessary for the development of photoreceptors.

Knockout of *RPGRIP1* in mouse (referred to as *RPGRIP1*^{tm1Tili}) resulted in early retinal degeneration with most of photoreceptors degenerating by 3 months of age, resembling the phenotypes in LCA patients. The abnormal photoreceptors were apparent at the age of postnatal day 15 (P15), showing disorganized outer segments and pyknotic nuclei, a sign of ongoing cell death [63]. *RPGRIP1* KO mice presented a normal structure of connecting cilia, suggesting RPGRIP1 is not needed for the connecting cilia development and maintenance. RPGR, however, lost localization to connecting cilia in *RPGRIP1* KO mice, suggesting RPGR correct localization is dependent on RPGRIP1. A recent N-ethyl-N-nitrosourea-induced RPGRIP1 null mouse model (referred to as *RPGRIP1*^{nmf247}) showed a more severe retinal degeneration when compared to that of *RPGRIP1*^{tm1Tili} mice. *RPGRIP1*^{tm1Tili} mice showed a rapid and progressive photoreceptor cell death. Outer segments were not seen in *RPGRIP1*^{nmf247} mice at P7 and P14. Only 3-4 photoreceptor nuclei layers remained by P21. Rhodopsin mislocalization was detected at P12, the earliest time point examined. Other outer segment proteins, ROM1, transducin, and arrestin, were also mislocalized, but neither transducin nor arrestin mislocalized in *RPGRIP1*^{tm1Tili} mice [63, 64]. The phenotype of *RPGRIP1*^{tm1Tili} mice suggested that RPGRIP1 is essential

for rod outer segment morphogenesis, whereas phenotypes in the *RPGRIP1*^{nmf247} mice suggested RPGRIP1 is essential not only for rod outer segment disc morphogenesis but also for outer segment formation. The phenotypic difference between the two mouse mutant strains was caused by a short alternative splice variant in *RPGRIP1*^{tm1Tili} mice, which may have a role in outer segment formation.

RPGRIP1L is implicated in different types of ciliopathies. Inactivation of the *RPGRIP1L* (*Ftm*) gene results in the death of mouse at midgestation and recapitulating similar malformation observed in human MKS fetues, including brain, liver, kidney, limb, and eye developmental defects [52, 65]. Morpholino knockdown of *RPGRIP1L* in zebrafish showed a broad range of ciliary defects, including shortened body axis, curved body, malformed somites, kinked notochord, abnormal tail extension, and hydrocephaly [53, 66]. In mouse cochlear hair cells, RPGRIP1L is required for planar cell polarity. In zebrafish, it is required for convergent extension and polarized positioning of motile cilia in floor plate and is also required for the stability of dishevelled protein (Dvl) at the cilium base [66].

Mislocalization of outer segment proteins has been observed in *RPGR* or *RPGRIP1* KO mice and in a patient carrying an *RPGR* mutation, suggesting RPGR and its interacting proteins are involved in protein trafficking in cilia [62–64, 67]. RPGR can regulate the ciliary trafficking of prenylated membrane-associated proteins by interacting with PDEδ, which is loaded with farnesylated cargo [68]. Since RPGR targeting to connecting cilia is dependent on RPGRIP1, RPGRIP1 may be involved in this process. RPGRIP1 is also essential for other ciliary protein trafficking. Mislocalization of NPHP4 and SDCCAG8, another ciliopathic protein [69], was observed in the photoreceptors of *RPGRIP1* KO mice (*RPGRIP1*^{nmf247}) [70]. RPGRIP1 and RPGRIP1L may function as scaffolds to recruit NEK4 to cilia, helping to maintain ciliary stability [56].

The primary cilium is a coordinating hub for different signaling pathways, such as Wnt (canonical and noncanonical), sonic hedgehog (SHH), fibroblast growth factor (FGF), Notch, platelet derived growth factor receptor α (PDGFR α), mTOR, and Hippo signaling pathways [71]. RPGR and its interacting protein may be directly or indirectly involved in these signaling pathways. Silencing of RPGR in hTERT-RPE1 caused defective cilia formation and abnormal remodelling of actin cytoskeleton [59]. The noncanonical Wnt pathway, also referred to as planar cell polarity (PCP) pathway, regulates actin cytoskeleton rearrangement by activating the small GTPase, RhoA, which plays a critical role in actin cytoskeleton dynamics. Our unpublished data suggest RPGR and its interacting protein regulate the stability of the key components of the PCP pathway. RPGRIP1L (Ftm) was shown to be involved in SHH pathway by controlling the production of Gli3 protein, which regulates SHH signaling [65]. RPGRIP1L is also involved in the PCP pathway through targeting Dvl to the cilium base and stabilizing the proteins there [66]. NPHP4, a direct interacting partner of both RPGRIP1 and RPGRIP1L, has been shown to stabilize Dvl [72]. In fact RPGRIP1L and NPHP4 coordinate to modulate dishevelled stability and control the Wnt pathway [66].

7. Conclusion

Mutations in the *RPGR* gene are the most common cause of RP, frequently associated with ciliopathies. RPGR directly or indirectly interacts with ciliary proteins to form one or more protein complexes. RPGR and its interacting proteins may regulate cilia genesis, maintenance, and function mainly through recruiting ciliary protein to cilia. RPGR protein complex is involved in cilia regulatory signaling pathways, but understanding the complicated RPGR-involved molecular mechanisms remains a challenge.

Conflict of Interests

The authors declare that there is no conflict of interests regarding the publication of this paper.

Acknowledgments

The authors would like to thank the National Eye Research Centre, Rosetrees Trust, Fight for Sight, Tenovus Scotland, the Visual Research Trust, the W. H. Ross Foundation, Yorkhill Children's Charity, and the Carnegie Trust for the Universities of Scotland for supporting this work.

References

[1] N. F. Berbari, A. K. O'Connor, C. J. Haycraft, and B. K. Yoder, "The primary cilium as a complex signaling center," *Current Biology*, vol. 19, no. 13, pp. R526–R535, 2009.

[2] V. Singla and J. F. Reiter, "The primary cilium as the cell's antenna: signaling at a sensory organelle," *Science*, vol. 313, no. 5787, pp. 629–633, 2006.

[3] K. G. Kozminski, K. A. Johnson, P. Forscher, and J. L. Rosenbaum, "A motility in the eukaryotic flagellum unrelated to flagellar beating," *Proceedings of the National Academy of Sciences of the United States of America*, vol. 90, no. 12, pp. 5519–5523, 1993.

[4] D. G. Cole, D. R. Diener, A. L. Himelblau, P. L. Beech, J. C. Fuster, and J. L. Rosenbaum, "Chlamydomonas kinesin-II-dependent intraflagellar transport (IFT): IFT particles contain proteins required for ciliary assembly in Caenorhabditis elegans sensory neurons," *The Journal of Cell Biology*, vol. 141, no. 4, pp. 993–1008, 1998.

[5] G. J. Pazour, B. L. Dickert, Y. Vucica et al., "Chlamydomonas IFT88 and its mouse homologue, polycystic kidney disease gene Tg737, are required for assembly of cilia and flagella," *The Journal of Cell Biology*, vol. 151, no. 3, pp. 709–718, 2000.

[6] K. G. Kozminski, P. L. Beech, and J. L. Rosenbaum, "The Chlamydomonas kinesin-like protein FLA10 is involved in motility associated with the flagellar membrane," *The Journal of Cell Biology*, vol. 131, no. 6 I, pp. 1517–1527, 1995.

[7] G. J. Pazour, B. L. Dickert, and G. B. Witman, "The DHC1b (DHC2) isoform of cytoplasmic dynein is required for flagellar assembly," *The Journal of Cell Biology*, vol. 144, no. 3, pp. 473–481, 1999.

[8] M. E. Porter, R. Bower, J. A. Knott, P. Byrd, and W. Dentler, "Cytoplasmic dynein heavy chain 1b is required for flagellar assembly in *Chlamydomonas*," *Molecular Biology of the Cell*, vol. 10, no. 3, pp. 693–712, 1999.

[9] J. M. Scholey, "Intraflagellar transport motors in cilia: moving along the cell's antenna," *Journal of Cell Biology*, vol. 180, no. 1, pp. 23–29, 2008.

[10] J. L. Rosenbaum and G. B. Witman, "Intraflagellar transport," *Nature Reviews Molecular Cell Biology*, vol. 3, no. 11, pp. 813–825, 2002.

[11] A. Hendrickson, "Organization of the adult primate fovea," in *Macular Degeneration*, P. L. Penfold and J. M. Provis, Eds., pp. 1–20, Springer, Berlin, Germany, 2005.

[12] C. J. Horst, L. V. Johnson, and J. C. Besharse, "Transmembrane assemblage of the photoreceptor connecting cilium and motile cilium transition zone contain a common immunologic epitope," *Cell Motility and the Cytoskeleton*, vol. 17, no. 4, pp. 329–344, 1990.

[13] S. G. Solomon and P. Lennie, "The machinery of colour vision," *Nature Reviews Neuroscience*, vol. 8, no. 4, pp. 276–286, 2007.

[14] B. M. Kevany and K. Palczewski, "Phagocytosis of retinal rod and cone photoreceptors," *Physiology*, vol. 25, no. 1, pp. 8–15, 2010.

[15] Q. Liu, G. Tan, N. Levenkova et al., "The proteome of the mouse photoreceptor sensory cilium complex," *Molecular and Cellular Proteomics*, vol. 6, no. 8, pp. 1299–1317, 2007.

[16] L. E. Ostrowski, K. Blackburn, K. M. Radde et al., "A proteomic analysis of human cilia: identification of novel components," *Molecular and Cellular Proteomics*, vol. 1, no. 6, pp. 451–465, 2002.

[17] M. R. Mahjoub, "The importance of a single primary cilium," *Organogenesis*, vol. 9, no. 2, pp. 61–69, 2013.

[18] S. C. Goetz and K. V. Anderson, "The primary cilium: a signalling centre during vertebrate development," *Nature Reviews Genetics*, vol. 11, no. 5, pp. 331–344, 2010.

[19] J. Hoefele, M. T. F. Wolf, J. F. O'Toole et al., "Evidence of oligogenic inheritance in nephronophthisis," *The Journal of the American Society of Nephrology*, vol. 18, no. 10, pp. 2789–2795, 2007.

[20] M. T. F. Wolf and F. Hildebrandt, "Nephronophthisis," *Pediatric Nephrology*, vol. 26, no. 2, pp. 181–194, 2011.

[21] A. Rattner, H. Sun, and J. Nathans, "Molecular genetics of human retinal disease," *Annual Review of Genetics*, vol. 33, pp. 89–131, 1999.

[22] D. T. Hartong, E. L. Berson, and T. P. Dryja, "Retinitis pigmentosa," *The Lancet*, vol. 368, no. 9549, pp. 1795–1809, 2006.

[23] C. Hamel, "Retinitis pigmentosa," *Orphanet Journal of Rare Diseases*, vol. 1, no. 1, article 40, 2006.

[24] D. K. Breuer, B. M. Yashar, E. Filippova et al., "A comprehensive mutation analysis of RP2 and RPGR in a North American cohort of families with X-linked retinitis pigmentosa," *The American Journal of Human Genetics*, vol. 70, no. 6, pp. 1545–1554, 2002.

[25] X. Shu, G. C. Black, J. M. Rice et al., "RPGR mutation analysis and disease: an update," *Human Mutation*, vol. 28, no. 4, pp. 322–328, 2007.

[26] Z. B. Jin, X. Q. Liu, M. Hayakawa, A. Murakami, and N. Naoi, "Mutational analysis of RPGR and RP2 genes in Japanese patients with retinitis pigmentosa: identification of four mutations," *Molecular Vision*, vol. 12, pp. 1167–1174, 2006.

[27] L. Huang, Q. Zhang, S. Li et al., "Exome sequencing of 47 chinese families with cone-rod dystrophy: mutations in 25 known causative genes," *PLoS ONE*, vol. 8, no. 6, Article ID e65546, 2013.

[28] A. Meindl, K. Dry, K. Herrmann et al., "A gene (RPGR) with homology to the RCC1 guanine nucleotide exchange factor is mutated in X-linked retinitis pigmentosa (RP3)," *Nature Genetics*, vol. 13, no. 1, pp. 35–42, 1996.

[29] R. Roepman, G. van Duijnhoven, T. Rosenberg et al., "Positional cloning of the gene for X-linked retinitis pigmentosa 3: homology with the guanine-nucleotide-exchange factor RCC1," *Human Molecular Genetics*, vol. 5, no. 7, pp. 1035–1041, 1996.

[30] R. Vervoort, A. Lennon, A. C. Bird et al., "Mutational hot spot within a new RPGR exon in X-linked retinitis pigmentosa," *Nature Genetics*, vol. 25, no. 4, pp. 462–466, 2000.

[31] R. Kirschner, T. Rosenberg, R. Schultz-Heienbrok et al., "RPGR transcription studies in mouse and human tissues reveal a retina-specific isoform that is disrupted in a patient with X-linked retinitis pigmentosa," *Human Molecular Genetics*, vol. 8, no. 8, pp. 1571–1578, 1999.

[32] D.-H. Hong and T. Li, "Complex expression pattern of RPGR reveals a role for purine-rich exonic splicing enhancers," *Investigative Ophthalmology and Visual Science*, vol. 43, no. 11, pp. 3373–3382, 2002.

[33] X. Shu, E. McDowall, A. F. Brown, and A. F. Wright, "The human retinitis pigmentosa GTPase regulator gene variant database," *Human Mutation*, vol. 29, no. 5, pp. 605–608, 2008.

[34] D. H. Hong, B. Pawlyk, M. Sokolov et al., "RPGR isoforms in photoreceptor connecting cilia and the transitional zone of motile cilia," *Investigative Ophthalmology and Visual Science*, vol. 44, no. 6, pp. 2413–2421, 2003.

[35] T. A. Mavlyutov, H. Zhao, and P. A. Ferreira, "Species-specific subcellular localization of RPGR and RPGRIP isoforms: implications for the phenotypic variability of congenital retinopathies among species," *Human Molecular Genetics*, vol. 11, no. 16, pp. 1899–1907, 2002.

[36] X. Shu, A. M. Fry, B. Tulloch et al., "RPGR ORF15 isoform co-localizes with RPGRIP1 at centrioles and basal bodies and interacts with nucleophosmin," *Human Molecular Genetics*, vol. 14, no. 9, pp. 1183–1197, 2005.

[37] X. Shu, Z. Zeng, M. S. Eckmiller et al., "Developmental and tissue expression of *Xenopus laevis* RPGR," *Investigative Ophthalmology and Visual Science*, vol. 47, no. 1, pp. 348–356, 2006.

[38] M. Linari, M. Ueffing, F. Manson, A. Wright, T. Meitinger, and J. Becker, "The retinitis pigmentosa GTPase regulator, RPGR, interacts with the delta subunit of rod cyclic GMP phosphodiesterase," *Proceedings of the National Academy of Sciences of the United States of America*, vol. 96, no. 4, pp. 1315–1320, 1999.

[39] J. P. Boylan and A. F. Wright, "Identification of a novel protein interacting with RPGR," *Human Molecular Genetics*, vol. 9, no. 14, pp. 2085–2093, 2000.

[40] R. Roepman, N. Bernoud-Hubac, D. E. Schick et al., "The retinitis pigmentosa GTPase regulator (RPGR) interacts with novel transport-like proteins in the outer segments of rod photoreceptors," *Human Molecular Genetics*, vol. 9, no. 14, pp. 2095–2105, 2000.

[41] D.-H. Hong, G. Yue, M. Adamian, and T. Li, "Retinitis pigmentosaGTPase regulator (RPGR)-interacting protein is stably associated with the photoreceptor ciliary axoneme and anchors

RPGR to the connecting cilium," *The Journal of Biological Chemistry*, vol. 276, no. 15, pp. 12091–12099, 2001.

[42] H. Khanna, T. W. Hurd, C. Lillo et al., "RPGR-ORF15, which is mutated in retinitis pigmentosa, associates with SMC1, SMC3, and microtubule transport proteins," *The Journal of Biological Chemistry*, vol. 280, no. 39, pp. 33580–33587, 2005.

[43] R. N. Wright, D.-H. Hong, and B. Perkins, "RpgrORF15 connects to the usher protein network through direct interactions with multiple whirlin isoforms," *Investigative Ophthalmology and Visual Science*, vol. 53, no. 3, pp. 1519–1529, 2012.

[44] E. A. Otto, B. Loeys, H. Khanna et al., "Nephrocystin-5, a ciliary IQ domain protein, is mutated in Senior-Loken syndrome and interacts with RPGR and calmodulin," *Nature Genetics*, vol. 37, no. 3, pp. 282–288, 2005.

[45] B. Chang, H. Khanna, N. Hawes et al., "In-frame deletion in a novel centrosomal/ciliary protein CEP290/NPHP6 perturbs its interaction with RPGR and results in early-onset retinal degeneration in the rd16 mouse," *Human Molecular Genetics*, vol. 15, no. 11, pp. 1847–1857, 2006.

[46] J. A. Sayer, E. A. Otto, J. F. O'Toole et al., "The centrosomal protein nephrocystin-6 is mutated in Joubert syndrome and activates transcription factor ATF4," *Nature Genetics*, vol. 38, no. 6, pp. 674–681, 2006.

[47] E. M. Valente, J. L. Silhavy, F. Brancati et al., "Mutations in CEP290, which encodes a centrosomal protein, cause pleiotropic forms of Joubert syndrome," *Nature Genetics*, vol. 38, no. 6, pp. 623–625, 2006.

[48] F. Coppieters, S. Lefever, B. P. Leroy, and E. de Baere, "CEP290, a gene with many faces: mutation overview and presentation of CEP290base," *Human Mutation*, vol. 31, no. 10, pp. 1097–1108, 2010.

[49] M. Barbelanne, J. Song, M. Ahmadzai, and W. Y. Tsang, "Pathogenic NPHP5 mutations impair protein interaction with Cep290, a prerequisite for ciliogenesis," *Human Molecular Genetics*, vol. 22, no. 12, pp. 2482–2494, 2013.

[50] T. P. Dryja, S. M. Adams, J. L. Grimsby et al., "Null RPGRIP1 alleles in patients with Leber congenital amaurosis," *The American Journal of Human Genetics*, vol. 68, no. 5, pp. 1295–1298, 2001.

[51] H. H. Arts, D. Doherty, S. E. C. van Beersum et al., "Mutations in the gene encoding the basal body protein RPGRIP1L, a nephrocystin-4 interactor, cause Joubert syndrome," *Nature Genetics*, vol. 39, no. 7, pp. 882–888, 2007.

[52] M. Delous, L. Baala, R. Salomon et al., "The ciliary gene *RPGRIP1L* is mutated in cerebello-oculo-renal syndrome (Joubert syndrome type B) and Meckel syndrome," *Nature Genetics*, vol. 39, no. 7, pp. 875–881, 2007.

[53] H. Khanna, E. E. Davis, C. A. Murga-Zamalloa et al., "A common allele in RPGRIP1L is a modifier of retinal degeneration in ciliopathies," *Nature Genetics*, vol. 41, no. 6, pp. 739–745, 2009.

[54] K. Remans, M. Bürger, I. Vetter, and A. Wittinghofer, "C2 domains as protein-protein interaction modules in the ciliary transition zone," *Cell Reports*, vol. 8, no. 1, pp. 1–9, 2014.

[55] R. Roepman, S. J. F. Letteboer, H. H. Arts et al., "Interaction of nephrocystin-4 and RPGRIP1 is disrupted by nephronophthisis or Leber congenital amaurosis-associated mutations," *Proceedings of the National Academy of Sciences of the United States of America*, vol. 102, no. 51, pp. 18520–18525, 2005.

[56] K. L. M. Coene, D. A. Mans, K. Boldt et al., "The ciliopathy-associated protein homologs RPGRIP1 and RPGRIP1L are linked to cilium integrity through interaction with Nek4 serine/threonine kinase," *Human Molecular Genetics*, vol. 20, no. 18, pp. 3592–3605, 2011.

[57] A. Eblimit, T. T. Nguyen, Y. Chen et al., "Spata7 is a retinal ciliopathy gene critical for correct RPGRIP1 localization and protein trafficking in the retina," *Human Molecular Genetics*, vol. 24, no. 6, pp. 1584–1601, 2015.

[58] C. A. Murga-Zamalloa, S. J. Atkins, J. Peranen, A. Swaroop, and H. Khanna, "Interaction of retinitis pigmentosa GTPase regulator (RPGR) with RAB8A GTPase: implications for cilia dysfunction and photoreceptor degeneration," *Human Molecular Genetics*, vol. 19, no. 18, Article ID ddq275, pp. 3591–3598, 2010.

[59] M. Gakovic, X. Shu, I. Kasioulis, S. Carpanini, I. Moraga, and A. F. Wright, "The role of RPGR in cilia formation and actin stability," *Human Molecular Genetics*, vol. 20, no. 24, Article ID ddr423, pp. 4840–4850, 2011.

[60] A. K. Ghosh, C. A. Murga-Zamalloa, L. Chan, P. F. Hitchcock, A. Swaroop, and H. Khanna, "Human retinopathy-associated ciliary protein retinitis pigmentosa GTPase regulator mediates cilia-dependent vertebrate development," *Human Molecular Genetics*, vol. 19, no. 1, pp. 90–98, 2010.

[61] X. Shu, Z. Zeng, P. Gautier et al., "Zebrafish Rpgr is required for normal retinal development and plays a role in dynein-based retrograde transport processes," *Human Molecular Genetics*, vol. 19, no. 4, pp. 657–670, 2009.

[62] D.-H. Hong, B. S. Pawlyk, J. Shang, M. A. Sandberg, E. L. Berson, and T. Li, "A retinitis pigmentosa GTPase regulator (RPGR)-deficient mouse model for X-linked retinitis pigmentosa (RP3)," *Proceedings of the National Academy of Sciences of the United States of America*, vol. 97, no. 7, pp. 3649–3654, 2000.

[63] Y. Zhao, D.-H. Hong, B. Pawlyk et al., "The retinitis pigmentosa GTPase regulator (RPGR)-interacting protein: Subserving RPGR function and participating in disk morphogenesis," *Proceedings of the National Academy of Sciences of the United States of America*, vol. 100, no. 7, pp. 3965–3970, 2003.

[64] J. Won, E. Gifford, R. S. Smith et al., "RPGRIP1 is essential for normal rod photoreceptor outer segment elaboration and morphogenesis," *Human Molecular Genetics*, vol. 18, no. 22, pp. 4329–4339, 2009.

[65] J. Vierkotten, R. Dildrop, T. Peters, B. Wang, and U. Rüther, "Ftm is a novel basal body protein of cilia involved in Shh signalling," *Development*, vol. 134, no. 14, pp. 2569–2577, 2007.

[66] A. Mahuzier, H.-M. Gaudé, V. Grampa et al., "Dishevelled stabilization by the ciliopathy protein rpgrip1l is essential for planar cell polarity," *Journal of Cell Biology*, vol. 198, no. 5, pp. 927–240, 2012.

[67] M. Adamian, B. S. Pawlyk, D.-H. Hong, and E. L. Berson, "Rod and cone opsin mislocalization in an autopsy eye from a carrier of X-linked retinitis pigmentosa with a Gly436Asp mutation in the RPGR gene," *American Journal of Ophthalmology*, vol. 142, no. 3, pp. 515–518, 2006.

[68] D. Wätzlich, I. Vetter, K. Gotthardt et al., "The interplay between RPGR, PDEδ and Arl2/3 regulate the ciliary targeting of farnesylated cargo," *EMBO Reports*, vol. 14, no. 5, pp. 465–472, 2013.

[69] E. A. Otto, T. W. Hurd, R. Airik et al., "Candidate exome capture identifies mutation of SDCCAG8 as the cause of a retinal-renal ciliopathy," *Nature Genetics*, vol. 42, no. 10, pp. 840–850, 2010.

[70] H. Patil, N. Tserentsoodol, A. Saha, Y. Hao, M. Webb, and P. A. Ferreira, "Selective loss of RPGRIP1-dependent ciliary targeting

of NPHP4, RPGR and SDCCAG8 underlies the degeneration of photoreceptor neurons," *Cell Death and Disease*, vol. 3, no. 7, article e355, 2012.

[71] E. C. Oh and N. Katsanis, "Cilia in vertebrate development and disease," *Development*, vol. 139, no. 3, pp. 443–448, 2012.

[72] C. Burcklé, H.-M. Gaudé, C. Vesque et al., "Control of the Wnt pathways by nephrocystin-4 is required for morphogenesis of the zebrafish pronephros," *Human Molecular Genetics*, vol. 20, no. 13, pp. 2611–2627, 2011.

[73] L. Yang, X. Yin, L. Feng et al., "Novel mutations of RPGR in Chinese retinitis pigmentosa patients and the genotype-phenotype correlation," *PLoS ONE*, vol. 9, no. 1, Article ID e85752, 2014.